

**EFFECT OF PALM METHYL ESTER BLENDING ON  
COMBUSTION AND PARTICULATE MATTER  
CHARACTERISTICS IN SMALL CI ENGINE**



**A THESIS SUBMITTED IN PARTIAL FULFILLMENT OF THE  
REQUIREMENT FOR THE DEGREE OF MASTER OF  
ENGINEERING IN AUTOMOTIVE ENGINEERING  
(INTERNATIONAL PROGRAM)  
INTERNATIONAL COLLEGE  
KING MONGKUT'S INSTITUTE OF TECHNOLOGY  
LADKRABANG  
ACADEMIC YEAR 2016  
KMUTL – 2016 – IC – M – 004 – 003**

This material is reserved for educational use only, not allowed for commercial use.

Forbidden to modify the content, and cite the document when use.



**COPYRIGHT 2016**  
**INTERNATIONAL COLLEGE**  
**KING MONGKUT'S INSTITUTE OF TECHNOLOGY**  
**LADKRABANG**

This material is reserved for educational use only, not allowed for commercial use.

Forbidden to modify the content, and cite the document when use.

<b>Thesis</b>	Effect of Palm Methyl Ester Blending on Combustion and Particulate Matter Characteristics in Small CI Engine
<b>Student</b>	Mr. Jiramed Boonsakda
<b>Student ID.</b>	57610021
<b>Degree</b>	Master of Engineering
<b>Program</b>	Automotive Engineering (International Program)
<b>Year</b>	2016
<b>Thesis Advisor</b>	Asst. Prof. Dr. Preechar Karin Dr. Nuwong Chollacoop Prof. Dr. Katsunori Hanamura

## ABSTRACT

Compression Ignition (CI) Engine is popularly used in vehicles due to high thermal efficiency. However CI engine has a particulate matter (PM) problem which biodiesel could be one of possible solution to solve this problem. The fuels chosen were commercial diesel (B7), blends of 20%, 40%, 60%, 80% and 100% of biodiesel by volume. This research separate into four parts. The first part focuses on fuel properties analysis such as fuel composition, distillation and heating value. The second part is engine performance which focusing on performance characteristic and efficiency when running on the engine. The third part is combustion analysis using combustion pressure sensor to capture the physical inside the combustion chamber. The last part is particulate matter which including particulate quantities, particle size distribution and particle composition.

**Keywords:** Biodiesel, Biofuel, Particulate matter, Soot, Emission

## ACKNOWLEDGEMENT

Initially, I would like to express my special thanks of gratitude to my advisor, Asst. Prof. Dr. Preechar Karin and co-advisor, Dr. Nuwong Chollacoop and Prof. Dr. Katsunori Hanamura for their spacious advice, guidance and encouragement throughout my thesis.

I am extremely grateful to thank National Metal and Materials Technology Center (MTEC), THAILAND for the financial and measuring equipment support in my research and Hino motors for scholarship which support my research and daily life.

I wish to express my gratitude to assistance from my senior and friends at KMITL automotive laboratory, Komkla Siricholathum, Prathan Srichai, Ekkawut Saenkhumvong, Park Watanawongskorn, Pop-Paul Ewphun, Watanyoo Phaireote, Sombat Marasri and Veerayut Wongpattharaworakul for their sincere advice and technical support such as the electronic program, equipment some comment and suggestion. I am pleased to have this opportunity to thank many colleagues and bachelor subordinate who have helped me with this dissertation.

I am also wish to thank Yanmar S.P. Co., Ltd for support the small the diesel engine to produce particulate matter.

# CONTENTS

ABSTRACT .....	I
ACKNOWLEDGEMENT .....	II
CONTENTS .....	III
LIST OF FIGURE.....	VI
LIST OF TABLE .....	IX
1. Chapter 1 INTRODUCTION .....	1
1.1. Background.....	1
1.2. Objectives .....	3
1.2.1. To study the efficiency of diesel blended with biodiesel. ....	3
1.2.2. To study combustion characteristic of biodiesel fuel. ....	3
1.2.3. To study the physical characteristics of diesel blended with biodiesel particulate matter in term of: .....	3
1.3. Scope of work.....	3
1.3.1. Analyze fuel properties such as viscosity, density, heating value, chemical formula, and carbon fraction and auto ignition temperature. ....	3
1.3.2. Operate the engine on engine dynamometer to see engine performance characteristic.....	3
1.3.3. To study the mechanical of biodiesel blended fuel combustion using combustion analyzer. ....	3
1.3.4. The analysis of the quantity of biodiesel blended fuel particulate matter using smoke meter. ....	3
1.3.5. The analysis of particle size distribution using laser diffraction technique. And compare with the previous work method.....	3
2. Chapter 2 RESEARCH THEORY .....	4
2.1. Diesel engine .....	4
2.2. Emission of diesel engine.....	6
2.3. Particulate matter.....	7
2.4. Alternative fuel: Biodiesel .....	9
2.5. Technical analysis .....	11

2.5.1. Scanning electron microscope .....	11
2.5.2. Transmission electron microscope.....	13
2.5.3. Laser diffraction particle sizing .....	14
2.6. Literature reviews.....	15
3. Chapter 3 EXPERIMENTAL APPARATUS AND PROCEDURE.....	21
3.1. Experimental apparatus .....	21
3.1.1. Diesel engine specification .....	21
3.1.2. Eddy current engine dynamometer .....	23
3.1.3. Fuel specification .....	24
3.1.4. Black smoke meter.....	26
3.1.5. Pressure sensor.....	26
3.1.6. Crank encoder .....	27
3.1.7. Data acquisition system .....	28
3.2. Experiment condition .....	30
3.3. Experiment procedure .....	30
3.3.1. Particulate matter quantities.....	30
3.3.2. Particulate matter size distribution.....	31
3.3.3. Combustion analysis .....	31
4. Chapter 4 RESULTS AND DISCUSSION.....	36
4.1. Fuel properties.....	36
4.2. Engine performance .....	39
4.2.1. Engine performance, efficiency, and exhaust temperature.....	39
4.3. Combustion characteristic .....	42
4.3.1. Injection timing .....	42
4.3.2. Effect of engine load .....	45
4.3.3. Effect of engine speed.....	47
4.3.4. Effect of fuel type .....	48
4.4. Particulate matter.....	49
4.4.1. Particulate matter quantities.....	49

4.4.2. Particulate matter size distribution.....	53
4.4.3. Morphology and nanostructures .....	55
4.4.4. Particle composition.....	59
5. Chapter 5 CONCLUSION.....	62
REFERENCE.....	63
APPENDICES .....	66
Appendix A:.....	67
Additional result.....	67
A-1: Pressure-Volume diagram.....	68
A-2: Pressure-Crank angle diagram .....	69
A-3: Derivation of pressure .....	70
A-4: Rate of heat release.....	71
A-5: Cumulative heat release .....	72
A-6: Etc.....	73
A-6.1: 2400rpm vary load20%,50%,80% .....	73
A-6.2: Full load.....	75
Appendix B: Material specification.....	81
B-1: Diesel engine specification.....	82
Appendix C: Standard and properties of fuels.....	84
C-1: Diesel fuel.....	85
C-2: Biodiesel fuel.....	87
Appendix D: Thailand emission standard .....	89
D-1: Thailand emission standards for small diesel engine vehicle .....	90
AUTHOR BIOGRAPHY.....	99

## LIST OF FIGURE

Figure 2.1 Diesel cycle [4].....	5
Figure 2.2 Stage of heat release rate [5] .....	6
Figure 2.3 Diesel combustion flame zone [6].....	6
Figure 2.4 Depicted schematically of particulate matter: coarse mode (largest, shown in part), nucleation mode (smallest); accumulation mode (midding) [7] .....	8
Figure 2.5 Particle size distribution of soot from a diesel engine [8].....	9
Figure 2.6 The greenhouse effect (Carbon dioxide) and the concept of carbon neutral of renewable bio-oxygenated fuels .....	10
Figure 2.7 Summary of influent of renewable bio-oxygenated fuel (Ethanol and Biodiesel) for economic, environmental and social .....	10
Figure 2.8 Transesterification of Vegetable Oil to Biodiesel [9] .....	11
Figure 2.9 Schematics of scanning electron microscopy operation [10].....	12
Figure 2.10 Schematics of transmission electron microscopy operation [11].....	13
Figure 2.11 The laser diffraction granulometer and associated dispersion units ....	14
Figure 2.12 Artist’s conception of diesel particulate matter [12].....	15
Figure 2.13 Relation between O/C ratio and activation energy[21].....	19
Figure 2.14 Relation between O/C ratio and size of carbon crystallite[21] .....	19
Figure 3.1 Diesel Engine and Specification for PM Quantities and Size Distribution Experiment .....	21
Figure 3.2 Diesel Engine Picture for Combustion Characteristic Experiment.....	22
Figure 3.3 Schematic diagram of engine dynamometer .....	23
Figure 3.4 smoke meter and paper filter .....	26
Figure 3.5 pressure sensor.....	27
Figure 3.6 crank encoder.....	28
Figure 3.7 data acquisition hardware .....	29
Figure 3.8 DEWESoft X2 software .....	29
Figure 3.9 Schematic diagram of particulate matter quantity measurement .....	30
Figure 3.10 Schematic diagram of particulate matter trapping .....	31
Figure 3.11 Schematic diagram of tested small CI engine operation on dynamometer for combustion characteristic .....	31
Figure 3.12 Pressure-crank angle diagram .....	32
Figure 3.13 Pressure-volume diagram .....	33
Figure 3.14 Rate of heat release.....	33
Figure 3.15 Combustion process.....	34
Figure 3.16 MFB, SOC, EOC .....	35

Figure 4.1 Distillation of conventional diesel and biodiesel fuel .....	37
Figure 4.2 Diesel, B60, and Biodiesel fuel composition from CHNS/O analyzer ..	38
Figure 4.3 Oxygen mass fraction of fuel .....	39
Figure 4.4 Engine performance curve.....	39
Figure 4.5 Brake specific fuel consumption and brake specific energy consumption at 80% load and 2400 rpm .....	40
Figure 4.6 Exhaust gas temperature at 80% load and 2400rpm on each fuel .....	41
Figure 4.7 Actual injection timing from heat release rate approximate 14-16 deg bTDC at full load (a) 1600rpm, (b) 2000rpm, (c) 2400rpm .....	43
Figure 4.8 Actual injection timing from heat release rate at partial load 2400rpm (a)20% load, (b)50% load, (c)80% load at 2400 rpm.....	44
Figure 4.9 Pressure-crank angle diagram of B7 on different engine load .....	45
Figure 4.10 Rate of heat release of B7 on different engine load .....	46
Figure 4.11 Cumulative heat release of B7 on different engine load .....	46
Figure 4.12 Rate of heat release of B7 on different engine speed .....	47
Figure 4.13 Rate of heat release of B7 on different fuel type and engine load .....	48
Figure 4.14 Smoke intensity of conventional diesel.....	49
Figure 4.15 Smoke intensity of B20 .....	50
Figure 4.16 Smoke intensity of B40 .....	50
Figure 4.17 Smoke intensity of B60 .....	51
Figure 4.18 Smoke intensity of B80 .....	51
Figure 4.19 Smoke intensity of B100 .....	52
Figure 4.20 comparison of particulate mass which emitted from biodiesel and commercial diesel [30].....	52
Figure 4.21 Particle size distribution at 80% load 2400rpm of each fuel .....	53
Figure 4.22 particle cumulative at 80% load 2400rpm of each fuel.....	54
Figure 4.23 SEM image of biodiesel blends diesel engine's PM10 in the condition of 80% load engine operation. ....	55
Figure 4.24 SEM image of conventional diesel particulate matter in condition of 80% load operation .....	56
Figure 4.25 SEM image of biodiesel particulate matter in condition of 80% load operation.....	56
Figure 4.26 TEM image of conventional diesel particulate matter ultrafine particles in the condition of 80% load operation.....	57
Figure 4.27 TEM image of biodiesel particulate matter ultrafine particles in the condition of 80% load operation.....	57

Figure 4.28 TEM image of conventional diesel nanoparticle in condition 80% load operation.....	58
Figure 4.29 TEM image of biodiesel nanoparticle in condition 80% load operation .....	58
Figure 4.30 particle composition result .....	59
Figure 4.31 Oxygen/Carbon ratio of particulate matter.....	60
Figure 4.32 relation between activation energy and O/C ratio[21] .....	60
Figure 4.33 Effect of O/C ratio to particle size[21].....	61
Figure 4.34 Ash fraction from particulate matter .....	61



## LIST OF TABLE

Table 3-1 Diesel Engine Specification for Combustion Characteristic Experiment .....	22
Table 3-2 Conventional diesel fuel properties .....	24
Table 3-3 Biodiesel fuel properties .....	25
Table 3-4 Experiment condition .....	30
Table 4-1 summary of fuel properties .....	36



# Chapter 1

## INTRODUCTION

### 1.1. Background

Recently, the shortage of energy is the one of main problem in the world. The global energy demand, reported by International Energy Agency, has been increasing continuously. The energy demand to year 2030 of transportation sector is growing approximately 1.7% per year as shown in Fig. 1.1 and the energy from oil is 36 % of global energy using which the biggest factor as shown in figure 1.2. Thus, the finding for using worthy or renewable energy is the way to solve this crisis. One of this is the using of high efficiency engine. As a well-known that a diesel engine has the highest thermal efficiency, where is more than 30% thermal efficiency, when compare with other internal combustion engine at the same load. The increasing number of diesel engine is an alternative to increase the efficiency of liquid fuel which limited in the world. However, the main pollutants from diesel engine are solid particles (Particulate Matter: PM) and nitrogen oxide (NOx) [1]. The pollutants should be removed from exhaust gas because of their effects on environment and human health, such as lung cancer. Hence, the regulation of pollution standard for diesel emission is proper way to control the emission that emitted to the atmosphere.

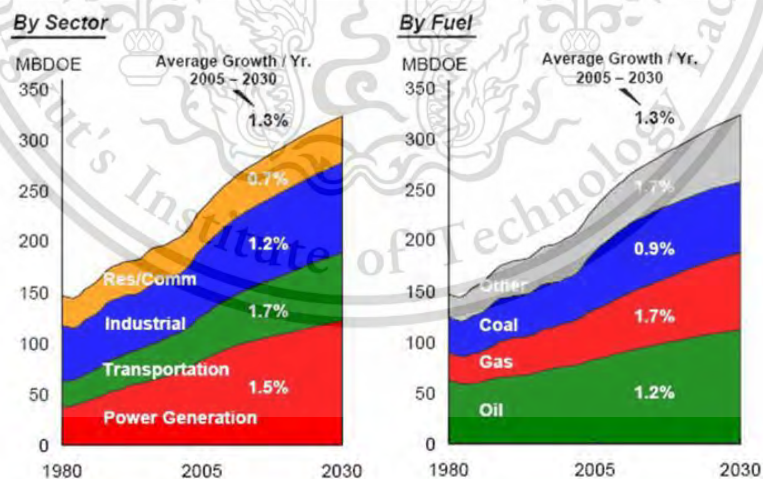


**Figure 1.1** Global energy demands, View to the year 2030 [2]

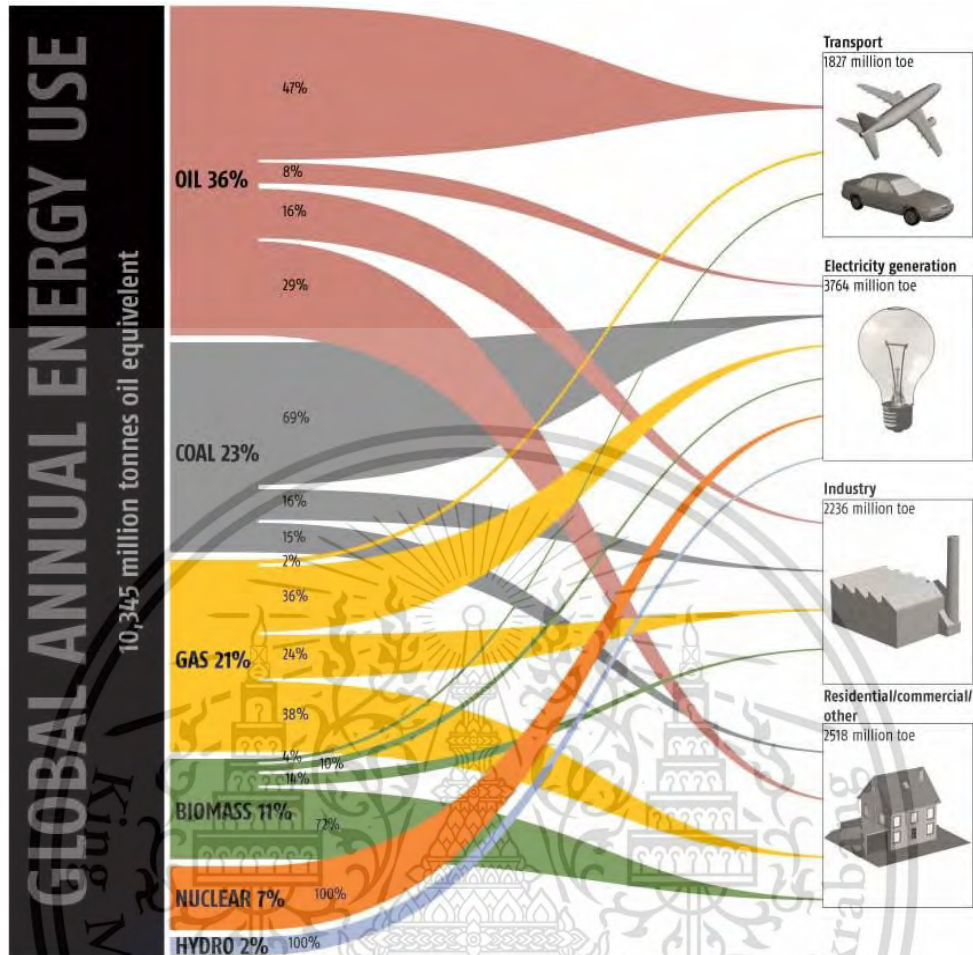


**Figure 1.2** World energy use and the sectorial split of fuel use [3]

In January 2012, the government of Thailand regulates to use the standard level 7 or Euro 4 to control the emission which release from diesel engine by the particulate matter must be not over 0.025 g/km.

The biofuel such as biodiesel diesel is the good option to substitute for fossil fuel. Because biofuel can be made from biomass and can re-produce faster than fossil fuel. Therefore, Thailand government promotes the using of biodiesel to Thai people. Due to, biodiesel can be produced in country with the domestic agriculture product of palm oil, jatropha oil, and etc. The advantage of biodiesel is low sulfur and aromatic hydrocarbon content. Beside, biodiesel has oxygen atom in fuel molecule and also acts like environmental friendly fuel. Even if, the combustion of biodiesel fuel emits greenhouse gas ( $\text{CO}_2$ ) to atmosphere as same as diesel fuel but in theoretical the biodiesel fuel can substantial reduce the net greenhouse gas. Due to, the biodiesel was made from biomass, as plants which the growth of plants pulls out the carbon dioxide gas from atmosphere by

photosynthesis. So the carbon dioxide gas was emitted from biofuel' s combustion and the carbon dioxide absorption by plants is balance, the increasing of greenhouse gas in the atmosphere can assume to be zero. Furthermore, the bio – oxygenated fuel also promote more completely combustion than fossil fuel that mean it emit low amount of particulate matter.

## **1.2.Objectives**

- 1.2.1. To study the efficiency of diesel blended with biodiesel.
- 1.2.2. To study combustion characteristic of biodiesel fuel.
- 1.2.3. To study the physical characteristics of diesel blended with biodiesel particulate matter in term of:
  - Quantity
  - Size
  - Composition
  - Activation energy

## **1.3. Scope of work**

- 1.3.1. Analyze fuel properties such as viscosity, density, heating value, chemical formula, and carbon fraction and auto ignition temperature.
- 1.3.2. Operate the engine on engine dynamometer to see engine performance characteristic.
- 1.3.3. To study the mechanical of biodiesel blended fuel combustion using combustion analyzer.
- 1.3.4. The analysis of the quantity of biodiesel blended fuel particulate matter using smoke meter.
- 1.3.5. The analysis of particle size distribution using laser diffraction technique. And compare with the previous work method.
- 1.3.6. To analysis particle composition using CHNS/O analyzer
- 1.3.7. Measure activation energy of particulate matter using thermal gravimetric analysis

## Chapter 2

### RESEARCH THEORY

#### 2.1. Diesel engine

A conventional internal combustion diesel engine works on “Diesel Cycle”. In the simple diesel engines, an injector injects diesel into the combustion chamber above the piston directly. Diesel engines are also commonly known as Compression-Ignition engines; since the diesel is burned due to hot compressed air. The temperature of the air inside the combustion chamber rises to above 400°C to 800°C, which in turn, ignites the diesel which was injected into the combustion chamber. The ‘Diesel Cycle’ does not use an external mechanism such as a spark-plug to ignite the air-fuel mixture. The principle of diesel cycle can be divided in to 4 stoke, as shown in Figure 2.1.

1. Suction – With pistons moving downwards and opening of the inlet valve creates suction of clean air into the cylinders.
2. Compression – With closing of Inlet valve the area above the piston gets closed. The piston moves up resulting in compression of the air in a confined space under higher compression-ratio.
3. Combustion – At this stage the injector sprays the diesel into the combustion chamber. The rise in temperature of the air caused by its compression; results in instantaneous burning of diesel with in an explosion. This causes heat to release resulting in generation of expanding forces known as power. These forces again push the pistons downwards resulting in their reciprocating motion.
4. Exhaust– On their way up, the pistons push the exhaust gases above them thru’ the exhaust valve which opens during exhaust stroke.

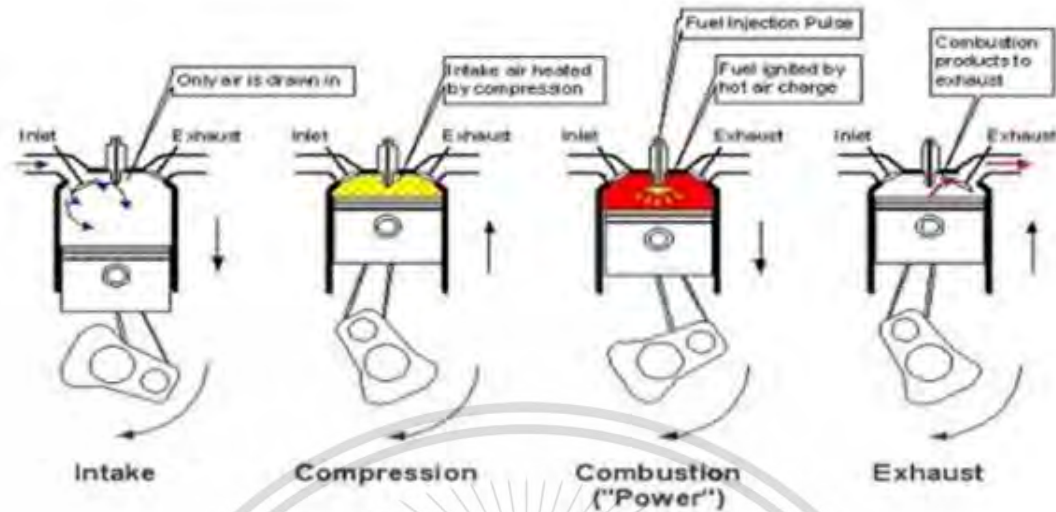


Figure 2.1 Diesel cycle [4]

The heat release rate (Figure 2.2) in combustion stroke of diesel cycle has 4 stage which consist of ignition delay phase, premixed combustion phase, mixing-controlled combustion phase and late combustion phase. The heat release rate explain the process as

- Ignition Delay Phase, a - b is the time period since the start of fuel injection in the combustion chamber until the fuel ignited.
- Premixed Combustion Phase, b - c is the time duration of the premixed fuel combustion after ignition delay phase which will initiate the rapid auto - ignition and increase heat release rate.
- Diesel Fuel Performance Mixing Combustion Phase, c - d is occurred in combustion chamber after the completely burned of premixed fuel. The combustion rate will be controlled by the formation rate of mixture between air - fuel that ready to be burned.
- Late Combustion Phase, d - e is the period that the heat release rate is low during the exhaust stroke. It is the combustion of the rest of the fuel and carbon residue which previously generated from the rich mixture.

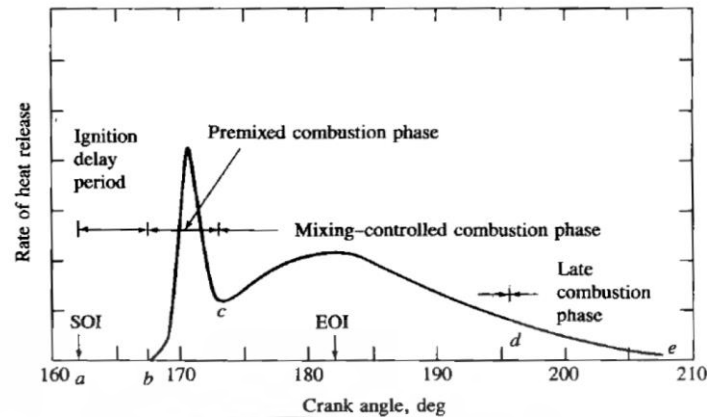


Figure 2.2 Stage of heat release rate [5]

## 2.2. Emission of diesel engine

Diesel engines convert the chemical energy contained in the fuel into mechanical power. Diesel fuel is injected under pressure into the engine cylinder where it mixes with air and where the combustion occurs. The exhaust gases which are discharged from the engine contain several constituents that are harmful to human health and to the environment. By the emission of diesel engine consist of CO, HC, NO<sub>x</sub>, SO<sub>2</sub> and particulate matter as shown on eq.2.1 and Figure 2.3 shown the combustion phenomena in combustion chamber.

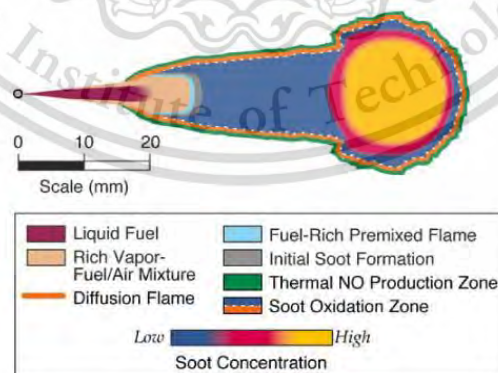


Figure 2.3 Diesel combustion flame zone [6]

Carbon monoxide (CO), hydrocarbons (HC), and aldehydes are generated in the exhaust as the result of incomplete combustion of fuel. A significant portion of exhaust hydrocarbons is also derived from the engine lube oil. When engines

operate in enclosed spaces, such as underground mines, buildings under construction, tunnels or warehouses, carbon monoxide can accumulate in the ambient atmosphere and cause headaches, dizziness and lethargy. Under the same conditions, hydrocarbons and aldehydes cause eye irritation and choking sensations. Hydrocarbons and aldehydes are major contributors to the characteristic diesel smell. Hydrocarbons also have a negative environmental effect, being an important component of smog.

Nitrogen oxides ( $\text{NO}_x$ ) are generated from nitrogen and oxygen under the high pressure and temperature conditions in the engine cylinder.  $\text{NO}_x$  consist mostly of nitric oxide (NO) and a small fraction of nitrogen dioxide ( $\text{NO}_2$ ). Nitrogen dioxide is very toxic.  $\text{NO}_x$  emissions are also a serious environmental concern because of their role in the smog formation.

Sulfur dioxide ( $\text{SO}_2$ ) is generated from the sulfur present in diesel fuel. The concentration of  $\text{SO}_2$  in the exhaust gas depends on the sulfur content of the fuel. Low sulfur fuels of less than 0.05% sulfur are being introduced for most diesel engine applications. Sulfur dioxide is a colorless toxic gas with a characteristic, irritating odor. Oxidation of sulfur dioxide produces sulfur trioxide which is the precursor of sulfuric acid which, in turn, is responsible for the sulfate particulate matter emissions. Sulfur oxides have a profound impact on environment being the major cause of acid rains.

Particulate matter (PM) is a complex aggregate of solid and liquid material. Its origin is carbonaceous particles generated in the engine cylinder during combustion. The primary carbon particles form larger agglomerates and combine with several other, both organic and inorganic, components of diesel exhaust.

### 2.3. Particulate matter

Particulate matter is the most characteristic of diesel emissions which responsible for the black smoke traditionally associated with diesel powered vehicles. The diesel particulate matter emission is usually abbreviated as PM or DPM. Particulate matter was divided into three characteristic ranges of size: nucleation mode, accumulation mode and coarse mode. The nucleation-mode particles are more arcane: most are probably formed from nucleated volatiles, Accumulation mode particles are constructed from a solid core of carbonaceous building blocks called 'spherules', together forming 'agglomerates' within the range of 60–100 nm. Spherules are fairly uniform in size, i.e. mostly 20–50 nm.

The coarse-mode particles are solid and are formed from the other two modes through a process of storage and release in the exhaust system, or through material disintegration. Composition-wise, there are five distinct ‘fractions’: ash, carbonaceous, organic, sulphate and nitrate as shown Figure 2.4. The diesel particulate matter has a complicated physical and chemical structure.

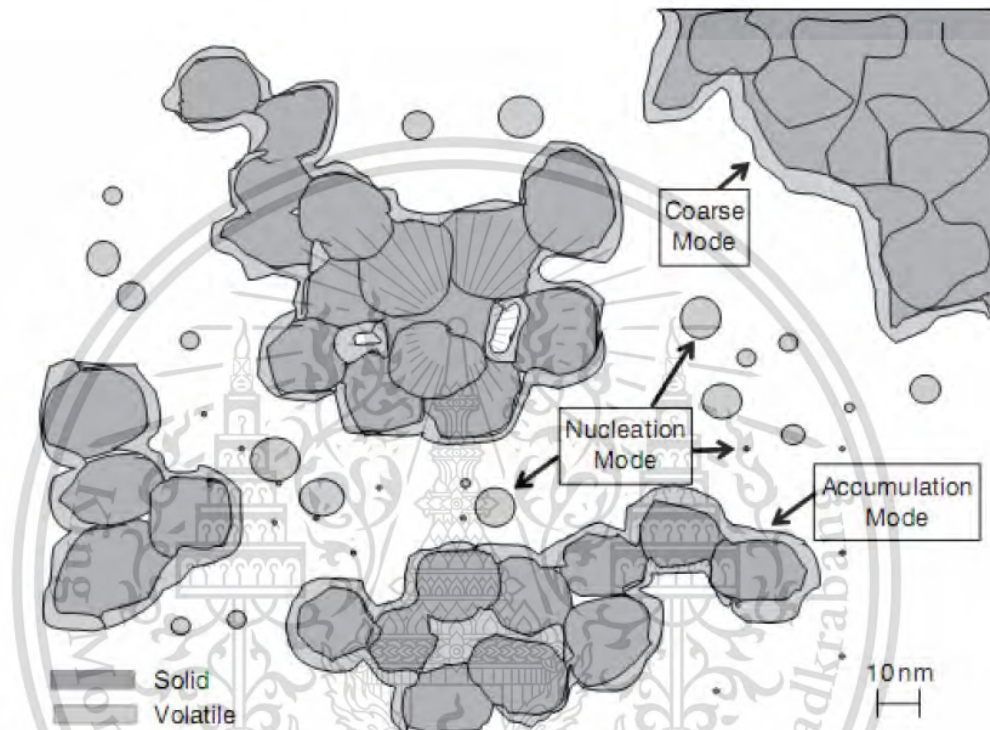


Figure 2.4 Depicted schematically of particulate matter: coarse mode (largest, shown in part), nucleation mode (smallest); accumulation mode (middling) [7]

Two main elements of diesel particulate matter are Solid Organic Fraction (SOL), consisting of carbon and metallic ash, and the Soluble Organic Fraction (SOF), consisting of hydrocarbon. Figure 2.5 is also illustrated the definition of size of atmosphere particles: PM<sub>10</sub>,  $D$  (diameter)  $< 10 \mu\text{m}$ ; fine particles,  $D < 2.5 \mu\text{m}$ ; ultrafine particles,  $D < 0.10 \mu\text{m}$ ; and nano - particles,  $D < 0.05 \mu\text{m}$  or 50 nm.

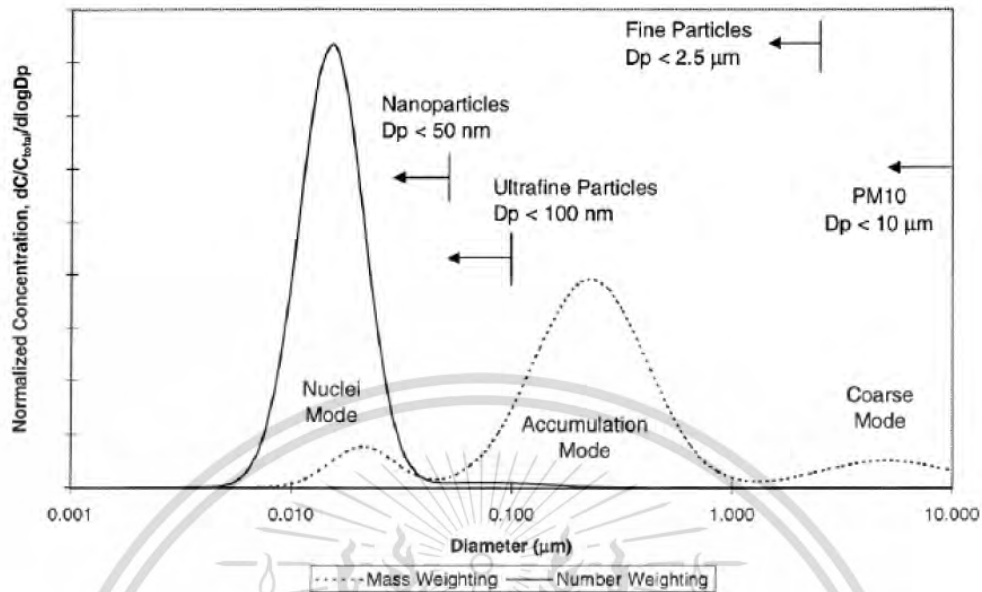


Figure 2.5 Particle size distribution of soot from a diesel engine [8]

#### 2.4. Alternative fuel: Biodiesel

Renewable bio-oxygenated fuels – liquid and gaseous fuels derived from organic matter – can play an important role in reducing CO<sub>2</sub> emissions (greenhouse gas effect and global warming) because of bio-fuels is the carbon neutral, as shown in Figure 2.6.

To reduce dependency on oil and to contribute to growing efforts to decarbonize the transport sector, bio-fuels release shifting to low-carbon, non-petroleum fuels, often with minimal changes to vehicle stocks and distribution infrastructure. While improving vehicle efficiency is by far the most important low-cost way of reducing co emissions in the transport sector, bio-fuels will need to play a significant role in replacing liquid fossil fuels suitable for planes, marine vessels and other heavy transport modes that cannot be electrified. Production and use of bio-fuel can also provide benefits such as increased energy security, by reducing dependency on oil imports, and reducing oil price volatility. In addition, bio-fuels can support economic development by creating new sources of income in rural areas, as shown in Figure 2.7.

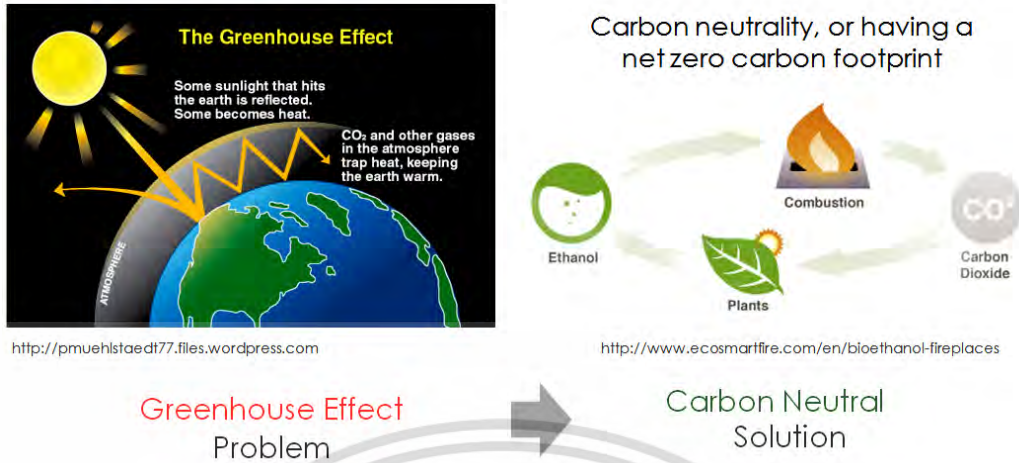


Figure 2.6 The greenhouse effect (Carbon dioxide) and the concept of carbon neutral of renewable bio-oxygenated fuels

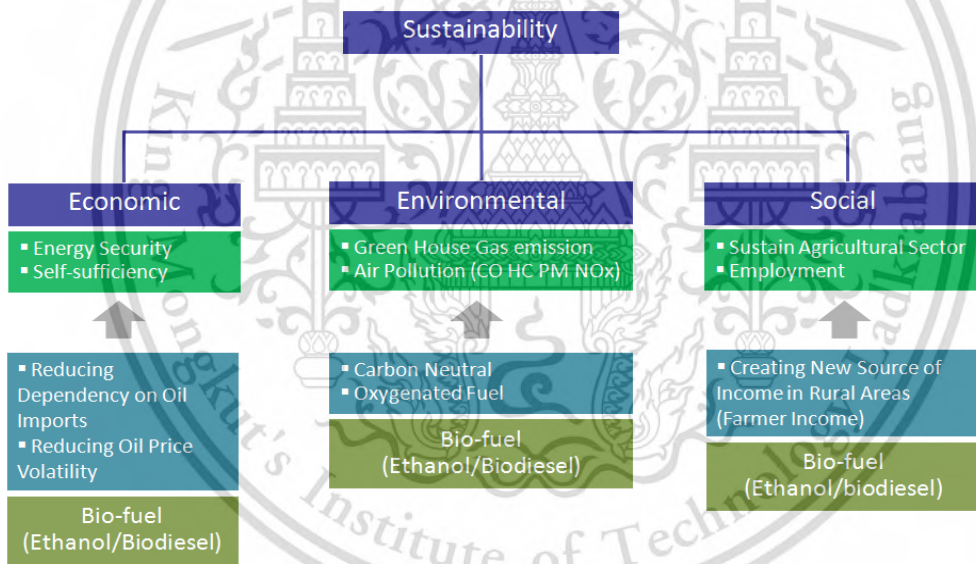


Figure 2.7 Summary of influent of renewable bio-oxygenated fuel (Ethanol and Biodiesel) for economic, environmental and social

Biodiesel is an alternative fuel for diesel engines that is produced by chemically reacting a vegetable oil or animal fat with an alcohol such as methanol. The reaction requires a catalyst, usually a strong base, such as sodium or potassium hydroxide, and produces new chemical compounds called methyl esters. It is these esters that have come to be known as biodiesel. Because its primary feedstock is a vegetable oil or animal fat, biodiesel is generally

considered to be renewable. Since the carbon in the oil or fat originated mostly from carbon dioxide in the air, biodiesel is considered to contribute much less to global warming than fossil fuels. Diesel engines operated on biodiesel have lower emissions of carbon monoxide, unburned hydrocarbons, particulate matter, and air toxics than when operated on petroleum-based diesel fuel. Biodiesel is produced through a process known as transesterification, as shown in Figure 2.8. By R1, R2, and R3 are long hydrocarbon chains, sometimes called fatty acid chains. There are only five chains that are most common in soybean oil and animal fats (others are present in small amounts)[9].

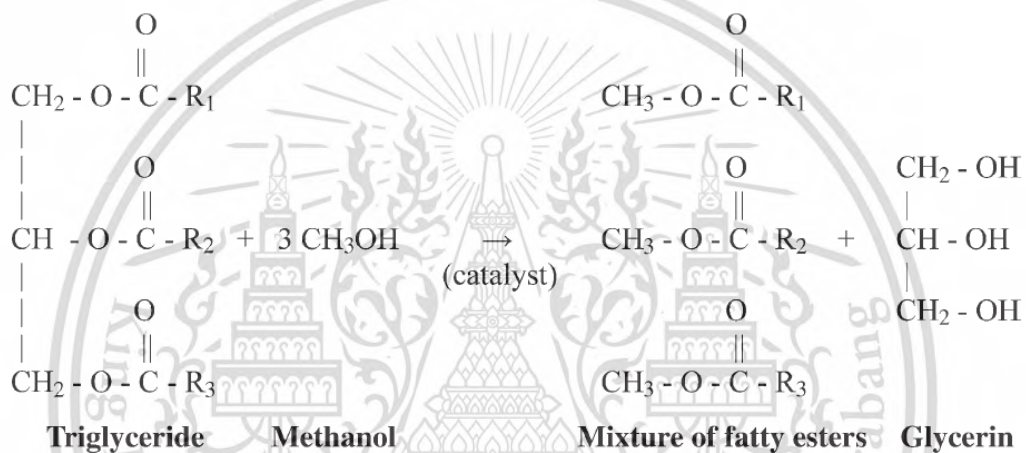


Figure 2.8 Transesterification of Vegetable Oil to Biodiesel [9]

## 2.5. Technical analysis

### 2.5.1. Scanning electron microscope

The scanning electron microscope (SEM) uses a focused beam of high-energy electrons to generate a variety of signals at the surface of solid specimens. The signals that derive from electron-sample interactions reveal information about the sample including external morphology (texture), chemical composition, and crystalline structure and orientation of materials making up the sample. In most applications, data are collected over a selected area of the surface of the sample, and a 2-dimensional image is generated that displays spatial variations in these properties. Areas ranging from approximately 1 cm to 5 microns in width can be imaged in a scanning mode using conventional SEM

techniques (magnification ranging from 20X to approximately 30,000X, spatial resolution of 50 to 100 nm). The main SEM components include: Source of electrons, Column down which electrons travel with electromagnetic lenses, Electron detector, Sample chamber and Computer and display to view the images as shown in Figure 2.9. Electrons are produced at the top of the column, accelerated down and passed through a combination of lenses and apertures to produce a focused beam of electrons which hits the surface of the sample. The sample is mounted on a stage in the chamber area and, unless the microscope is designed to operate at low vacuums, both the column and the chamber are evacuated by a combination of pumps. The level of the vacuum will depend on the design of the microscope. The position of the electron beam on the sample is controlled by scan coils situated above the objective lens. These coils allow the beam to be scanned over the surface of the sample. This beam scanning, as the name of the microscope suggests, enables information about a defined area on the sample to be collected. As a result of the electron-sample interaction, a number of signals are produced. These signals are then detected by appropriate detectors.

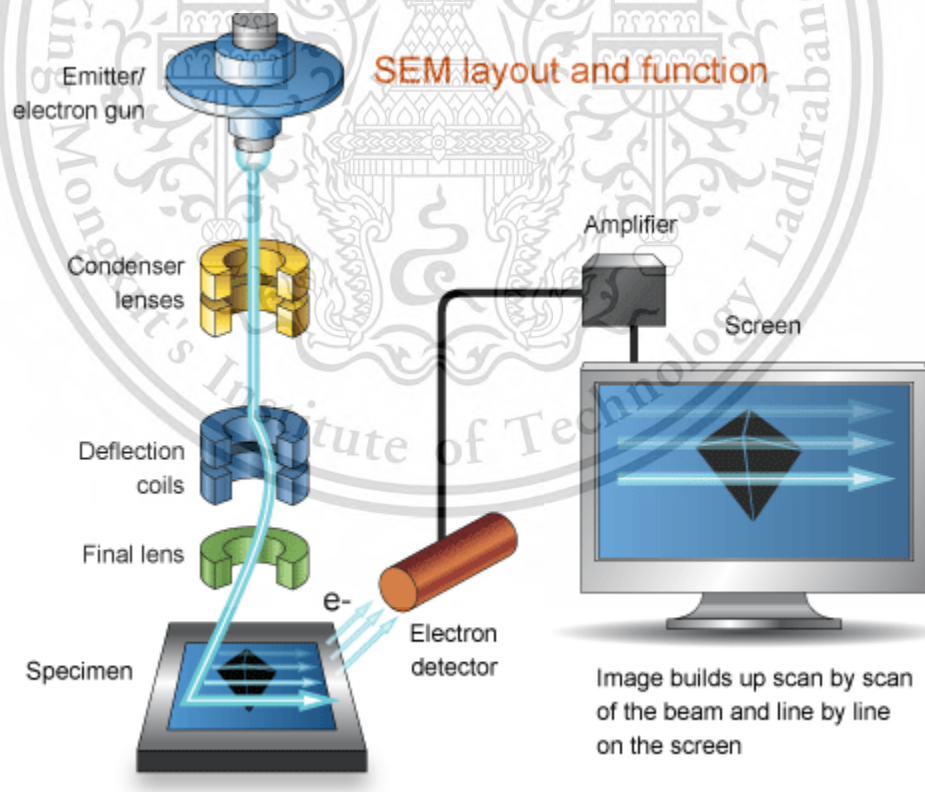


Figure 2.9 Schematics of scanning electron microscopy operation [10]

### 2.5.2. Transmission electron microscope

The transmission electron microscope (TEM) is a very powerful tool for material science. A Figure 2.10 shown schematic of transmission electron microscopy operation by a high energy beam of electrons is shone through a very thin sample, and the interactions between the electrons and the atoms can be used to observe features such as the crystal structure and features in the structure like dislocations and grain boundaries. Chemical analysis can also be performed. TEM can be used to study the growth of layers, their composition and defects in semiconductors. High resolution can be used to analyze the quality, shape, size and density of quantum wells, wires and dots. The TEM operates on the same basic principles as the light microscope but uses electrons instead of light. Because the wavelength of electrons is much smaller than that of light, the optimal resolution attainable for TEM images is many orders of magnitude better than that from a light microscope. Thus, TEMs can reveal the finest details of internal structure - in some cases as small as individual atoms.

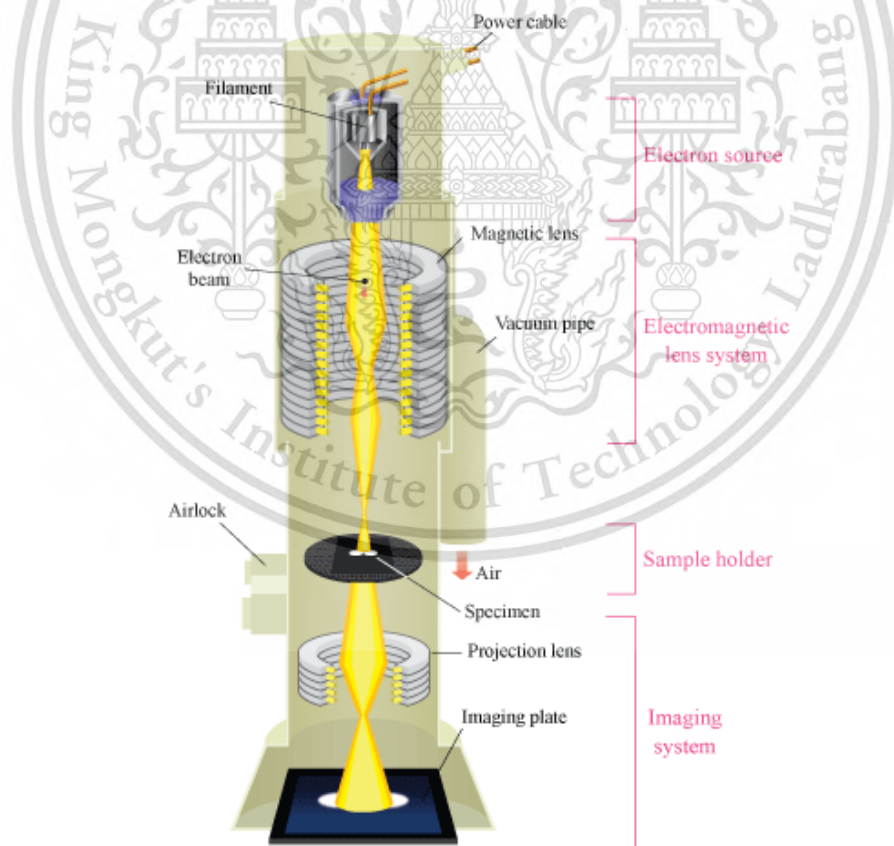


Figure 2.10 Schematics of transmission electron microscopy operation [11]

This material is reserved for educational use only, not allowed for commercial use.

Forbidden to modify the content, and cite the document when use.

### 2.5.3. Laser diffraction particle sizing



Figure 2.11 The laser diffraction granulometer and associated dispersion units

Figure 2.11 shows the laser diffraction granulometer and associated dispersion units, laser diffraction technique. It is used in a wide range of applications to give accurate measurement of particle size. The method is usually applicable for a particle range from 0.1 to 2,000  $\mu\text{m}$  depending on the setup of the system, a particle volume fraction from 0.001 to 1.0 vol. % can normally be measured. The laser diffraction technique is based on Mie scattering developed by Gustav Mie.

In order to solve for a spherical particle Mie assumed that the particle has to be isotropic, in effect no difference in which direction the incident beam strikes the particle. He also assumed that the waves of the incident light were of constant frequency, constant amplitude and parallel.

The particle size distribution of all samples were performed with the laser diffraction granulometer and associated dispersion units This laser diffraction particle size analyzer is designed to measure particle sizes ranges from 0.02 to 2000  $\mu\text{m}$  by using a blue (488.0  $\mu\text{m}$  wavelength LED) and red (633.8  $\mu\text{m}$  wavelength He-Ne laser) light dual-wavelength, single-lens detection system. The light energy diffracted by the dilute suspension circulating through the cell is measured by 52 sensors.

## 2.6. Literature reviews

M. M. Maricq (2007) [12] proposed the characteristics of the particulate matter from diesel engine. Figure 2.12 shown the diesel particulate matter consists of two types of particles: (a) fractal-like agglomerates of primary particles 15–30 nm in diameter, composed of carbon and traces of metallic ash, and coated with condensed heavier end organic compounds and sulfate; (b) nucleation particles composed of condensed hydrocarbons and sulfate.

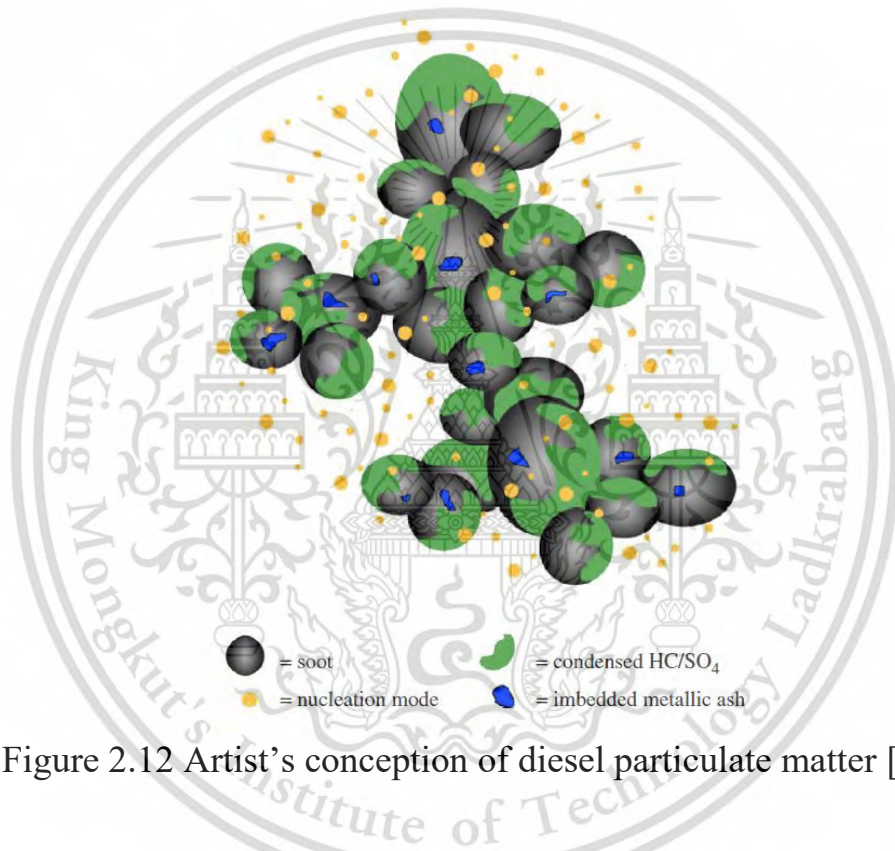


Figure 2.12 Artist's conception of diesel particulate matter [12]

O. I. Smith (1981) [13] presented the basic structure of primary particles. A primary particle is consisted by carbon atoms which are bonded together in hexagonal face – centered arrays in planes, referred to as platelets. Platelets are arranged in layers to form crystallites. There are typically 2–5 platelets per crystallite, and on the order of  $10^3$  crystallites per spherical soot particle. The crystallites are arranged with their planes more or less parallel to the particle surface. This structure of unordered layers is called turbostatic. Spherules, diameter of 10–50 nm, are fused together to form particles. A single spherule contains 105 to 106 carbon atoms.

D. B. Kittelson (1997) [8] concluded the particulate matter composition and structure. Diesel exhaust particles consist mainly of highly agglomerated solid carbonaceous material and ash, and volatile organic and sulfur compounds. Solid carbon is formed during combustion in locally rich regions. Much of it is subsequently oxidized. The residue is exhausted in the form of solid agglomerates. A tiny fraction of the fuel and atomized and evaporated lube oil escape oxidation and appear as volatile or soluble organic compounds (generally described as the soluble organic fraction, SOF) in the exhaust. The SOF contains polycyclic aromatic compounds containing oxygen, nitrogen, and sulfur. Metal compounds in the fuel and lube oil lead to a small amount of inorganic ash. The idealized of diesel particles number and mass weighted size distributions. Most of the particle mass exists in accumulation mode in the 0.1 - 0.3  $\mu\text{m}$  diameter range. This is where the carbonaceous agglomerates and associated adsorbed materials reside. The nuclei mode typically consists of particles in the 0.005 - 0.05  $\mu\text{m}$  diameter range. This mode usually consists of volatile organic and sulfur compounds that form during exhaust dilution and cooling, and may also contain solid carbon and metal compounds. The nuclei mode typically contains 1 - 20% of the particle mass and more than 90% of the particle number. The coarse mode contains 5 - 20% of the particle mass. It consists of accumulation mode particles that have been deposited on cylinder and exhaust system surfaces and later re-entrained.

Y. Songsaengchan et al (2012) [14] investigated the chemical characteristic of biodiesel and diesel particulate matter at various engine loads (0%, 50% and 80%). The research result represented particulate matter of diesel combustion is consisted approximately 4% moisture, 71% unburned HC and 25% carbon of no-load condition, 50% load condition is 6% moisture, 46% unburned HC and 48% carbon and 80% load condition is 4% moisture, 29% unburned HC and 67% carbon while particulate matter of biodiesel combustion is consisted approximately 4% moisture, 86% unburned HC and 10% carbon of no-load condition, 50% load condition is 9% moisture, 66% unburned HC and 25% carbon and 80% load condition is 4% moisture, 40% unburned HC and 56% carbon. The biodiesel engine particulate matter is faster oxidized than that of diesel engine particulate matter. In addition, the engine particulate matter from low load condition is faster oxidized that higher load for both of diesel and biodiesel fuels. So, particulate matter in high load condition has lower unburned HC fraction than that lower load condition. The combustion temperature in high

load condition is more than that of low load. The unburned HC might be oxidized with remain oxygen in high temperature exhaust gas. Moreover, particulate matter from biodiesel engine combustion has more unburned HC fraction than that of diesel engine combustion. Biodiesel fuel has lower heating value than that of diesel fuel. In the same load condition, biodiesel must be used more fuel injection in combustion chamber in combustion duration. More of fuel remaining in combustion duration is burned to be more HC in particulate matter.

A. K. Agarwal et al. (2011) [15] studied the effect of particulate matter emitted from a mid-size engine running on petroleum-based diesel versus biodiesel. They found that biodiesel and its blends (B20) gave more SOF in engine exhaust particulates than mineral diesel at all operating conditions because biodiesel has more viscosity value than mineral diesel so biodiesel drop was combusted harder than mineral diesel. But all operating conditions of studies, the peak particle for B100 and B20 were always smaller size than mineral diesel because of oxygen atom in fuel molecule.

T. Lu et al (2012) [16] analyzed the size and nanostructure of particulate matter that Effects from engine operating conditions by using transmission electron microscope (TEM). This research revealed that the size of primary particles is determined by the combustion conditions. It is found that primary particle size decreases with engine speed as a consequence of the shorter combustion duration but increases with increase of engine load (as reflected by a decrease in the air/fuel ratio) due to the longer duration of diffusion combustion and higher combustion temperature.

H. Kim et al. (2010) [17] explored the effect of biodiesel blended diesel fuel on nanoparticles. The number of particles smaller than 50 nm was increased under 5% and 20% biodiesel–diesel blends (BD05 and BD20) in comparison with diesel (D100). The number of particles smaller than 50 nm was increased by 8.7% (1.6%) when migrating from D100 to BD05 (BD20). With respect to particles smaller than 100 nm, the use of BD05 exhibited a 5.4% - higher particle number concentration than that of D100; however, under BD20, the corresponding value was 6.3% less than under D100. Therefore, compared with the particle number concentration under D100 there are more particles smaller than 50 nm – but fewer large particles – were emitted under BD20. The increased number of particles less than 50 nm that were emitted through the use of biodiesel–diesel blends possibly originated from the increase in the SOF particles. Under BD05, the rate

of reduction in particle numbers in the catalyst was higher than that under D100, probably because a large number of SOF particles were oxidized in the oxidation catalyst. The total number of particles emitted under BD05 in the entire range of measurement ( $10 < D_p < 385$  nm) increased by 4.4%. However, under BD20, the corresponding number decreased by 9.4%, and in terms of the converted particle weight, the particle mass reduced by 25%. The use of biofuel-blended diesel fuels reduced the total number of particles emitted from the engine. However, when compared to the use of diesel, the use of biodiesel–diesel blends caused the emission of more particles smaller than 50 nm, which are harmful to human body.

D. Dwivedi et al. (2006) [18] investigated about characterization particulate emissions from diesel engines fuelled by mineral diesel and B20 which operated at idling, 25%, 50% and 75% engine load. They found that oxygenated fuel B20 (biodiesel blend) showed superior engine performance in reducing particulate emissions at all operating conditions compared to mineral diesel (particulate in DE; 22–59 mg/m<sup>3</sup> and in BDE; 17–48 mg/m<sup>3</sup>). This may be due to lower sulphur and aromatic content of biodiesel.

M. Salamanca et al. (2012) [19] attempted the influence on the chemical composition of the particle matter produced in an automotive diesel engine operated with palm biodiesel (PB100) and its blends with diesel fuel by 5%, 20% and 50% of biodiesel. The result shown that biodiesel does not affect significantly the average size of PM emitted compared to diesel. However, biodiesel and biodiesel-diesel blends tend to produce PM with a higher number of diameters below 25 nm. In general, the higher oxygen content of biodiesel affects the chemical and morphological characteristics of the particulate matter produced in diesel engines.

P. Karin et al. (2012) [20] cultivated the particulate matter trapping which emitted from biodiesel and diesel fuel by using conventional diesel particulate filter (DPF). The studies presented DPF trapping duration of biodiesel fuel has longer than that of diesel fuel around two times because of PM concentration emitted from bio-oxygenated fuel combustion frame is lower than that of diesel combustion. Due to biodiesel fuel consisting of more oxygen atom in fuel molecule is readily oxidized with available oxygen in the flame zone.

The research from Jun Hamada et al.[21], which show the relation between oxygen/carbon ration with activation energy and particle size. The biodiesel particle has lower activation energy and smaller particle size due to

oxygen/carbon ratio in particle which biodiesel has higher oxygen/carbon ratio as shown in Figure 2.13 and Figure 2.14.

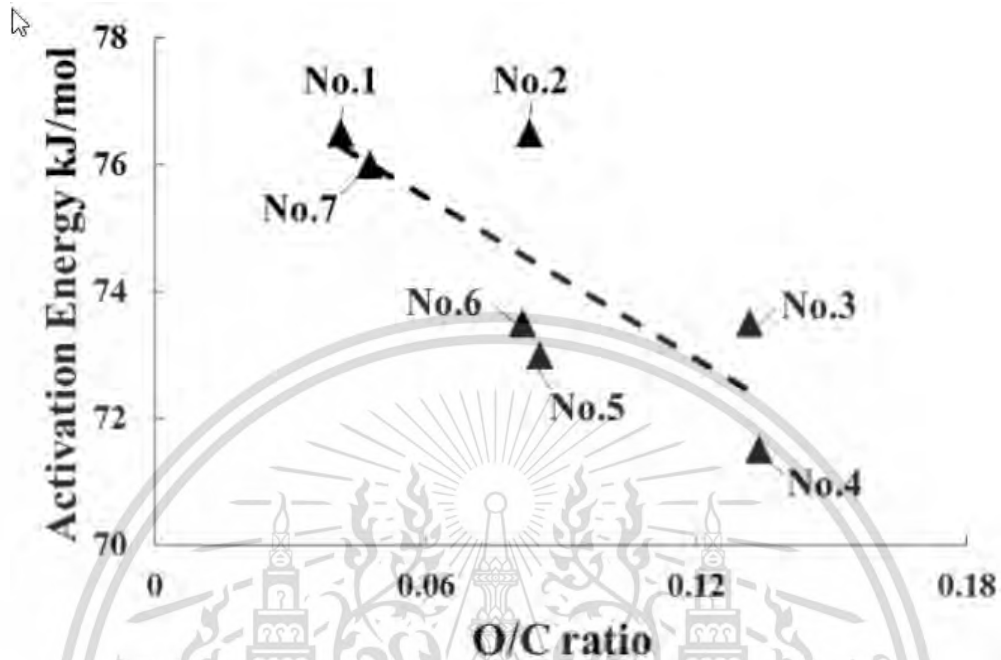


Figure 2.13 Relation between O/C ratio and activation energy[21]

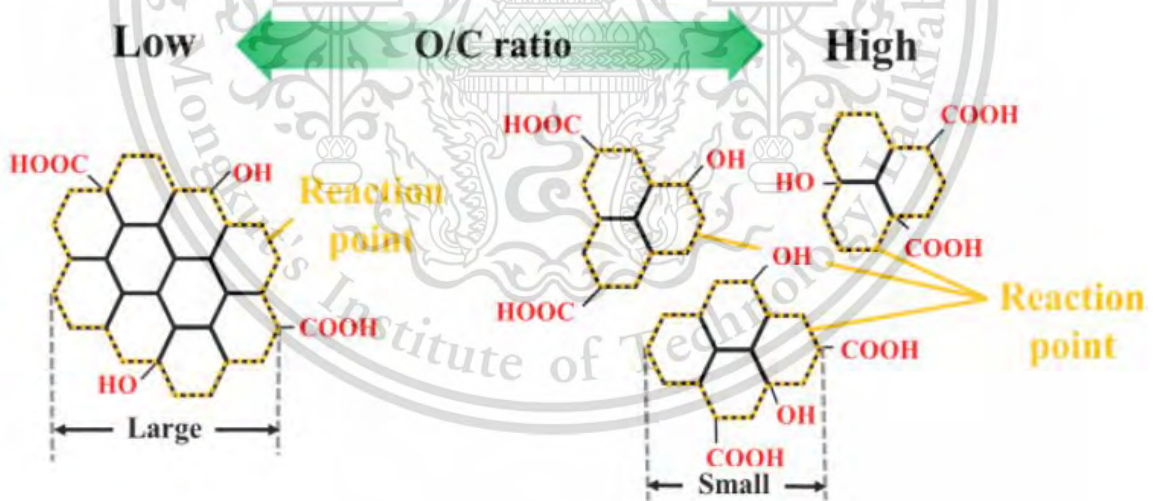


Figure 2.14 Relation between O/C ratio and size of carbon crystallite[21]

K.Vijararaj et al. (2014) [22] Biodiesel is an alternative fuel for conventional diesel engines and can be used without major modification of the engines. When compared to diesel, biodiesel has a higher cetane number which results in shorter ignition delay and hence results in low particulate emissions.

The research of S.Srihari et al.,[23] , the reason of lower EGT for biodiesel is” Early start of the combustion due to shorter premixed combustion phase and lower calorific value can also lead to reduction in exhaust gas temperature as is seen for the DEE blends[24].”. And it has some other research which get biodiesel EGT lower than diesel as well such as [25] and [26].



## Chapter 3

### EXPERIMENTAL APPARATUS AND PROCEDURE

#### 3.1. Experimental apparatus

##### 3.1.1. Diesel engine specification

The two small diesel engines were used for produce particulate matter in condition of diesel and biodiesel fuel.

The first engine is “YANMAR TF120DI” which were used for PM quantities and PM size distribution experiment. The engine is four stoke, single cylinder, 638 cm<sup>3</sup> displacement, direct injection and 16.1:1 compression ratio. Fuel injection pressure is 19.6 MPa and other specification is shown in Figure 3.1. The engine was operated and controlled on eddy current dynamometer.

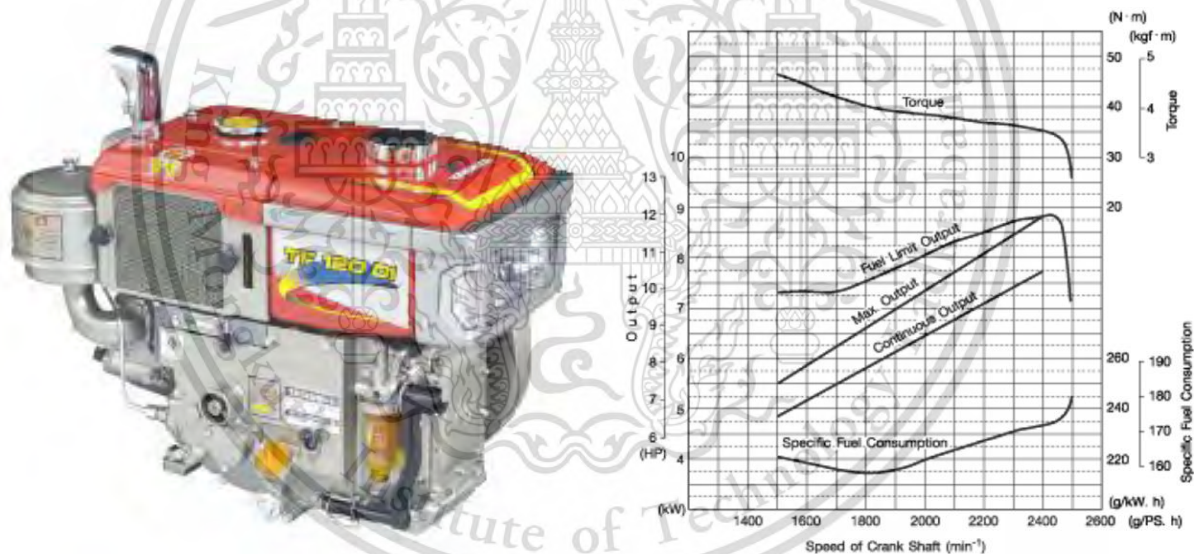


Figure 3.1 Diesel Engine and Specification for PM Quantities and Size Distribution Experiment

The second engine is “KUBOTA RT140 DI plus ES” which picture and specification shown in Figure 3.2 and Table 3-1 respectively. This engine was used for combustion characteristic experiment. The engine was operated and controlled on eddy current dynamometer. This engine was fitted with pressure sensor on a cylinder head to measure the pressure in the combustion chamber.



Figure 3.2 Diesel Engine Picture for Combustion Characteristic Experiment

Table 3-1 Diesel Engine Specification for Combustion Characteristic Experiment

Model	KUBOTA RT140 DI Plus ES
Type	diesel, 4 stroke, 1 cylinder, water cooled
Injection type	direct injection
Bore x stroke	97x96
Displacement	709cc
Maximum power	14hp/2400rpm
Maximum torque	5kg-m/1600rpm
Continuous power	12.5hp/2400rpm
Compression ratio	18:01

### 3.1.2. Eddy current engine dynamometer

The engine dynamometer, Tokyo Plant model ED-60-LC, was used in the experiment for applying a load on the tested engine and also measuring force, moment of force (torque) and power that the tested engine can produce against the load. The type of the engine dynamometer is Eddy current with external water cooling systems. Eddy current dynamometer can provide a quick load change rate for rapid load setting. Eddy current dynamometer consists of an electrically conductive core moving across a magnetic field to produce resistance to brake the movement. The magnetic field is generated by using variable electromagnets that can change the magnetic field strength to control the amount of braking. The electromagnet voltage is control by a desktop computer, using changes in the magnetic field to match the power output.

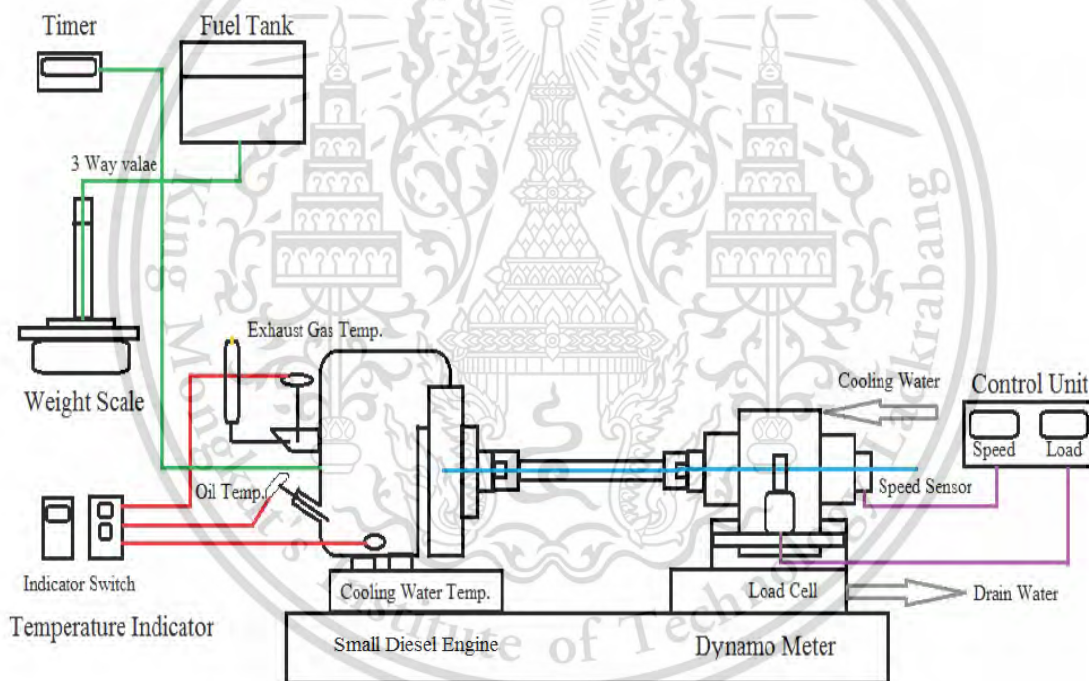


Figure 3.3 Schematic diagram of engine dynamometer

### 3.1.3. Fuel specification

The fuels chosen in this experiment has six fraction of biodiesel. Commercial grade diesel (B7) and Biodiesel were used as substrate for another fuel which are 20%, 40%, 60%, and 80% of biodiesel by volume called B20, B40, B60, and B80 respectively. The properties of substrate fuel are shown in Table 3-2 and Table 3-3.

Table 3-2 Conventional diesel fuel properties

Test Parameter	Result
Appearance	Clear & Bright
Calculated Cetane Index	55.5
Density, kg/m <sup>3</sup>	844.78
Heating value(kJ/kg)	45860
Bulk modulus(MPa)	1282
API Gravity @60 °F, Average, °API	38.0
API Gravity @60 °F, Upper, °API	38.1
Specific Gravity 15.6/15.6 °C, Upper	0.8344
API Gravity @60 °F, Middle, °API	38.0
Specific Gravity 15.6/15.6 °C, Middle	0.8347
API Gravity @60 °F Lower, °API	38.0
Specific Gravity 15.6/15.6 °C, Lower	0.8346
API Gravity @60 °F, Bottom, °API	38.0
Pour Point, °C	-3
Flash Point, (P.M.), Upper, °C	64
Flash Point, (P.M.), Lower, °C	66
Sulfur Content, mg/kg	68
Distillation :Initial Boiling Point, °C	178.3
Distillation :10 %Vol. Recovered, °C	214.3
Distillation :50 %Vol. Recovered, °C	281.5
Distillation :90 %Vol. Recovered, °C	352.3
Kinematic Viscosity at 40°C,mm <sup>2</sup> /s	3.092
Water and Sediment, % vol	<0.005
Gross Heat of combustion, BTU/lb	19,703
Methyl Ester of fatty Acid, % vol.	4.7

Table 3-3 Biodiesel fuel properties

Test Parameter	Result
Methyl Ester, %wt	97.9
Density at 30°C, kg/m <sup>3</sup>	864.1
Heating value(kJ/kg)	39890
Bulk modulus(MPa)	1482
Viscosity at 40°C, cSt	4.5
Flash Point, °C	184.5
Sulphur Content, %wt	< 0.0001
Carbon, on 10% distillation residue, %wt	< 0.1
Cetane Number	68.2
Sulphated Ash, %wt	< 0.001
Water, %wt	0.028
Total Contaminate, %wt	0.0003
Copper Strip Corrosion, %wt	1a
Oxidation Stability at 110 °C, hr	26.3
Acid Value, mgKOH/g	0.1
Iodine Value, gI <sub>2</sub> /100g	51.5
Linolenic Acid Methyl Ester, %wt	0.18
Methanol, %wt	0.03
Monoglyceride, %wt	0.31
Diglyceride, %wt	0.05
Triglyceride, %wt	0.01
Free Glycerin, %wt	0.00
Total Glycerin, %wt	0.09
Group I metals, mg/kg	0.39
Group II metals, mg/kg	0.69
Phosphorus, %wt	<0.00001
Additive	No
Appearance	Clear
Cloud Point, °C	14.0

### 3.1.4. Black smoke meter

Particulate matter emitted from engine combustion is measured in black smoke percentage. The smoke meter is applied to measure the concentration between particulate matter in exhaust gas before the filter and remaining after trapping in particulate filter by light emitting method. The zero percentage black smoke mean that is no particulate on filter and the other hand 100 percentage is mean the filter is covered by particulate all of area. This smoke meter percentage can be summarized that the filtration efficiency of particulate filter. However, the smoke meter, Okuda DSM - 240, is shown in Figure 3.4 which is used in investigation of particulate matter concentration and particulate filter efficiency.



Figure 3.4 smoke meter and paper filter

### 3.1.5. Pressure sensor

To measure the pressure in the combustion chamber this research choose “Kistler 6052C31” which can measure up to 250 bar mounted on the cylinder head”. This sensor is piezoelectric crystal which achieves high sensitivity.



Figure 3.5 pressure sensor

### 3.1.6. Crank encoder

Tracing the position of crank angle by using an optical crankshaft encoder is cost-efficient and convenient, as long as the signal is well calibrated. Nowadays, this type of shaft encoder usually generates at least two different signals: one is position identifying normally with a frequency of one pulse per revolution; the other one is the crank-angle marking signal.

To measure crankshaft position for calculate combustion chamber volume, “CA-RIE-360” encoder was chosen and mounted on the end of brake shaft for serviceability. 360 pulses per revolution so the resolution is 1 degree. The function is based on transmission light principle. An infrared beam is emitted and received at the sensor unit. The customized marker disk (with slits) is mounted in-between the sensors gate. The slits will interrupt the infrared beam, the receiver transforms the light to voltage signal.



Figure 3.6 crank encoder

### 3.1.7. Data acquisition system

For understanding the combustion inside an engine cylinder, many researchers work on either experimental tests or computer model simulations. Because of booming computing technology and growing hardware ability, mathematic simulations methods have become increasingly popular and economic. However, an experimental result is the fundamental validation measure for complex mathematic models, hence it is necessary and needs to be accurate and reliable, moreover, easy and efficient.

The pressure in combustion chamber and crank angle position data was kept by data acquisition system. The hardware which used in the experiment were SIRIUSi Custom with CHG and CHG+ as shown in Figure 3.7. And the software were DEWESoft X2 SP8 as shown in Figure 3.8 which can calculate many parameter in real time such as combustion chamber volume in that moment, heat release rate, IMEP, PMEP, and etc.



Figure 3.7 data acquisition hardware



Figure 3.8 DEWESoft X2 software

This material is reserved for educational use only, not allowed for commercial use.

Forbidden to modify the content, and cite the document when use.

### 3.2. Experiment condition

Table 3-4 Experiment condition

Experiment	Engine load (%)	Engine speed	Fuel
Particulate matter quantities	0,20,40,60,80,100	1600,1800...2400	commercial diesel B20 B40 B60 B100
SEM, TEM, Optical			
Particulate matte size distribution	80	2400	
BSFC,BSEC,Thermal efficiency	20,50,80	2400	
combustion characteristic	100	1400,1500....2600	

### 3.3. Experiment procedure

#### 3.3.1. Particulate matter quantities

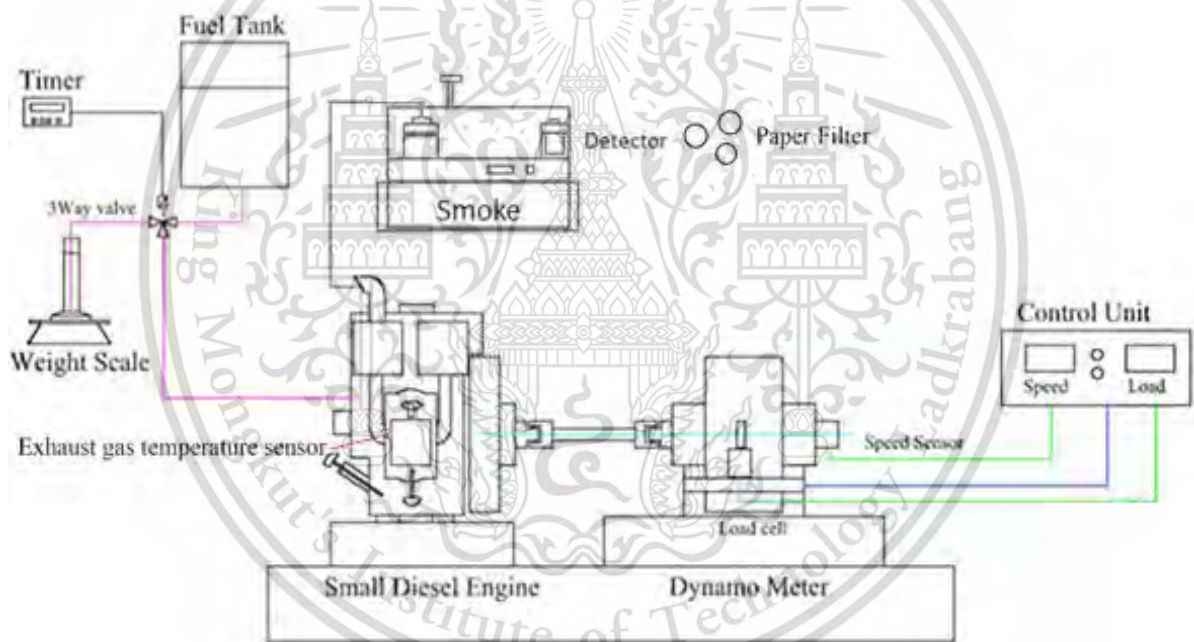


Figure 3.9 Schematic diagram of particulate matter quantity measurement

### 3.3.2. Particulate matter size distribution

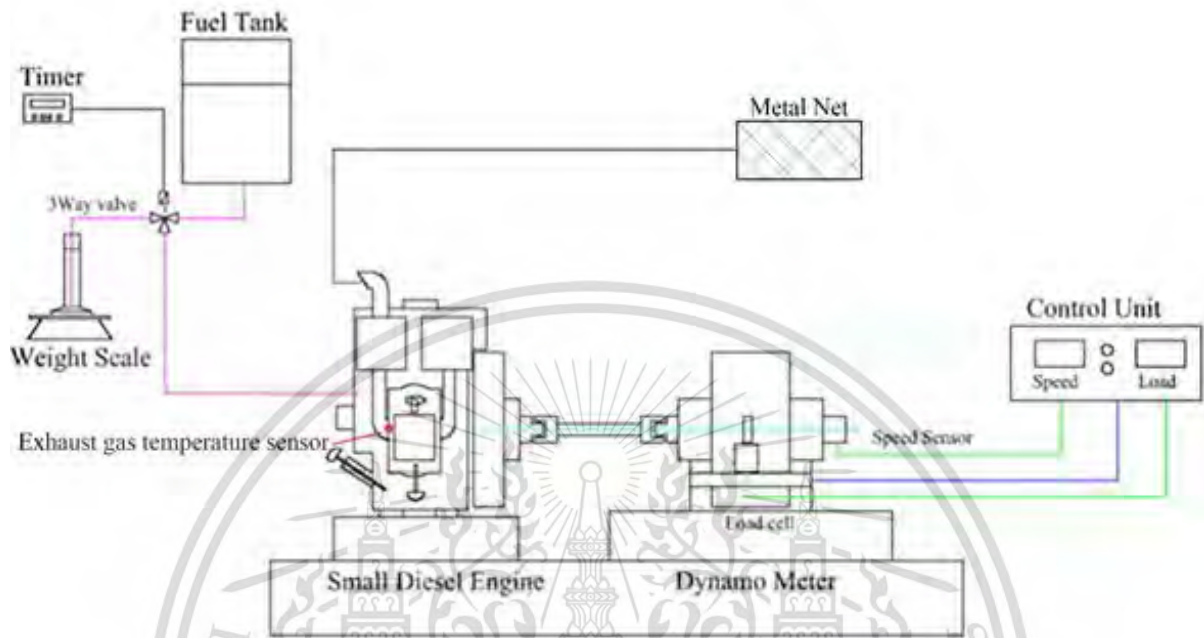


Figure 3.10 Schematic diagram of particulate matter trapping

### 3.3.3. Combustion analysis

The raw data from data acquisition start from pressure at each crank angle. It's collect 720 engine cycle for each engine condition and then calculate to find the average pressure of each crank angle as shown in "Figure 3.12".

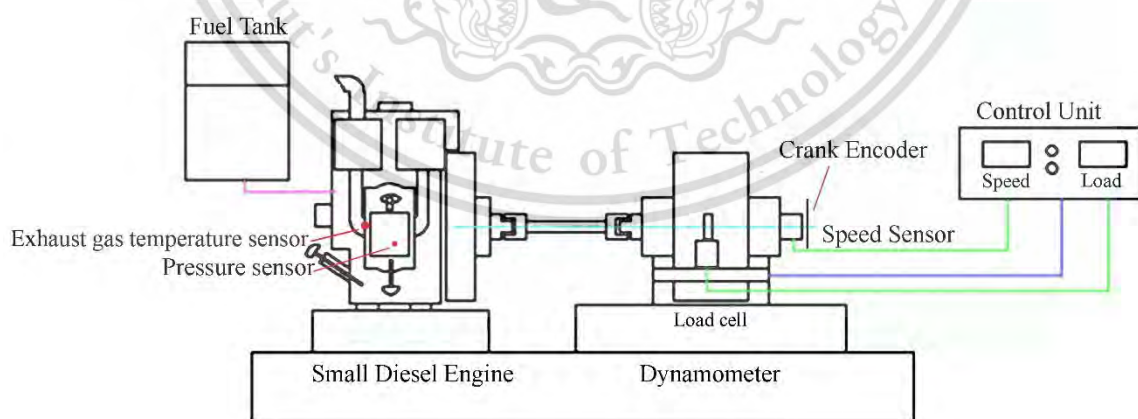


Figure 3.11 Schematic diagram of tested small CI engine operation on dynamometer for combustion characteristic

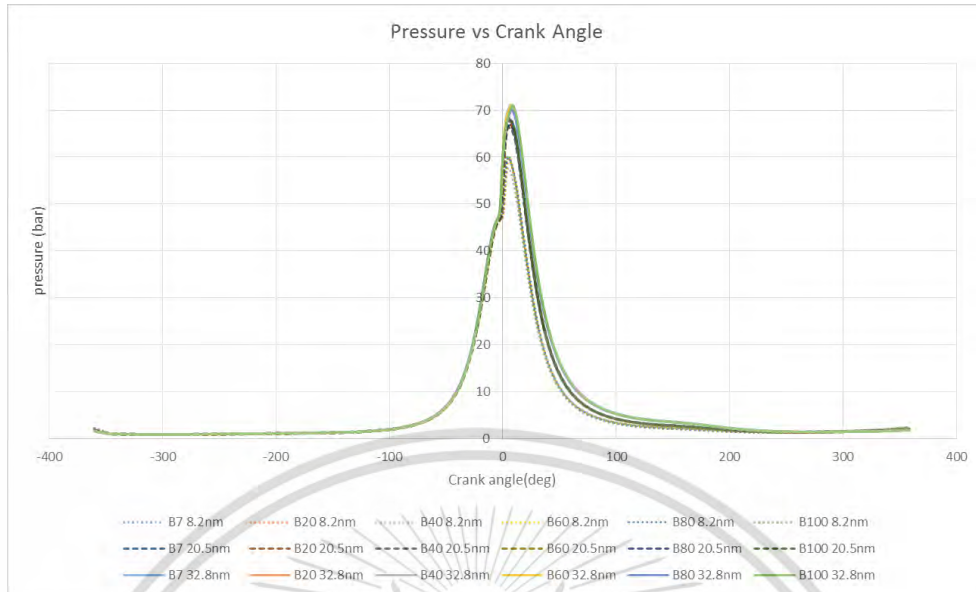


Figure 3.12 Pressure-crank angle diagram

After get the data in “Figure 3.12” then calculate the volume at each crank angle and will get a Pressure-volume diagram as shown in “Figure 3.13”. For the rate of heat release can calculate follow the “Equation 3-1” and calculate integrated heat release follow “Equation 3-2”.

$$TQ_i \text{ [kJ/m}^3\text{/}^\circ\text{CA]} = \frac{1}{\kappa - 1} \cdot [\kappa \cdot P_i \cdot (V_{i+1} - V_{i-1}) + V_i \cdot (P_{i+1} - P_{i-1})]$$

*i* ... measurement point

$\kappa$  ... polytropic exponent (user input)

*V* ... volume

*P* ... pressure

Equation 3-1 Heat release TQ calculation

$$TI_i \text{ [kJ/m}^3\text{]} = TQ_i + TI_{i-1}$$

*i* ... measurement point

Equation 3-2 Integrated heat release TI calculation

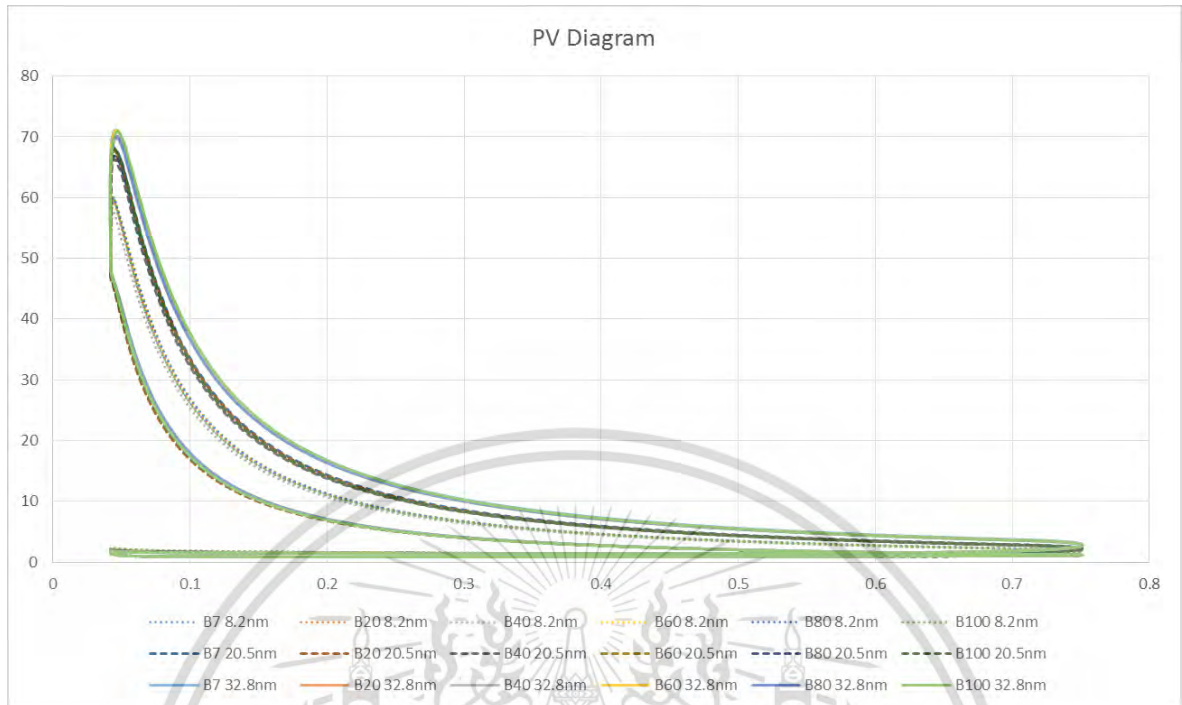


Figure 3.13 Pressure-volume diagram

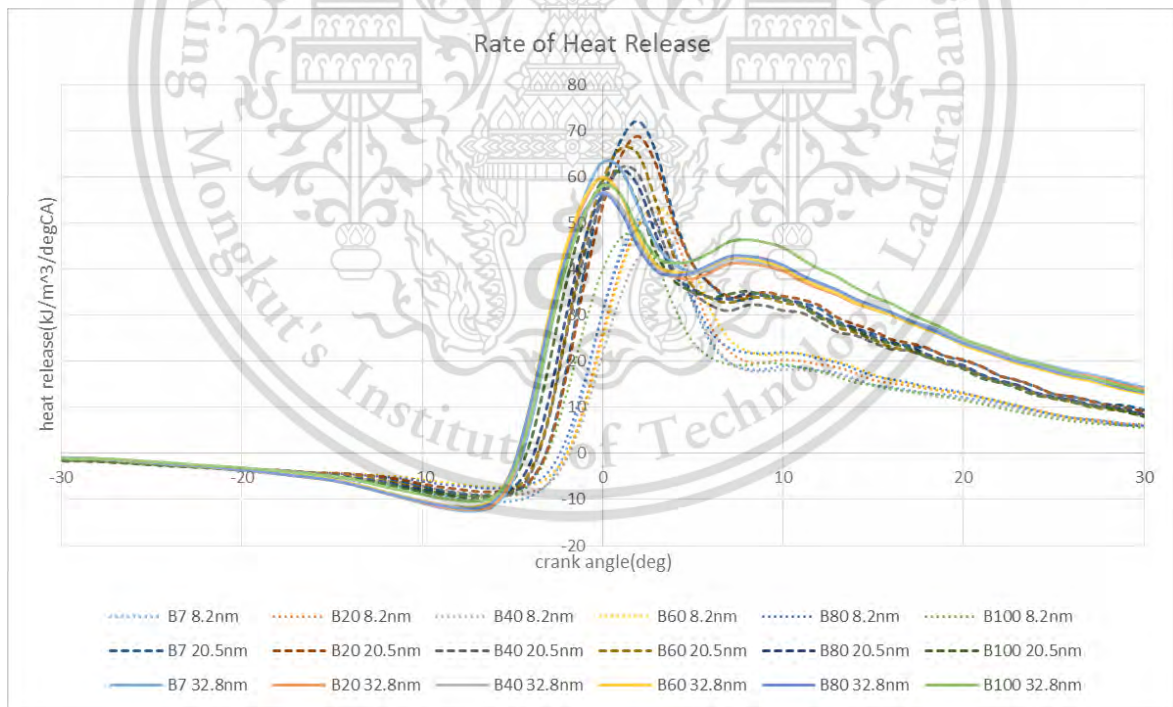


Figure 3.14 Rate of heat release

The combustion process which will be consider separate into 3 zone. The first is vaporization which fuel and air is mixing and absorb energy due to fuel

change the phase from liquid to gas. The second is premix combustion which is start of combustion. And the last process is mixing control combustion which still combust due to continuous fuel injection.

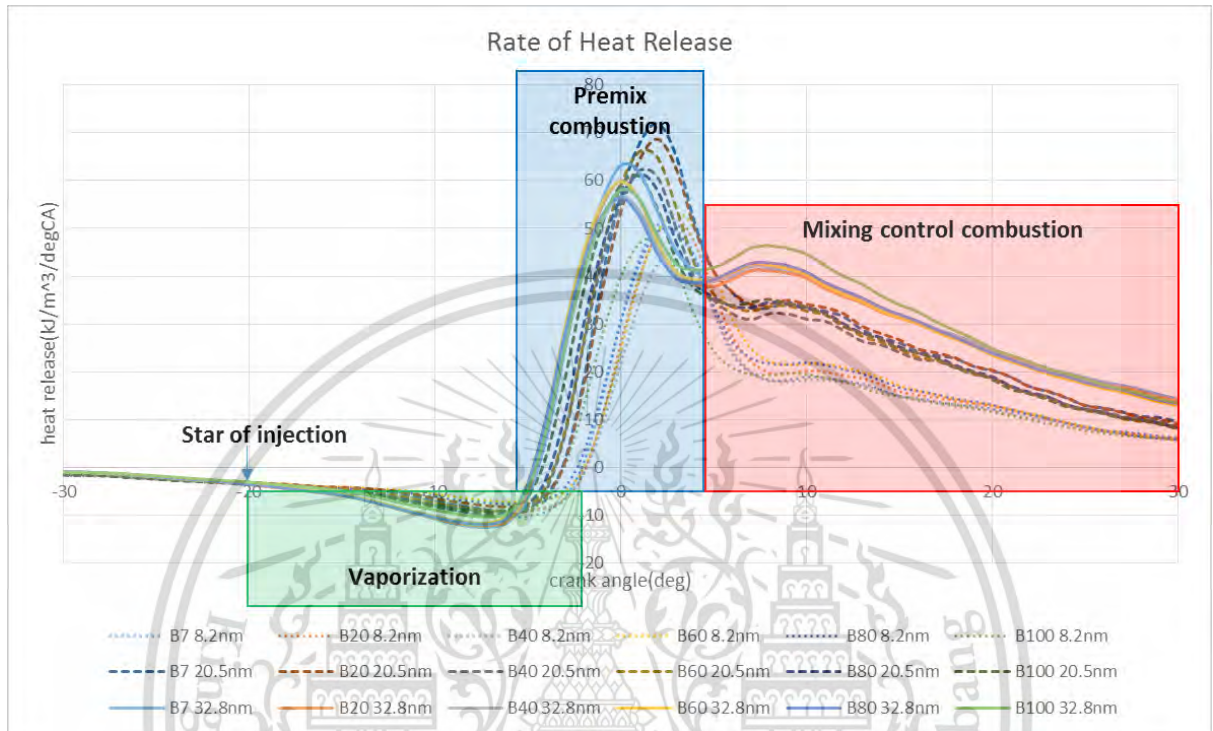


Figure 3.15 Combustion process

Mass fraction burn (MFB) is calculated from integrated heat release divide by total heat release.

Start of combustion (SOC) is defined when the integrated heat release crosses 0% (Due to the injection of diesel fuel the integrated heat release goes negative first)

End of combustion (EOC) is defined where integrated heat release reaches 95%.

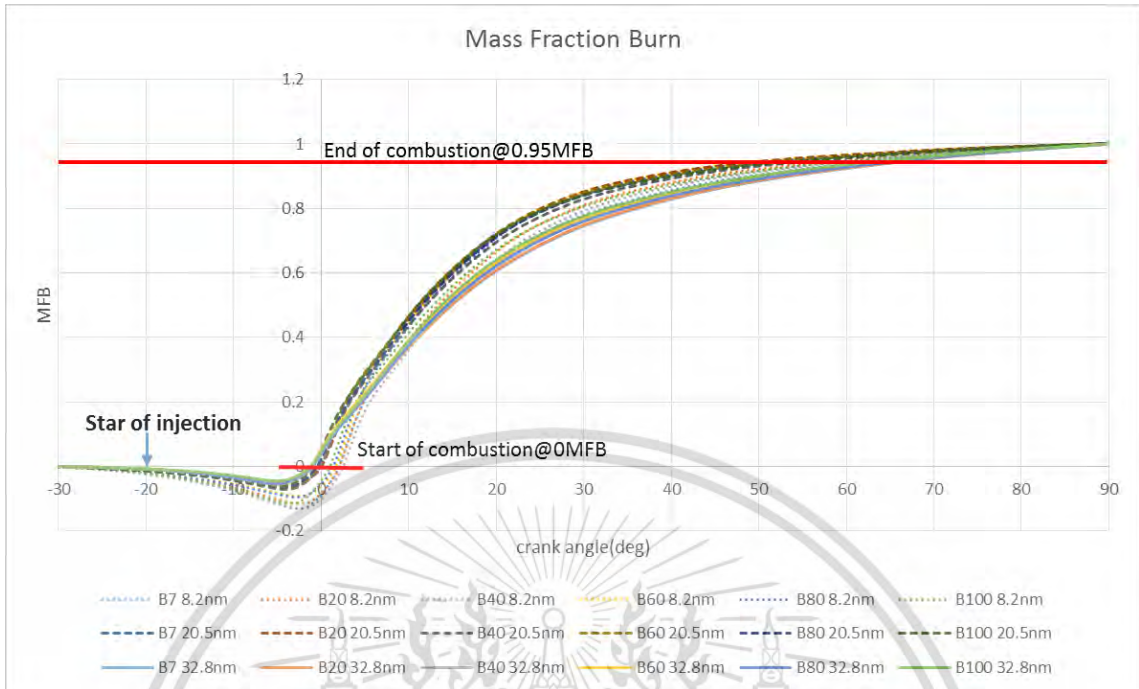


Figure 3.16 MFB, SOC, EOC

## Chapter 4

### RESULTS AND DISCUSSION

#### 4.1. Fuel properties

When compare the fuel properties between commercial diesel and biodiesel fuel, it has many parameter which have the effect with the combustion but for the main different properties are shown in "Table 4-1".

The higher viscosity of biodiesel make less amount of fuel injected in each cycle and worse air-fuel mixed together [27]. The density, biodiesel have higher value which promote more amount fuel per cycle. So when the viscosity and density can be compensated in term of amount of fuel in each cycle. But the heating value of biodiesel it has less than diesel approximately 13 percent so in the same load condition biodiesel must injected more mass per cycle to compensate the lower heat output which fuel consumption should be worse. The chemical formula show that biodiesel has Oxygen atom in fuel which call oxygenate fuel, it would be promote the better combustion. The carbon fraction show that commercial diesel which has higher value, should emitted more PM [28].

Table 4-1 summary of fuel properties

Fuel properties	Diesel	Biodiesel
Viscosity (centistokes)	3.32	4.44
Density (kg/m <sup>3</sup> )	823	862
Heating Values (kJ/kg)	45860	39890
Chemical Formula	C <sub>16.17</sub> H <sub>32.00</sub>	C <sub>15.26</sub> H <sub>29.48</sub> O <sub>1.70</sub>
Carbon Fraction	85	76
Auto ignition temperature(degC)	288	294

Distillation curve Figure 4.1 below shows the relationship between temperature and percentage of fuel volume which change from liquid to gas phase. Biodiesel is more homogeneous fuel which shown by vaporize temperature. It is very narrow around 340 to 350 degree Celsius. When compare with conventional fuel, biodiesel has higher vaporization temperature due to heavier atomic weight and higher density Table 3-2 and Table 3-3 so the heat of vaporization of biodiesel should be higher than conventional diesel.

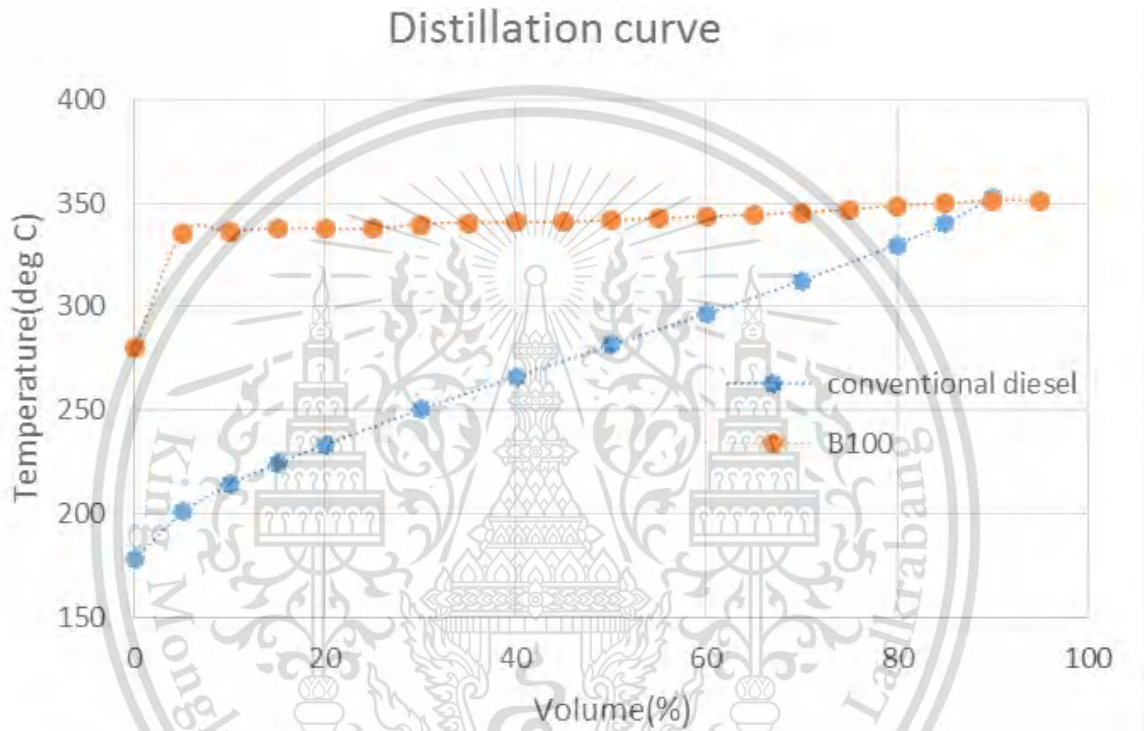


Figure 4.1 Distillation of conventional diesel and biodiesel fuel

Fuel composition in

Figure 4.2 and Figure 4.3 clearly show that biodiesel is oxygenate fuel due to high concentration of oxygen in the fuel. It should provide high oxidative reaction during the initial stage of oxidation.

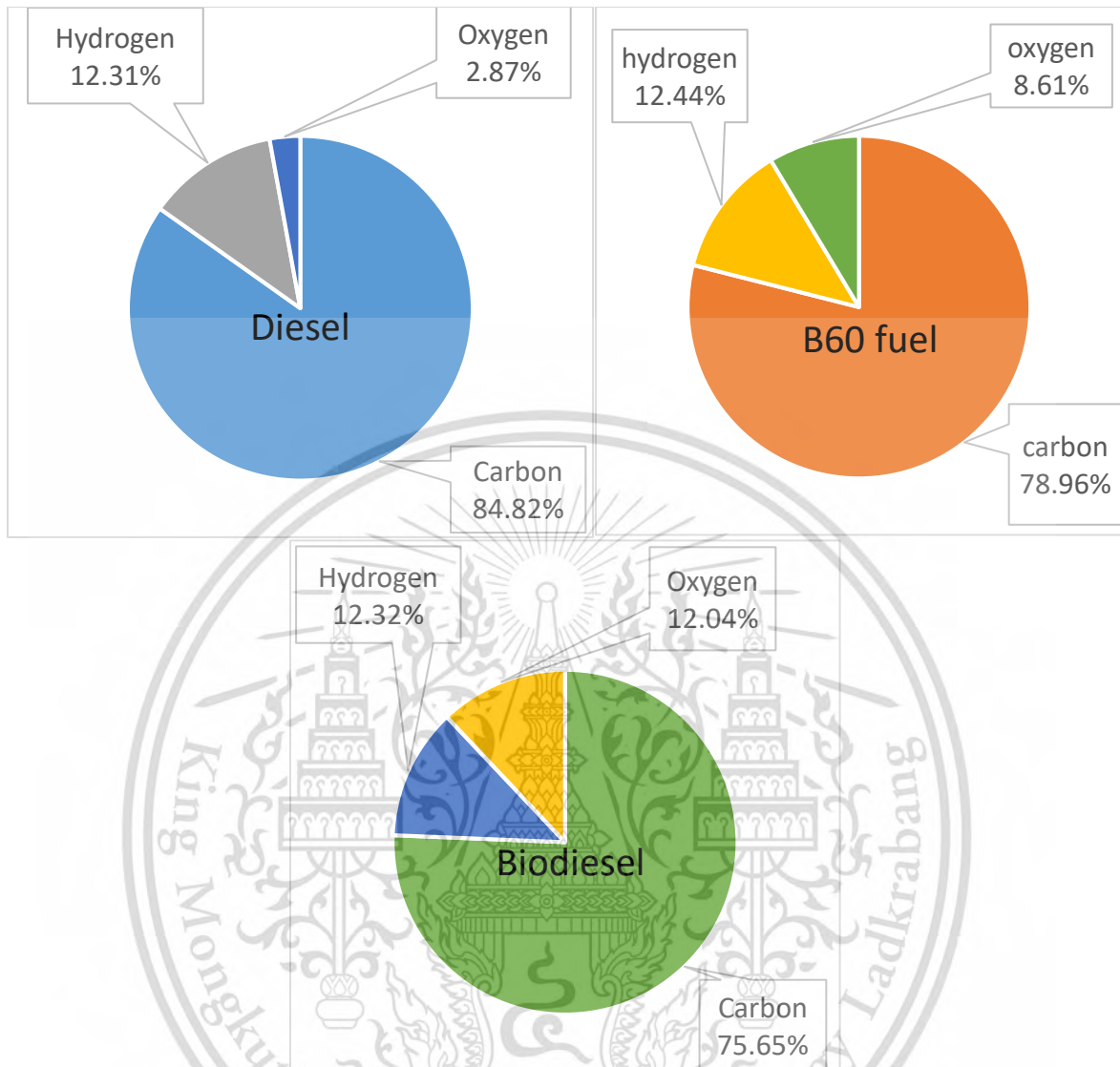


Figure 4.2 Diesel, B60, and Biodiesel fuel composition from CHNS/O analyzer

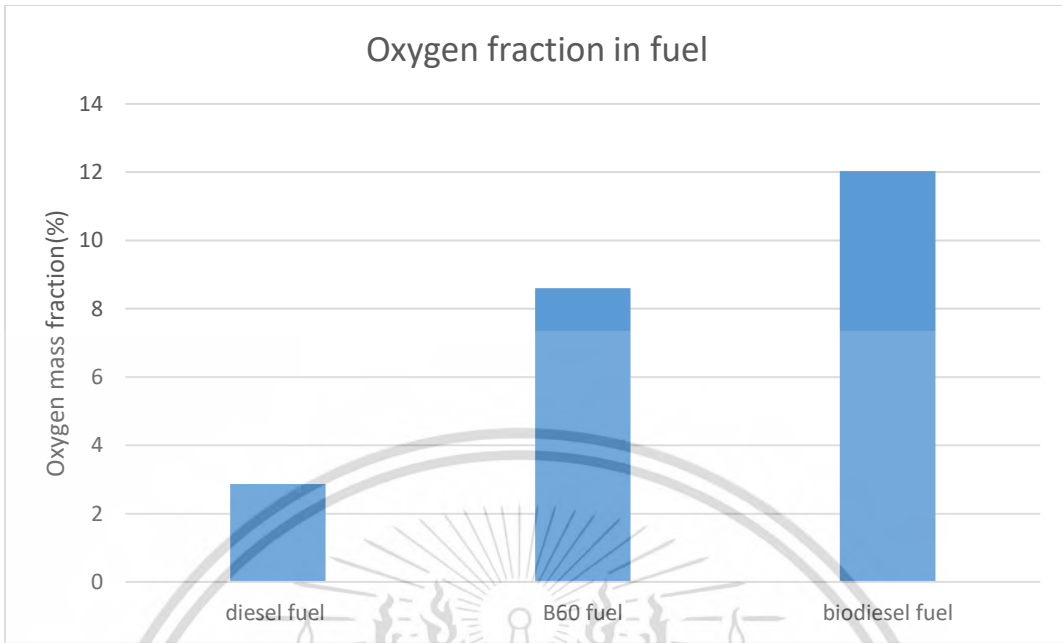


Figure 4.3 Oxygen mass fraction of fuel

#### 4.2.Engine performance

##### 4.2.1. Engine performance, efficiency, and exhaust temperature

The different fuel properties which biodiesel has lower heating value and worse air fuel mixing than diesel due to higher viscosity. However biodiesel which is oxygenate fuel, can perform very well in term of engine performance that doesn't have significant different in every fuel concentration.

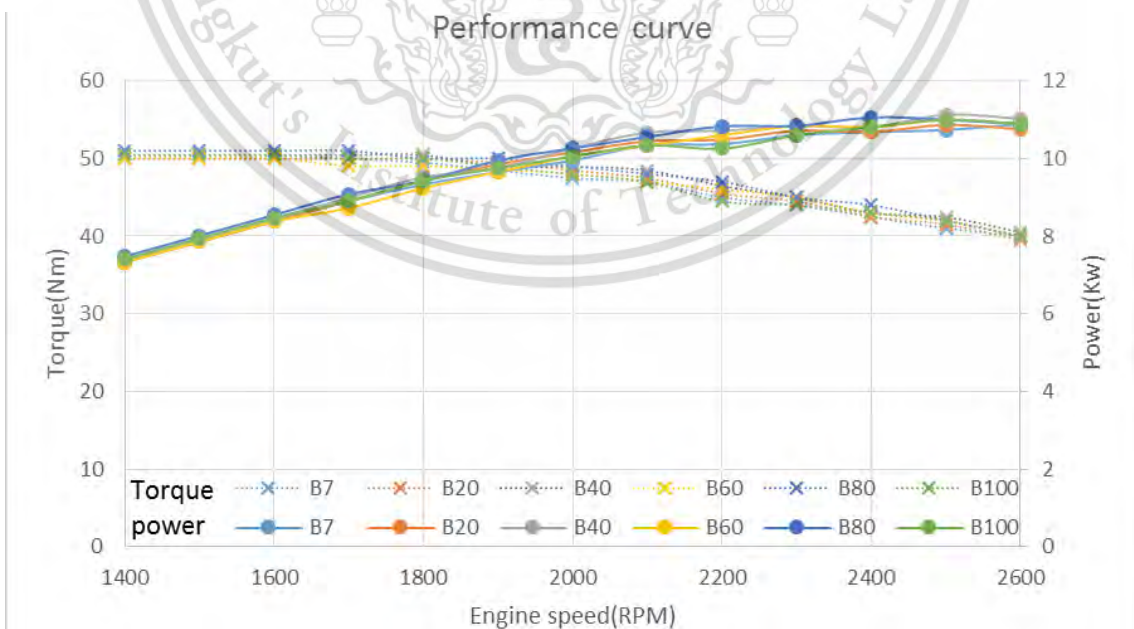


Figure 4.4 Engine performance curve

From the experiment result Figure 4.5 has shown when increase content of biodiesel, brake specific fuel consumption (BSFC) significantly increase around six percent. When engine dynamometer try to control the same power output of each fuel, biodiesel which has lower heating value have to inject more amount of fuel to compensate the lower energy output.

Although biodiesel has a worse brake specific fuel consumption but when consider on brake specific energy consumption (BSEC), trend is decrease inversely proportional with content of biodiesel. According to biodiesel is an oxygenate fuel which can combust more completely. So the thermal efficiency is increase and energy demand to create the power output is decrease.

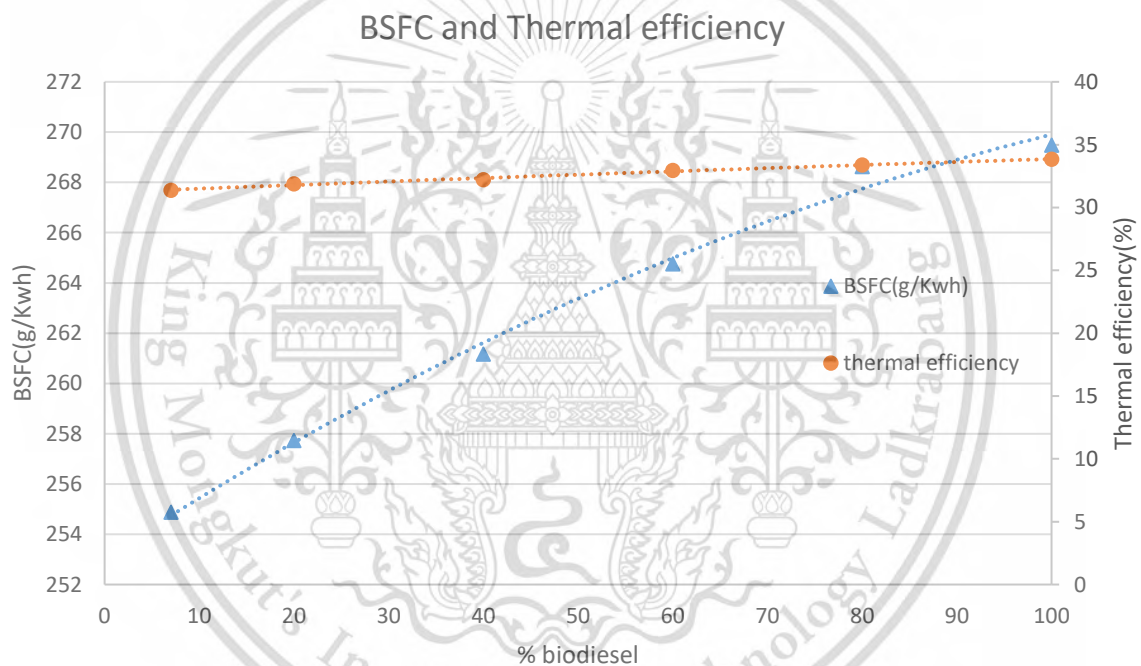


Figure 4.5 Brake specific fuel consumption and brake specific energy consumption at 80% load and 2400 rpm

Trend of exhaust gas temperature Figure 4.6 is inversely proportional with biodiesel fraction. Due to two reason, first is distillation curve in Figure 4.1 which biodiesel start to change their phase from liquid to gas phase at higher temperature than conventional diesel. And mass of biodiesel which use for combustion per cycle is more than conventional diesel from BSFC in Figure 4.5. It mean in the combustion reaction biodiesel have to absorb much more energy than conventional diesel to change their phase before combustion process. And

the second reason is Biodiesel has higher cetane number thus the advance combustion (premixed combustion phase) should be found lead to the shorter combustion duration lead to the lower temperature with biodiesel fuel blends. From those reason, the higher content of biodiesel, the lower exhaust gas temperature.

The research of S.Srihari et al.,[23] , the reason of lower EGT for biodiesel is” Early start of the combustion due to shorter premixed combustion phase and lower calorific value can also lead to reduction in exhaust gas temperature as is seen for the DEE blends[24].” And it has some other research which get biodiesel EGT lower than diesel as well such as [25] and [26].

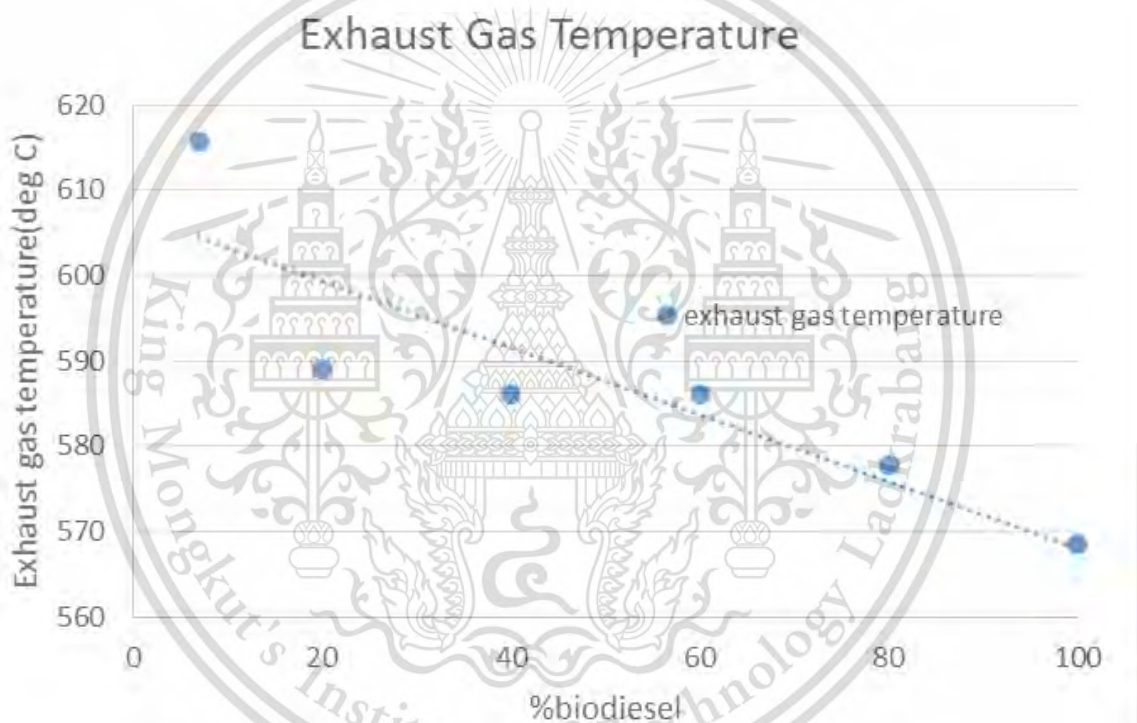


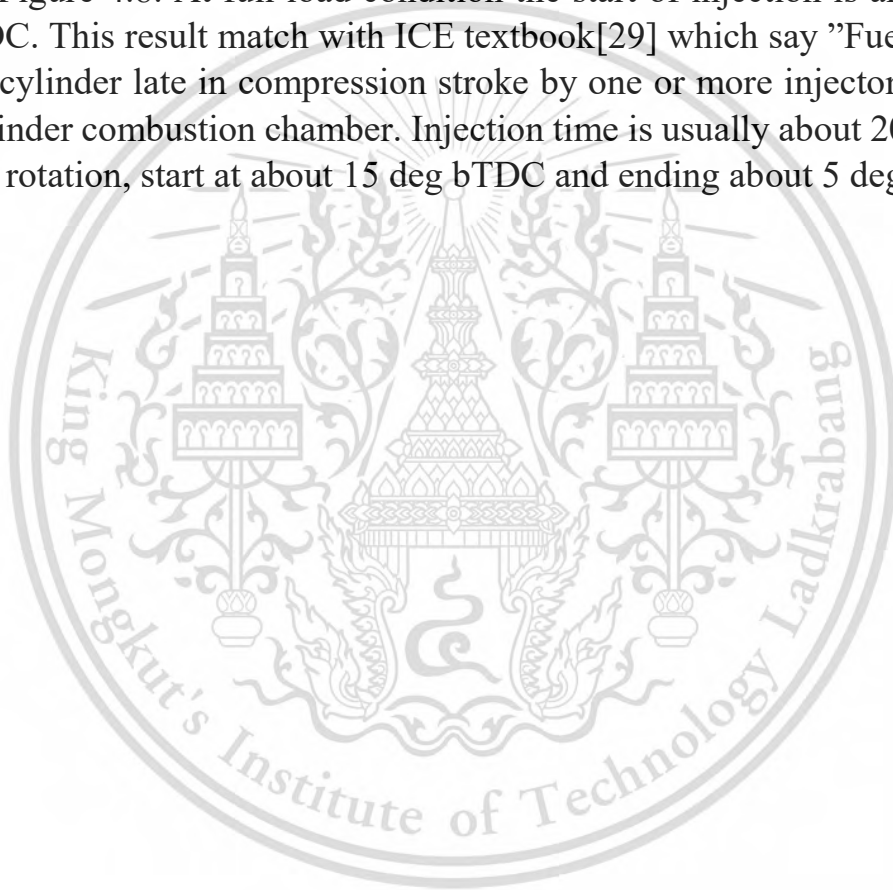
Figure 4.6 Exhaust gas temperature at 80% load and 2400rpm on each fuel

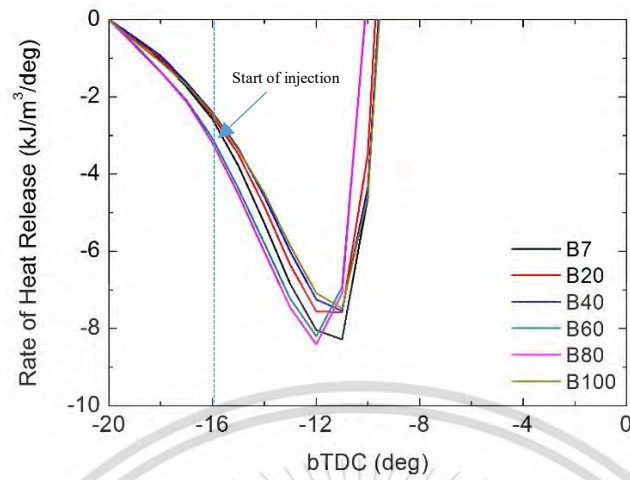
### 4.3. Combustion characteristic

Combustion characteristic is separated the analysis into three part, the effect of engine load, engine speed, and fuel type. And the raw data are shown in section0-0.

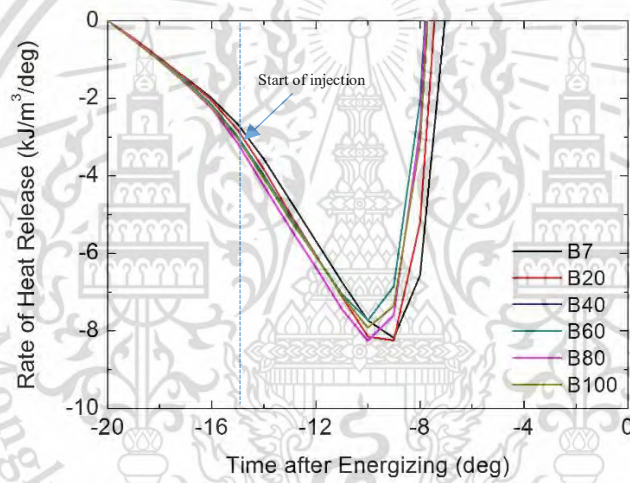
#### 4.3.1. Injection timing

From the engine specification (see appendix B-2), the stat of fuel injection is at 17.5-19.5 bTDC but in PV diagram the start of injection point is the point which slope change rapidly due to fuel start to vaporize which shown in Figure 4.7 and Figure 4.8. At full load condition the start of injection is around 14-16 deg bTDC. This result match with ICE textbook[29] which say "Fuel is injected into the cylinder late in compression stroke by one or more injectors located in each cylinder combustion chamber. Injection time is usually about 20 deg bTDC of crank rotation, start at about 15 deg bTDC and ending about 5 deg aTDC"

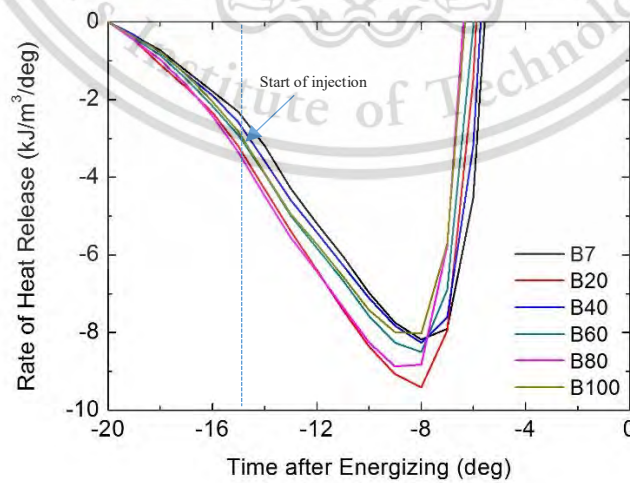




(a)



(b)



(c)

Figure 4.7 Actual injection timing from heat release rate approximate 14-16 deg bTDC at full load (a) 1600rpm, (b) 2000rpm, (c) 2400rpm

This material is reserved for educational use only, not allowed for commercial use.

Forbidden to modify the content, and cite the document when use.

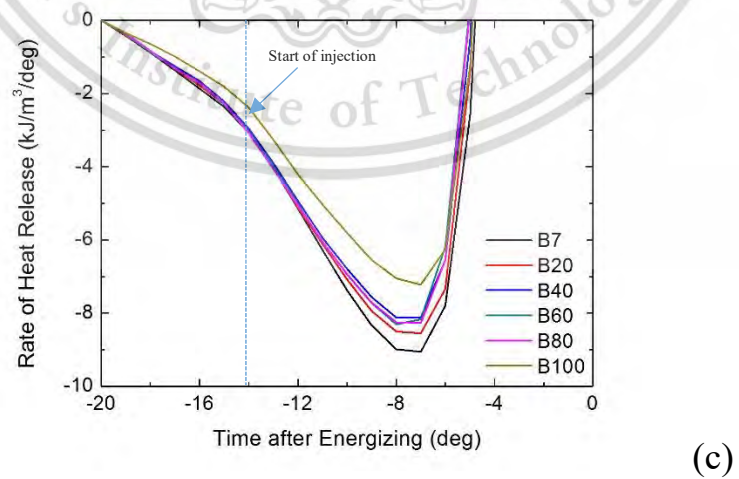
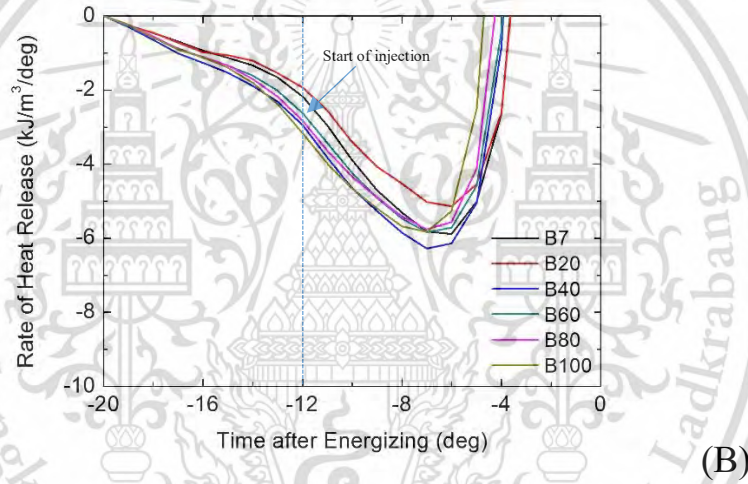
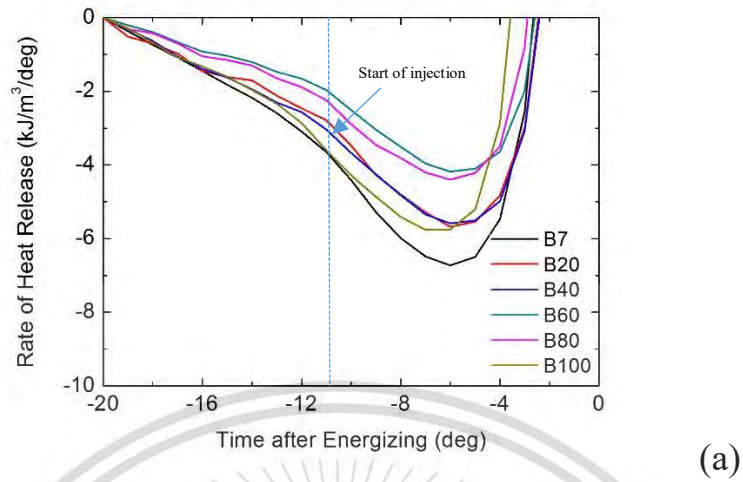


Figure 4.8 Actual injection timing from heat release rate at partial load 2400rpm  
(a)20% load, (b)50% load, (c)80% load at 2400 rpm

This material is reserved for educational use only, not allowed for commercial use.

Forbidden to modify the content, and cite the document when use.

### 4.3.2. Effect of engine load

The effect of engine load, because of higher engine load need more amount of fuel to combust and convert to energy output. The more amount of fuel the more pressure occur in the combustion chamber Figure 4.9. For the heat release analysis, higher load make shorter ignition delay in Figure 4.10 and Figure 4.11. The start premix combustion phase ignite earlier in Figure 4.10. The mixing control phase is more clearly see on higher load because of remaining fuel still burning. In Figure 4.11 the higher load, the higher total heat because of longer injection duration. And the trend for different fuel and different engine speed is similar to this mechanism.

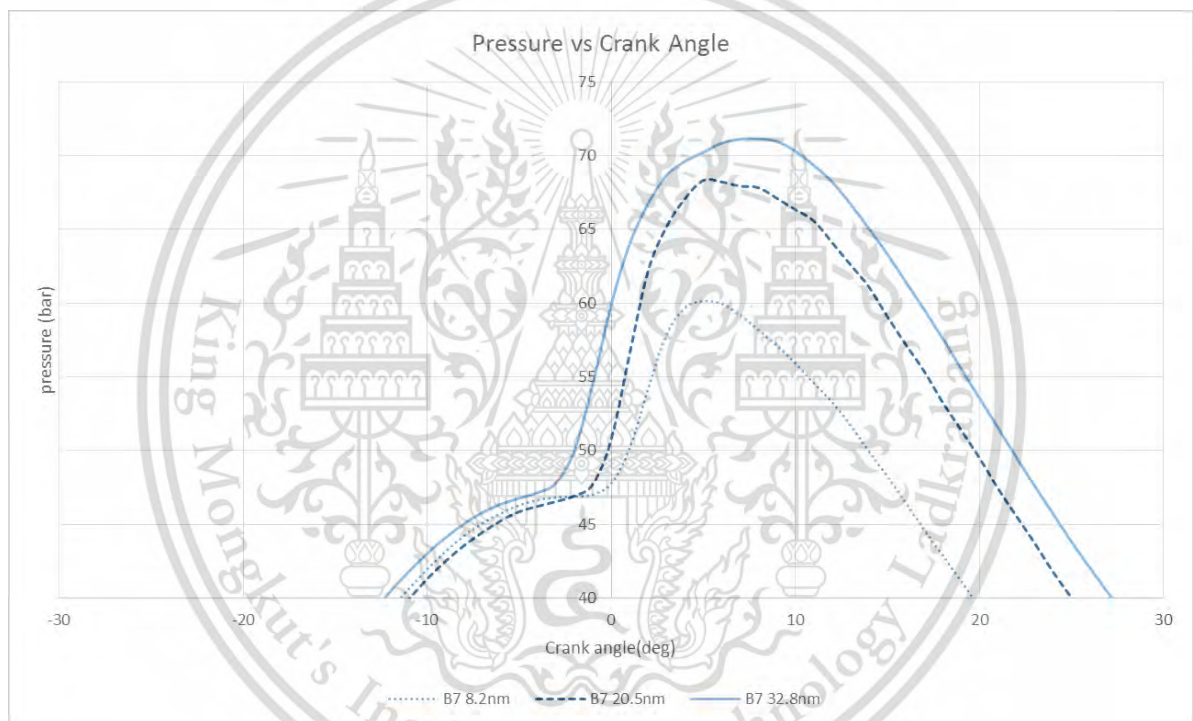


Figure 4.9 Pressure-crank angle diagram of B7 on different engine load

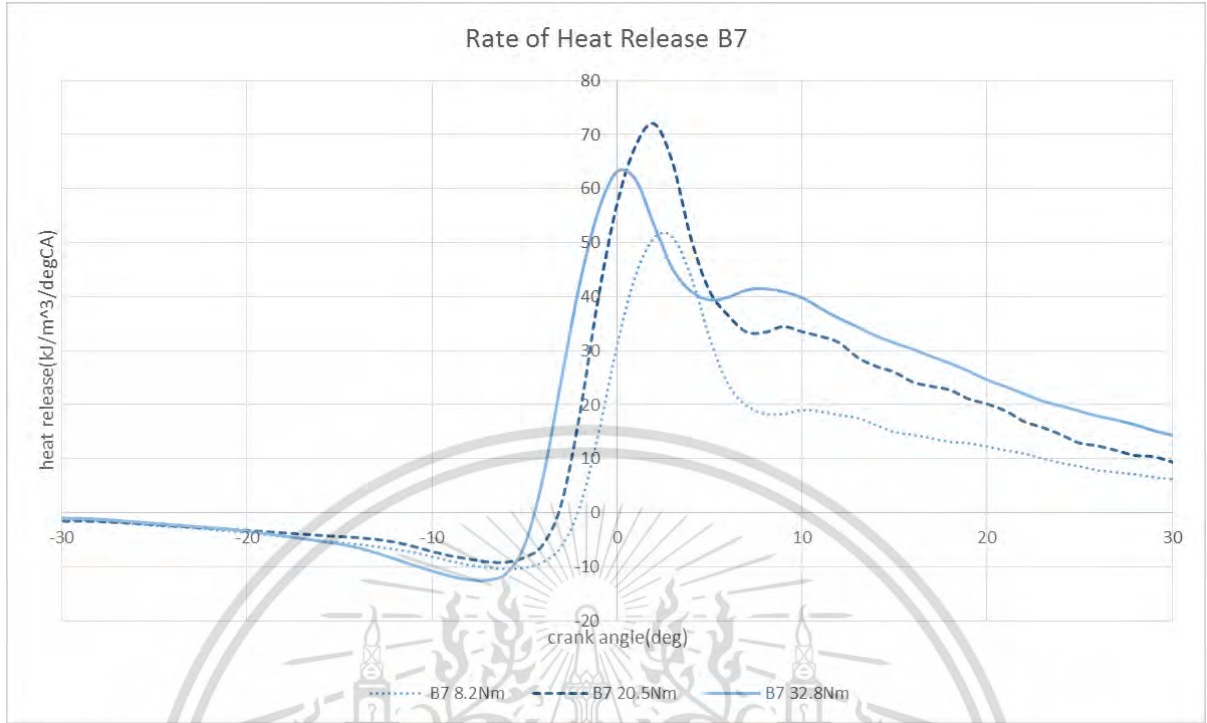


Figure 4.10 Rate of heat release of B7 on different engine load

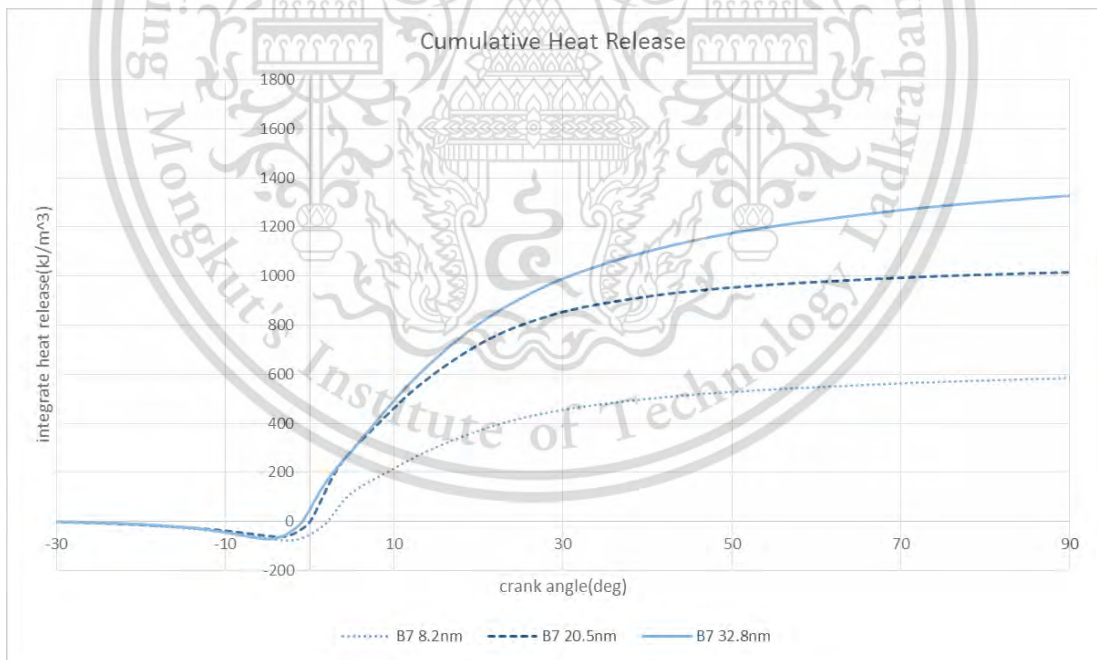


Figure 4.11 Cumulative heat release of B7 on different engine load

### 4.3.3. Effect of engine speed

In Figure 4.12, due to faster engine speed, it make the crankshaft rotate further in the same amount of time. If assume the ignition delay time is constant in every engine speed, the lowest engine speed will start to ignite first because crankshaft can rotate just a few angle in the same amount of time and then faster engine speed will ignite respectively. The phase of combustion in low engine speed is quiet difficult to identify because two peak of heat release is very close due to crankshaft rotate just a few degree in the same amount of time so it look like it has only one step of heat release. The characteristic of engine speed is similar in different type of fuel.

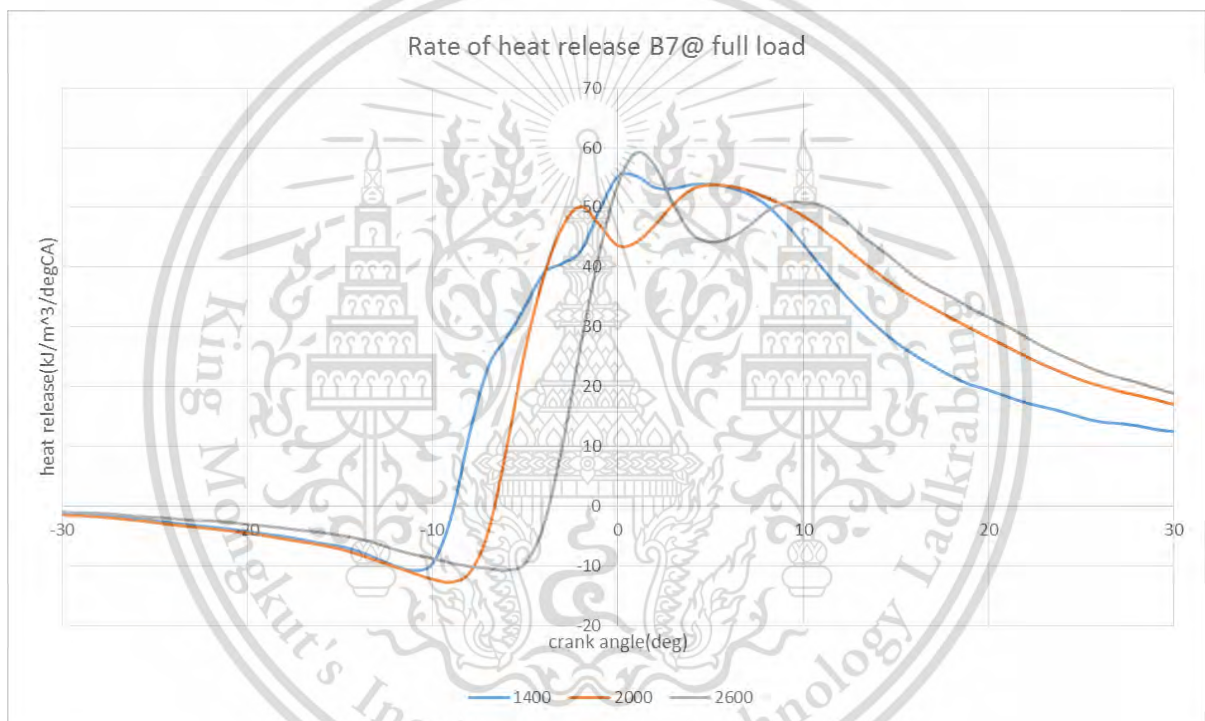


Figure 4.12 Rate of heat release of B7 on different engine speed

#### 4.3.4. Effect of fuel type

Biodiesel which is oxygenate fuel has a shorter ignition delay in every engine load condition and engine speed even though diesel fuel which has lower viscosity can mix with the air better than biodiesel.

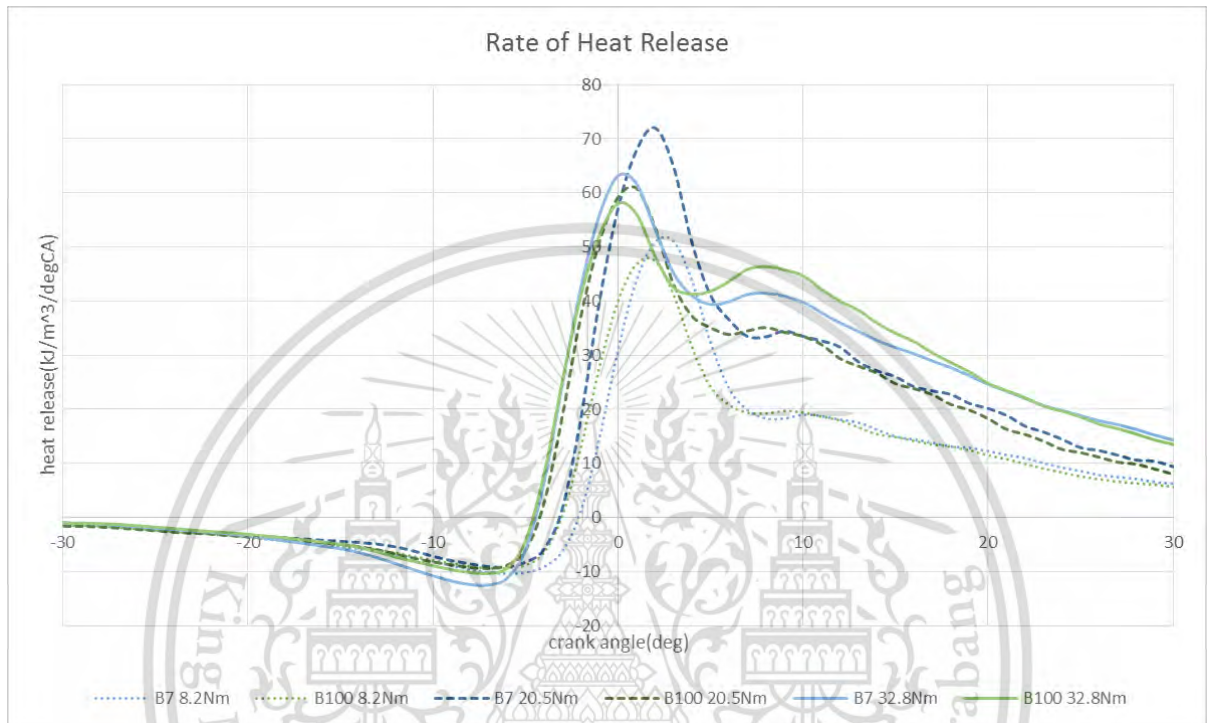


Figure 4.13 Rate of heat release of B7 on different fuel type and engine load

## 4.4. Particulate matter

### 4.4.1. Particulate matter quantities

Figure 4.14-Figure 4.19 show smoke intensities of each fuel, engine load, and engine speed. Conventional diesel emitted the highest amount of smoke. The PM reduced by concentration of biodiesel due to oxygenate fuel. It was clearly observed that biodiesel engine's particulate matter was approximately a half of conventional diesel engine's particulate matter. When increase engine load, smoke intensity increased because more fuel was supplied to the engine. For engine speed it has a little different amount of smoke due to the engine efficiency of each engine speed. The lowest amount of smoke in each engine load usually occurs around 1800-2000rpm. When increase concentration of biodiesel, trend of engine speed which emitted lowest particulate matter(in the same load) shift to faster engine speed because bio diesel has a faster chemical reaction rate due to Biodiesel is oxygenate fuel which has oxygen in their molecule.

In addition, when operating at high engine speed, particulate matter was increase because of shorter oxidation time in combustion period.

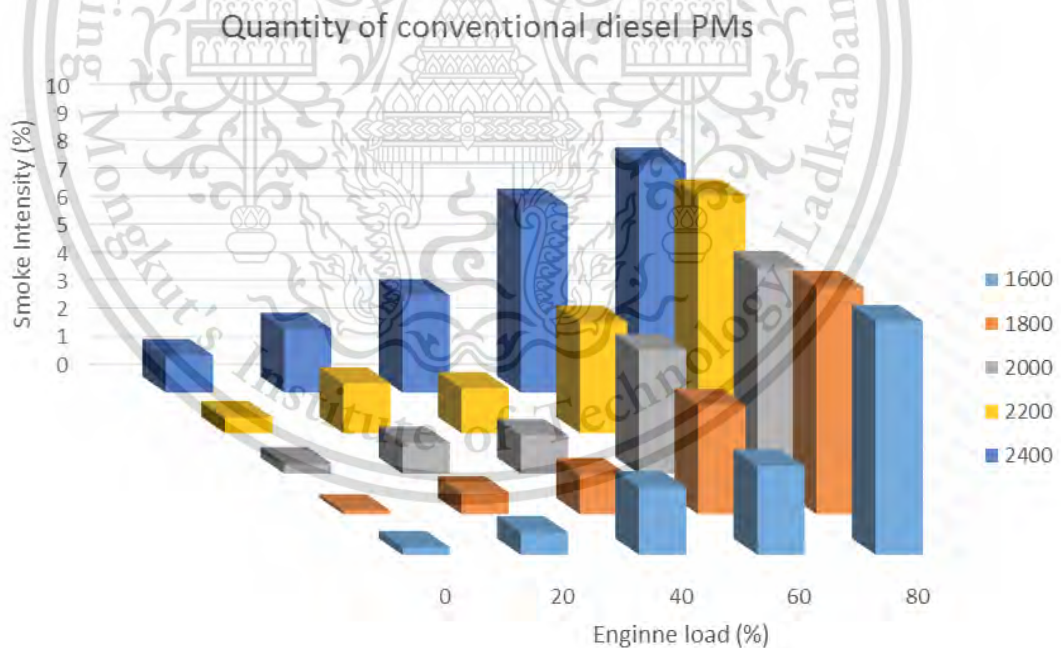


Figure 4.14 Smoke intensity of conventional diesel

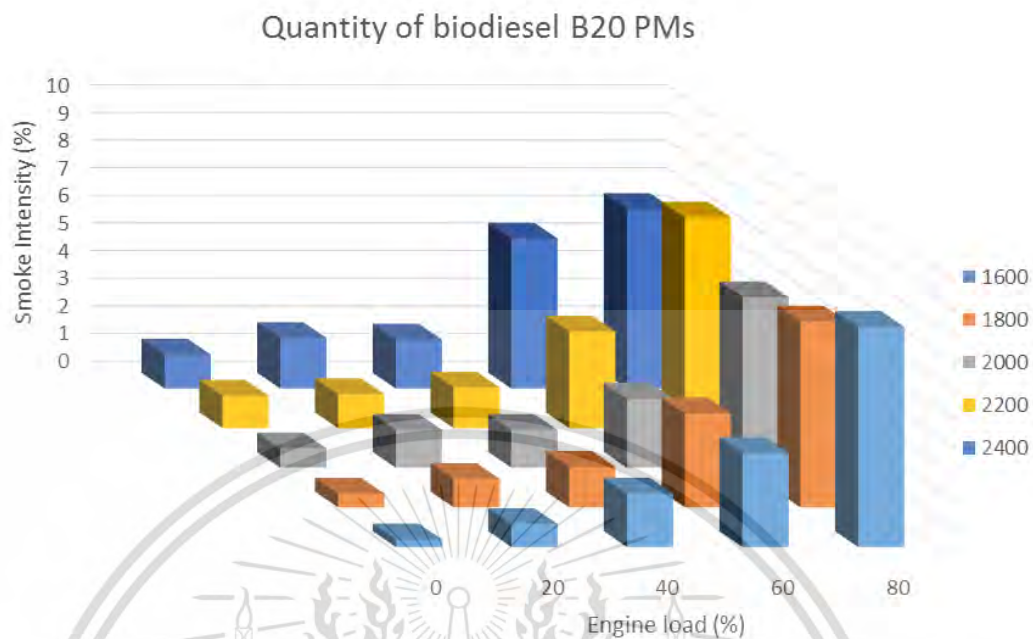


Figure 4.15 Smoke intensity of B20

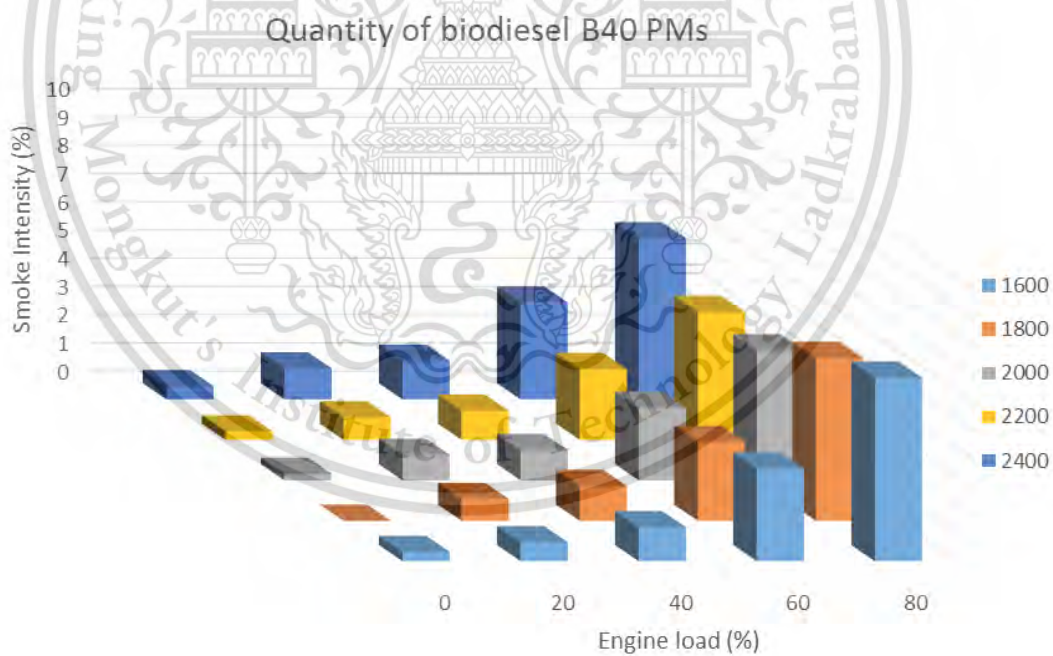


Figure 4.16 Smoke intensity of B40

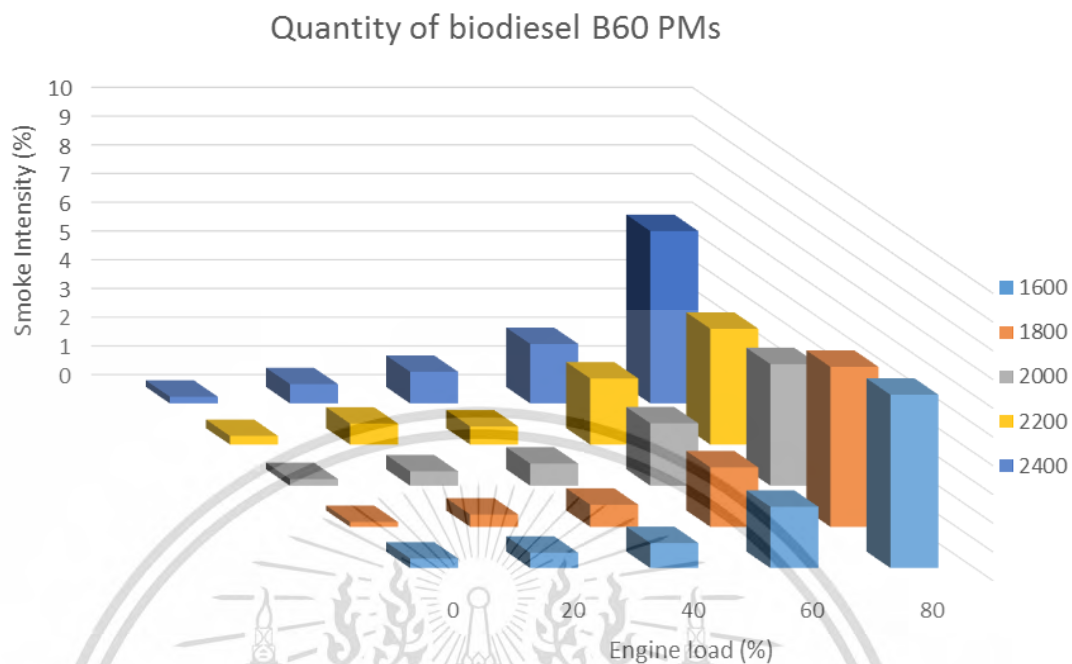


Figure 4.17 Smoke intensity of B60

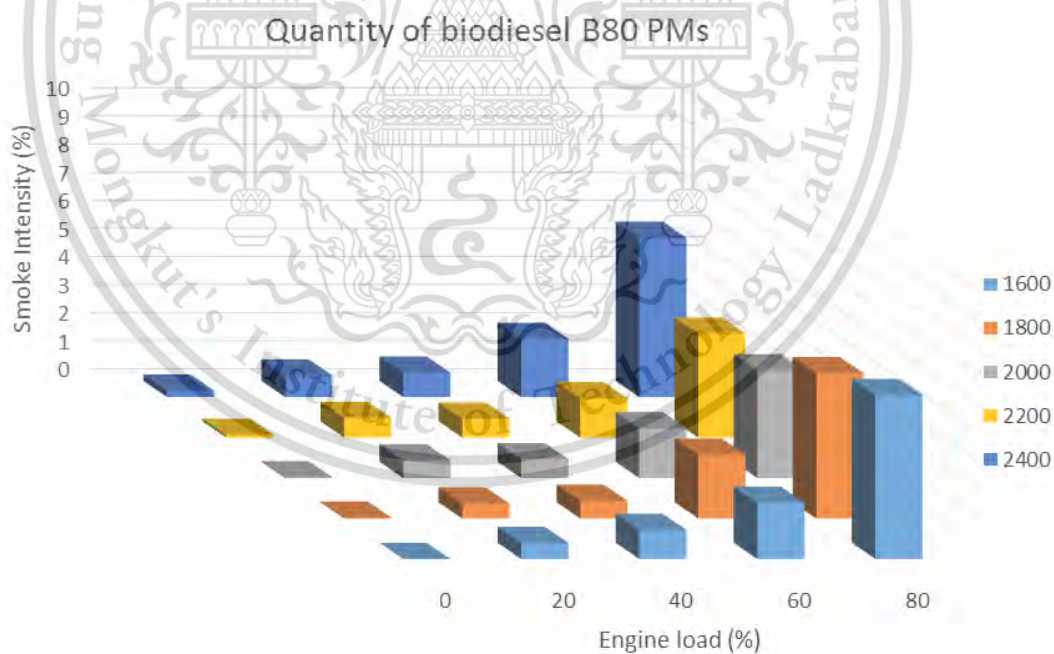


Figure 4.18 Smoke intensity of B80

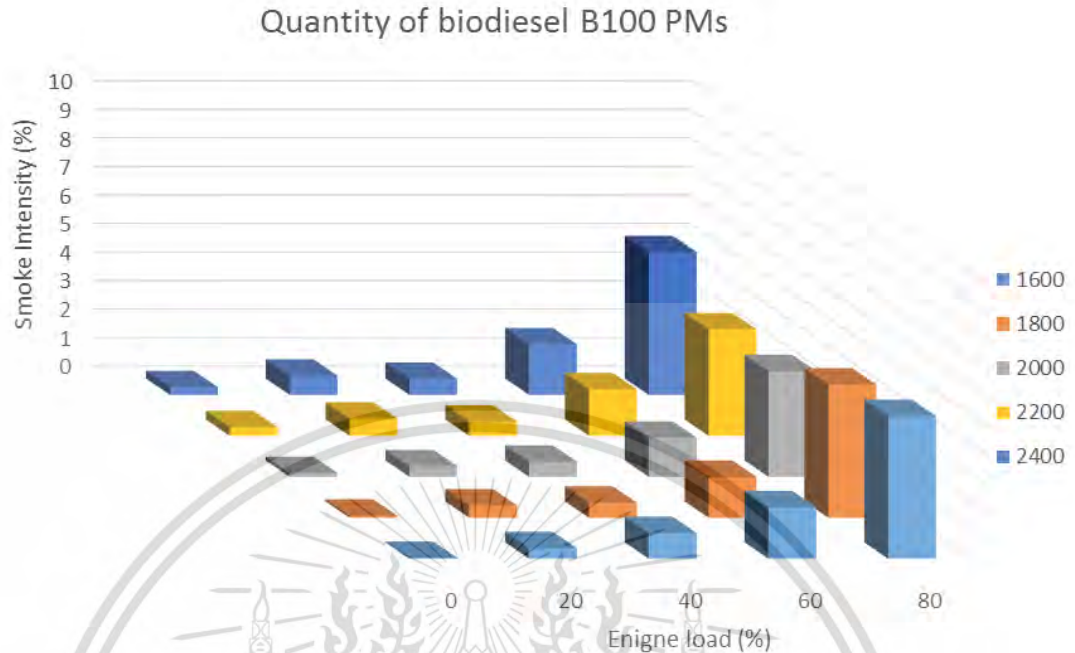


Figure 4.19 Smoke intensity of B100

The amount of particle quantities has been confirmed by Komkla Siricholathum research [30] which the mass of the biodiesel particle is approximately half of the diesel fuel as shown in the “.

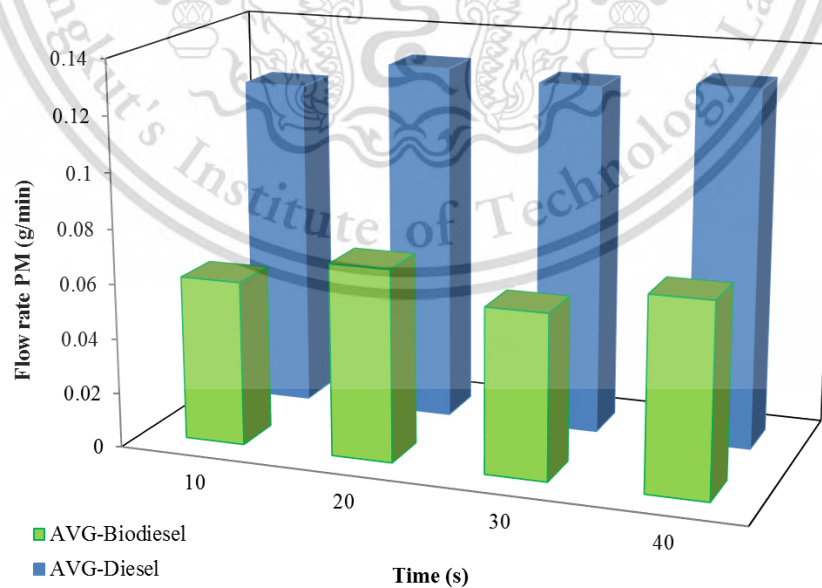


Figure 4.20 comparison of particulate mass which emitted from biodiesel and commercial diesel [30]

#### 4.4.2. Particulate matter size distribution

Particle which emitted from internal combustion engine clearly separate into 3 modes [8].

First is nucleation mode, but the nuclei particles are too small for the particle size distribution measure instrument.

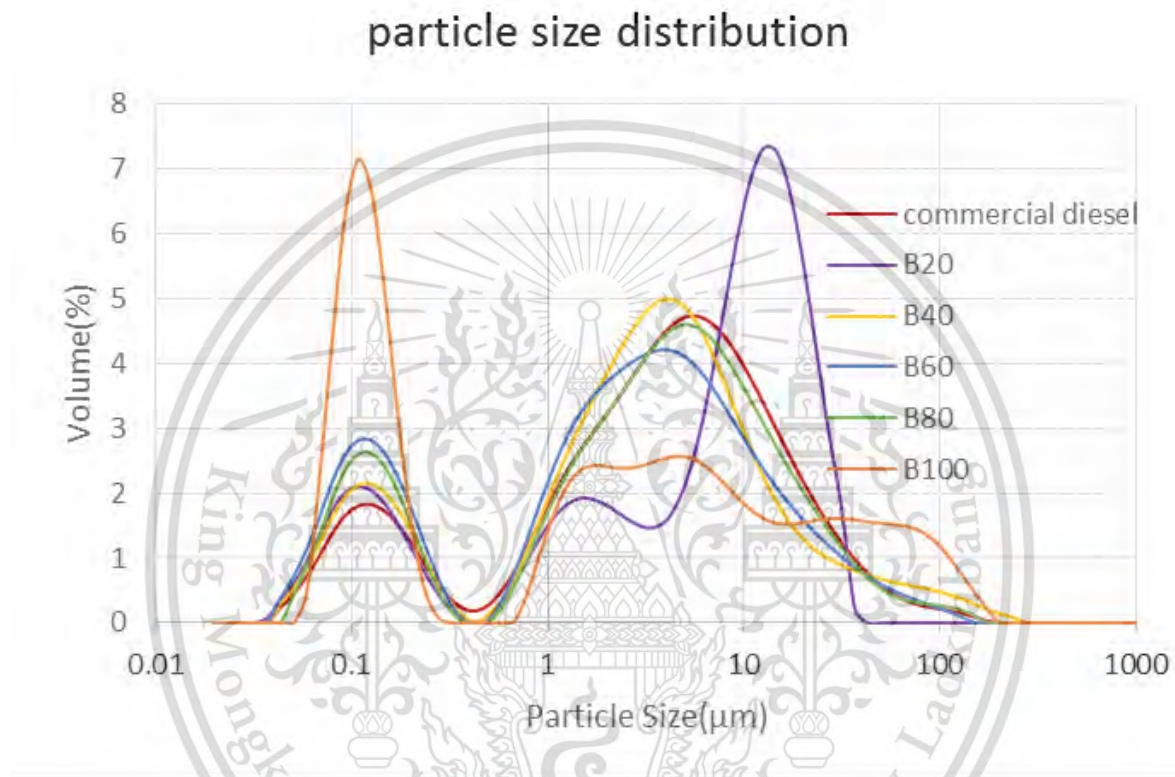


Figure 4.21 Particle size distribution at 80% load 2400rpm of each fuel

Second is accumulation mode which shown in first peak of Figure 4.21. The size range of agglomerate is  $\sim 40$ - $400$ nm, average size is  $\sim 130$ - $142$ nm, and mode size is  $\sim 100$ - $120$ nm. The higher content of oxygen in fuel, the higher amount and smaller size of agglomerate because of more complete combustion. Which can see in better BSEC.

Third is coarse mode such as PM<sub>2.5</sub> and PM<sub>10</sub> which shown in second peak of the Figure 4.21. The higher content of conventional diesel, the higher amount of particle in coarse mode.

The result of particle size distribution in every fuel show the similar trend of particle mode separation. The size of each modes are similar but the amount is different by the fraction of biodiesel.

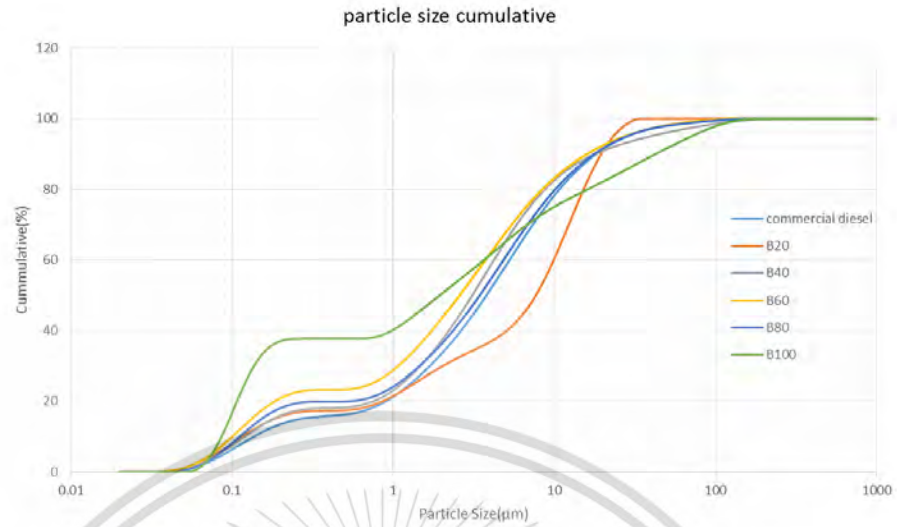
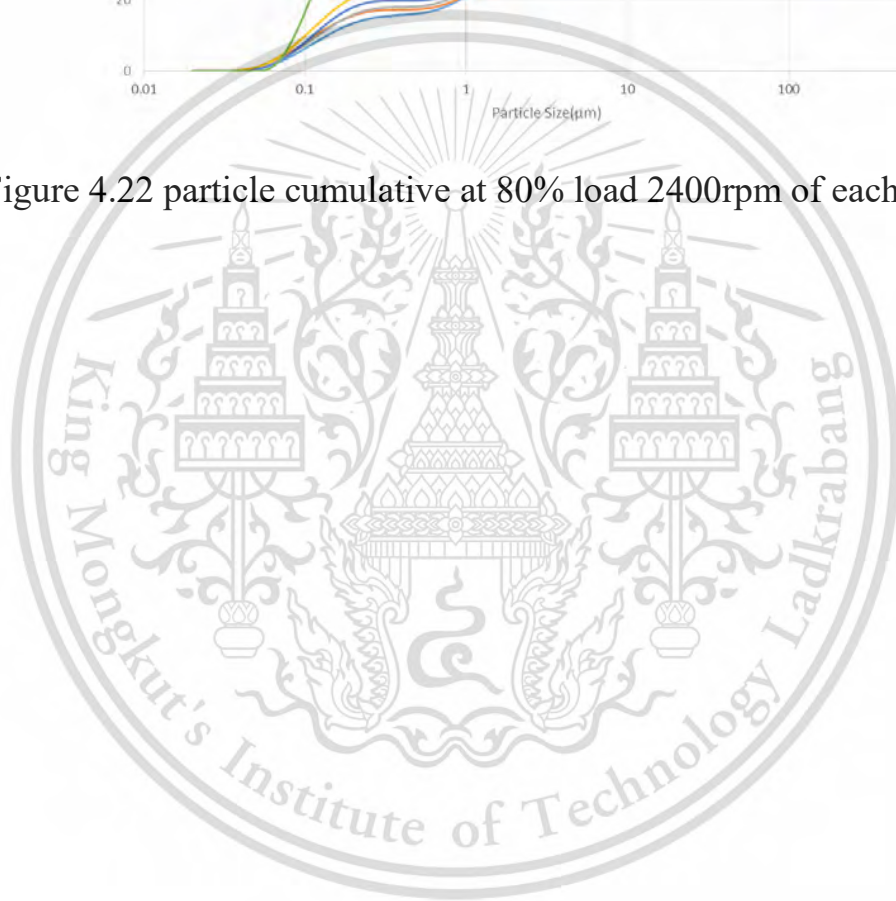


Figure 4.22 particle cumulative at 80% load 2400rpm of each fuel



#### 4.4.3. Morphology and nanostructures

The morphology of engine's particulate matter was successfully investigated using electron microscopy. Several type of PM spread all of the filters for example PM10 which have size around 10 micron, PM2.5 or fine particle, ultrafine particle and nanoparticle were clearly seen using SEM and TEM. Figure 4.23 shows SEM image of PM10 from biodiesel engine in the condition of 80% load engine operation. In Figure 4.24 and Figure 4.25 shows PM2.5 from the same condition with Figure 4.23.

Both of PM10 and PM2.5 of diesel and biodiesel engine's particulate matter consist of many single nanoparticles.

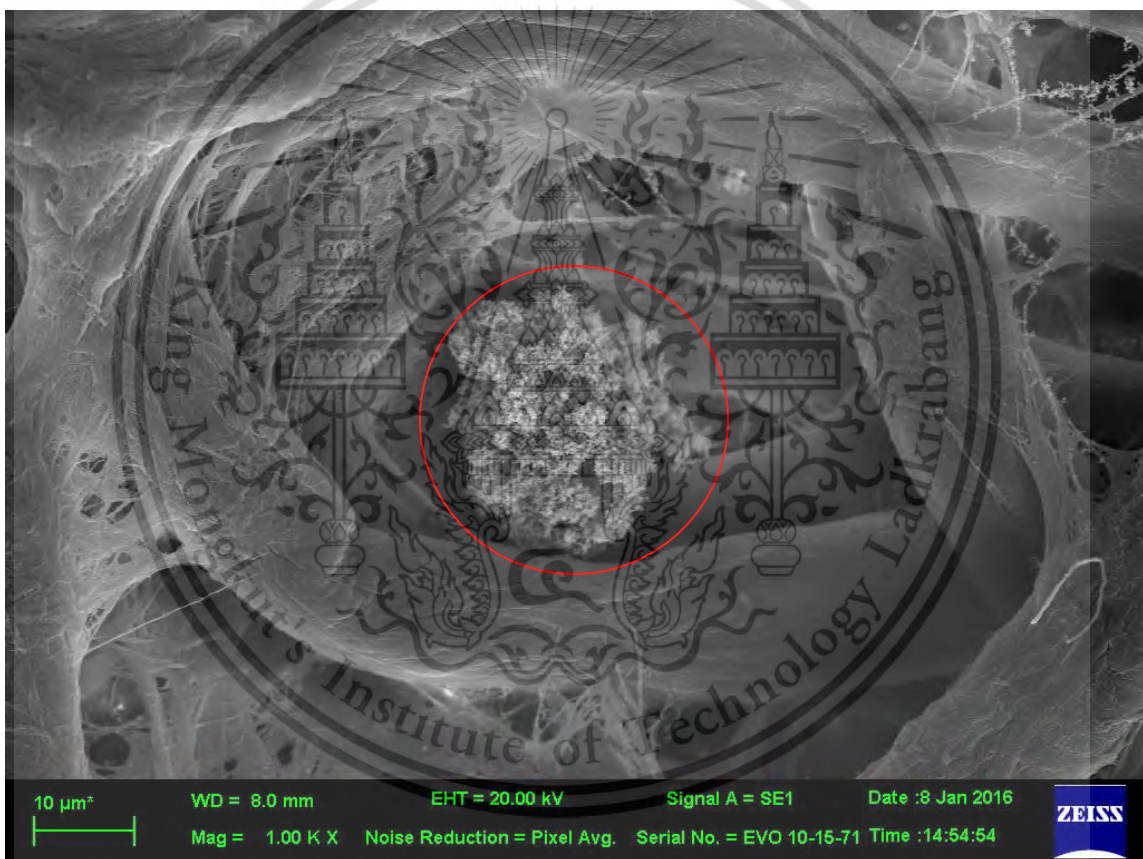


Figure 4.23 SEM image of biodiesel blends diesel engine's PM10 in the condition of 80% load engine operation.

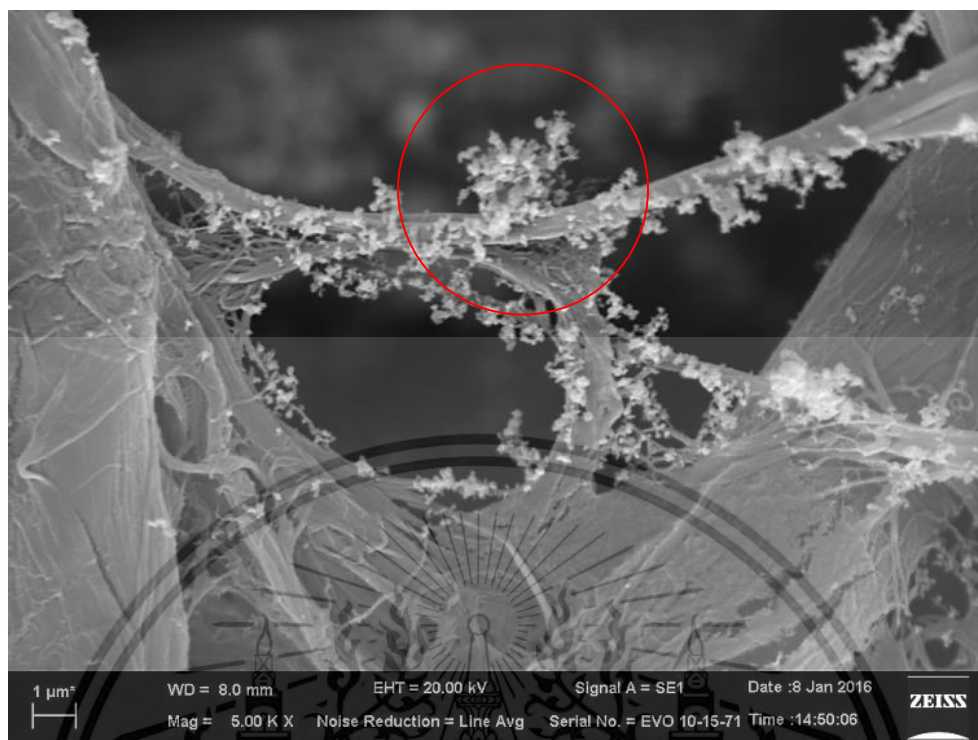


Figure 4.24 SEM image of conventional diesel particulate matter in condition of 80% load operation



Figure 4.25 SEM image of biodiesel particulate matter in condition of 80% load operation

This material is reserved for educational use only, not allowed for commercial use.

Forbidden to modify the content, and cite the document when use.

In addition, ultrafine particles and nanostructure of PM single particle were investigated using TEM for better understanding. Figure 4.26 and Figure 4.27 shows TEM images of diesel and biodiesel engine's particulate matter ultrafine particles, respectively, in the condition of 80% load engine operation. The average agglomerated particle diameter size are in the range of 40-400nm.

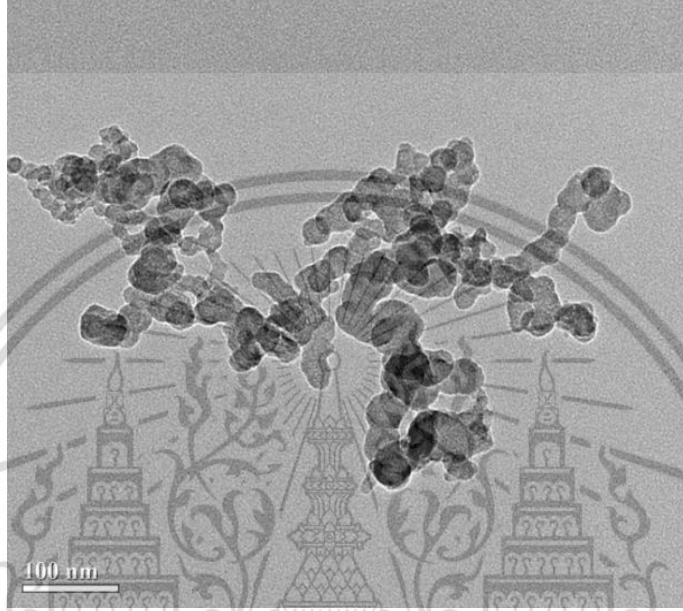


Figure 4.26 TEM image of conventional diesel particulate matter ultrafine particles in the condition of 80% load operation

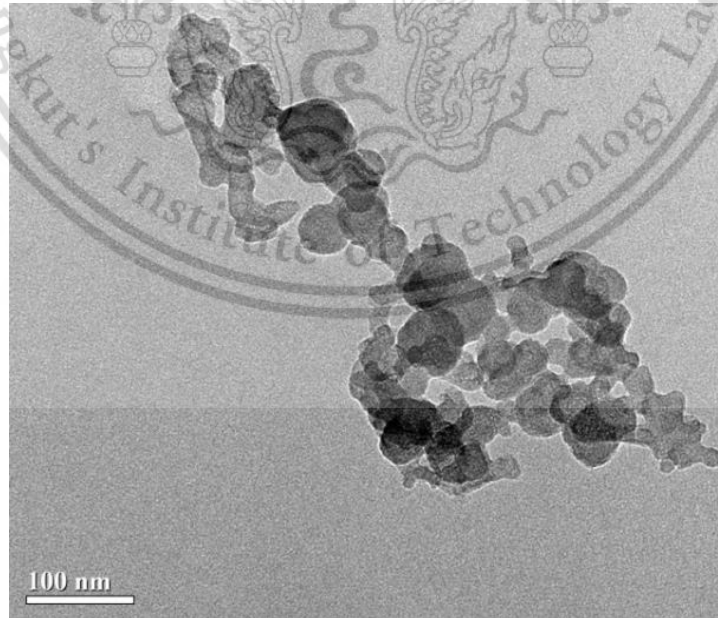


Figure 4.27 TEM image of biodiesel particulate matter ultrafine particles in the condition of 80% load operation

Moreover, single nanoparticles of diesel and biodiesel engines was also clearly observed using TEM as shown in Figure 4.28 and Figure 4.29, respectively. The average agglomerated particle diameter size are in the range of 20-50nm. Each carbon platelet, inner core and outer shell of single nanoparticle was also clearly observed by TEM.

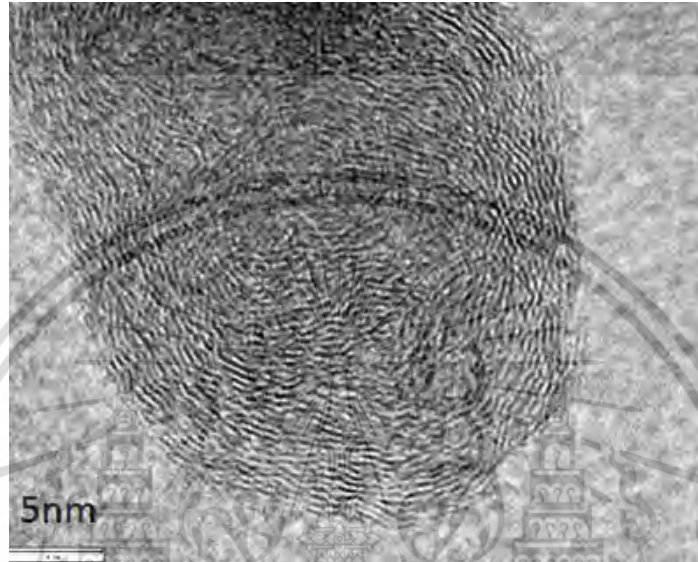


Figure 4.28 TEM image of conventional diesel nanoparticle in condition 80% load operation

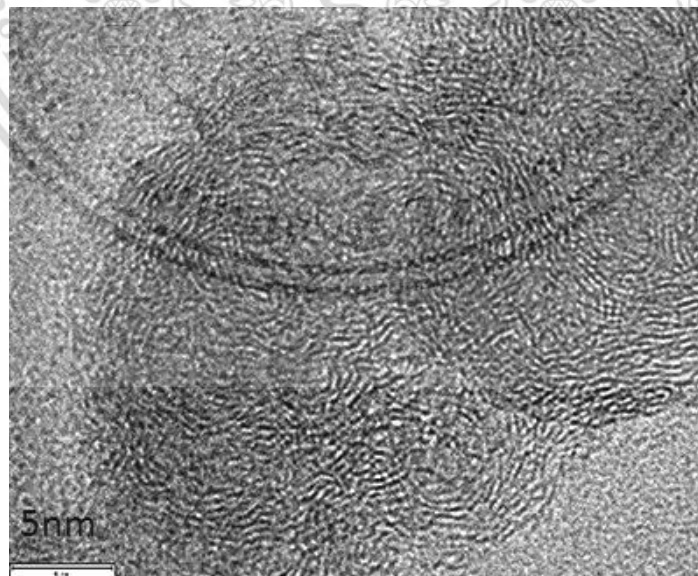


Figure 4.29 TEM image of biodiesel nanoparticle in condition 80% load operation

#### 4.4.4. Particle composition

From the CHNS/O analyzer result (Figure 4.30) biodiesel could contain larger amount of oxygen than does diesel PM, due to its intrinsic oxygenate fuel formation. The devolatilization of oxygen group bonded at the edge site provides high oxidative reactivity during the initial stage of oxidation. The edge site is known to have a high tendency toward oxidation, so that it can facilitate external surface burning.

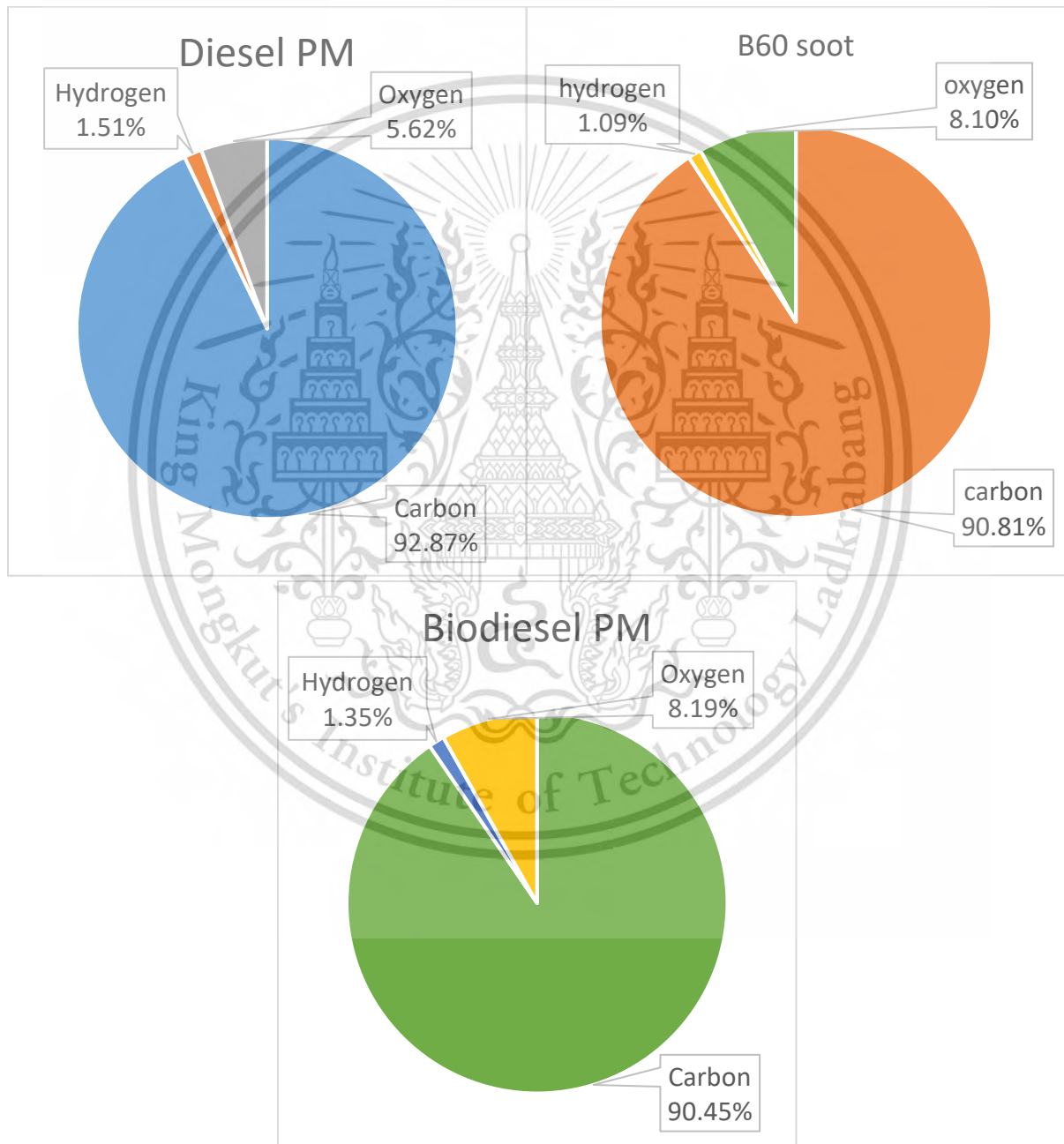


Figure 4.30 particle composition result

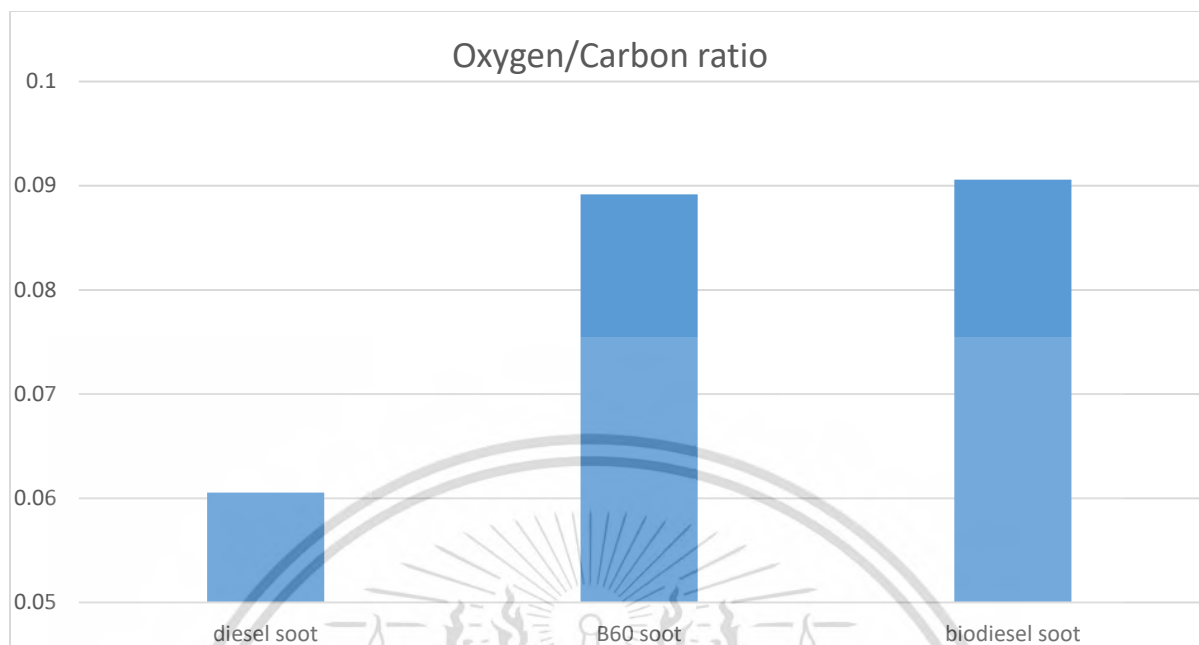


Figure 4.31 Oxygen/Carbon ratio of particulate matter

The research from Jun Hamada et al.[21], which show the relation between oxygen/carbon ration with activation energy and particle size. The biodiesel particle has lower activation energy and smaller particle size due to oxygen/carbon ratio in particle which biodiesel has higher oxygen/carbon ratio as shown in Figure 4.32 and Figure 4.33.

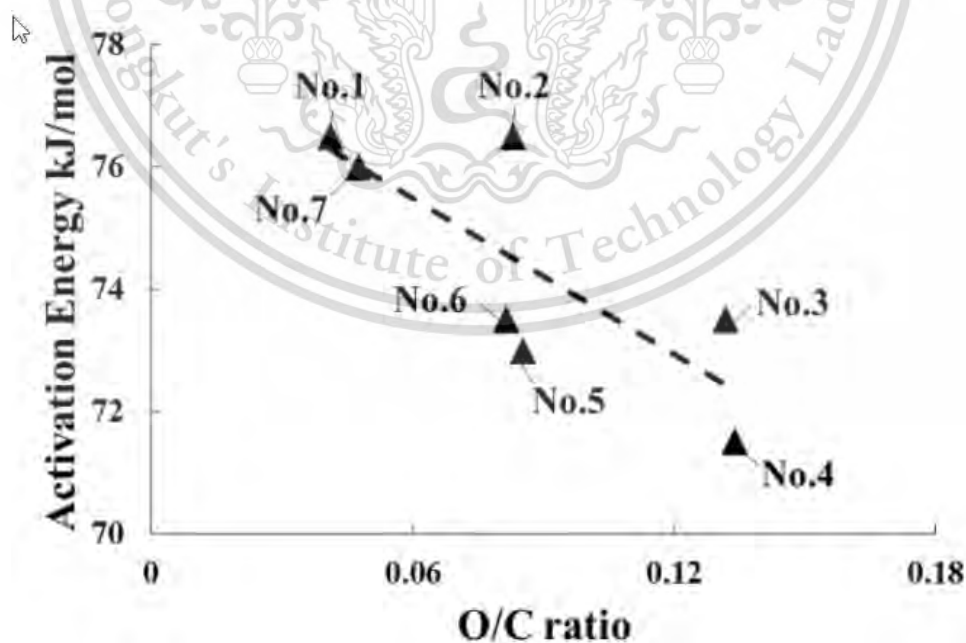


Figure 4.32 relation between activation energy and O/C ratio[21]

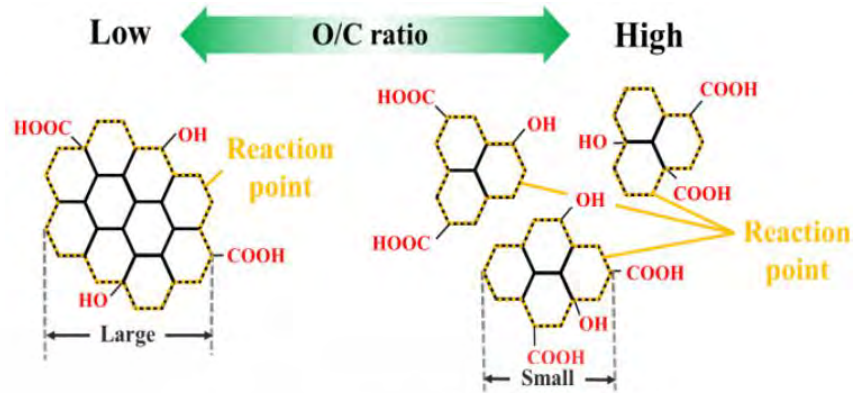


Figure 4.33 Effect of O/C ratio to particle size[21]

Another interest point is ash fraction which the amount of ash increase by the concentration of biodiesel which shown in Figure 4.34.

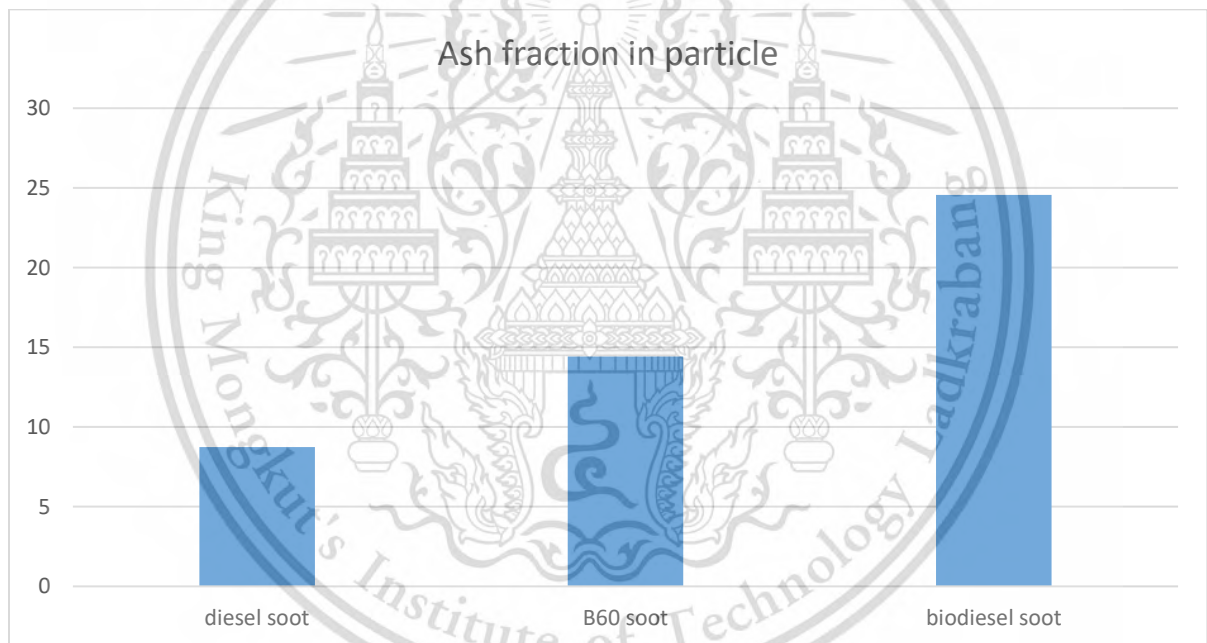


Figure 4.34 Ash fraction from particulate matter

## Chapter 5

### CONCLUSION

In term of Engine performance, there are no different on engine performance when use in standard engine. And biodiesel has better thermal efficiency because of oxygenate fuel.

In term of combustion characteristic, biodiesel have shorter ignition delay due to oxygenate fuel promote the earlier oxidation

For particulate matter, Parameters which have major effect on amount of PM are engine load, fuel type, and engine respectively.

Quantities of particulate matter increases when load is increased because amount of fuel injection in combustion chamber is higher. That means more of fuel injection makes bigger rich zone in spray which affected to incomplete combustion.

For the fuel, biodiesel fuel produces particulate matters about half of that from diesel combustion and because biodiesel fuel contain more oxygen atom in fuel molecule which provide better oxidation.

If consider on engine speed, quantities of particulate matter in middle engine speed are lowest compare with low and high engine speed because the middle engine speed is the condition best efficiency. At low engine speed, efficiency loss from heat lost and at the high engine speed, efficiency loss from friction lost.

The size of primary biodiesel particulate matter is smaller than the diesel particulate matter because biodiesel has larger amount of oxygen in PM from CHNS/O analyzer result. And the TGA result which show biodiesel particle has better oxidation, can be used to confirm why biodiesel PM are smaller than diesel particle.

## REFERENCE

- [1] J.B.Heywood, "Internal Combustion Engine Fundamental. McGraw-Hill series in Mechanical Engineering," vol. 1998, .
- [2] "Oil, coal, natural gas seen as fuels of the future,."
- [3] D.A. Coley, "Energy and Climate Change Creating a Sustainable Future, John Wiley & Sons, Ltd. 2008."
- [4] "<http://carenginecooling.blogspot.com/2012/07/diesel-engines-diesel-engine-also-known.html>."
- [5] "Diesel-Engine Management:An Overview. The Bosch Yellow Jackets Edition 2003 Expert Know-How on Automotive TechnologyDiesel-Engine Management. Published by:© Robert Bosch GmbH, 2003Postfach 1129,D-73201Plochingen.Automotive Aftermarket Business Sector,Department of Product Marketing Diagnostics &Test Equipment (AA/PDT5).," .
- [6] Dec, J. E, "A Conceptual Model of DI Diesel Combustion Based on Laser Sheet Imaging SAE Paper 970873," vol. 1997.
- [7] W. Addy Majewski, "Diesel Particulate Filters. Copyright © Ecopoint Inc. Revision 2001.07b."
- [8] D.B.Kittelson, "Engines and nanoparticles: a review," *J. Aerosol Sci.*, 1998, no. 29, pp. 575–588.
- [9] J.V. Gerpen, "Biodiesel processing and production,," *Fuel Process. Technol.*, 2015, 86, pp. 1097–1107.
- [10] "Schematics of scanning electron microscopy operation ,."
- [11] "Schematics of transmission electron microscopy operation,."
- [12] M.M. Maricq, "Review Chemical Characterization of particulate emissions from diesel engine: A review," *J. Aerosol Sci.*, 2007, 38, pp. 1079–1118.
- [13] O.I. Smith, "Fundamentals of soot formation in flames with application to diesel engine particulate emissions," *Prog. Energy Combust. Sci.*, 1981, 7, pp. 275–291.
- [14] Y. Songsaengchan, M. Tongroon, P. Karin, N. Chollacoop, C. Chareonphonphanich, and K. Hanamura, "Investigation of Biodiesel Particulate Matter in Nanostructure," *Int. Conf. Automot. Technol. Engine Altern. Fuels*, 2012, 2.
- [15] A.K. Agarwal, T. Gupta, and A. Kothari, "Particulate emissions from biodiesel vs diesel fuelled compression ignition engine,," *Renew. Sustain. Energy Rev.*, 2011, 15, pp. 3278–3300.
- [16] T. Lu, C.S. Cheung, and Z. Huang, "Effects of engine operating conditions on the size and nanostructure of diesel particles,," *J. Aerosol Sci.*, 2012, 47, pp. 27–38.

- [17] K. Kim and B. Choi, "The effect of biodiesel and bioethanol blended diesel fuel on nanoparticles and exhaust emissions from CRDI diesel engine.," *Renew. Energy*, 2010, 35, pp. 157–163.
- [18] D. Dwivedi, A.K. Agarwal, and M. Sharma, "Particulate emission characterization of a biodiesel vs diesel-fuelled compression ignition transport engine: A comparative study. Atmospheric Environment," 2006, 40, pp. 5586–5595.
- [19] M. Salamanca, F. Mondragón, J.R. Agudelo, and A. Santamaría, "Influence of palm oil biodiesel on the chemical and morphological characteristics of particulate matter emitted by a diesel engine," *Atmos. Environ.*, 2012, 62, pp. 220–227.
- [20] P. Karin, Y. Songsaengchan, S. Laosuwan, C. Charoenphonphanicha, N. Chollacoop, and K. Hanamura, "Nanostructure Investigation of Particle Emission by Using TEM Image Processing Method.," *Energy Procedia*, 2013, 34, pp. 757–766.
- [21] Jun Hamada *et al.*, "Research on internal transfer phenomena of the Diesel Particulate Filter (Sixth Report) -A study on effect of engine operating condition at Soot loading on PM structure and oxidation rate-."
- [22] K. Vijayaraj and A. P. Sathiyagnanam, "A comprehensive review on combustion of compression ignition engines using biodiesel."
- [23] S. Srihari, S. Thirumalini, and K. Prashanth, "An Experimental Study on the Performance and Emission Characteristics of PCCIDI Engine Fuelled with Diethyl ether-Biodiesel-Diesel Blends," *Renewable Energy*, 2017, 107, pp. 440–447.
- [24] S. Ramchandr, Jahagidar, E.R. Deore, M. S. Patil, and P.S. Desale, "Performance characterization of single cylinder DI diesel engine fuelled with karanja biodiesel," *World Cong Eng*, 2011.
- [25] Amar Pandhare and Atul Padalkar, "Investigations on Performance and Emission Characteristics of Diesel Engine with Biodiesel (Jatropha Oil) and Its Blends," *J. Renew. Energy*, 2013.
- [26] Y. V. Hanumantha Rao, Ram Sudheer Voleti, V. S. Hariharan, A. V. Sitarama Raju, and P. Nageswara Redd, "Use of Jatropha Oil Methyl Ester and Its Blends as an Alternative Fuel in Diesel Engine," *ABCM*, 2009.
- [27] Prathan Srichai, "Experimental investigation of spray combustion with biodiesel - blended in a constant volume combustion chamber," 2016.
- [28] P. Eastwood, *Particulate emissions from vehicles*. Chichester: Wiley, 2008.
- [29] Willard W. Pulkrabek, University of Wisconsin - Platteville, *Engineering Fundamentals of the Internal Combustion Engine, 2nd Edition*. .

- [30] Siricholathum, K, “The Impact of biodiesel particulate matter morphology and oxidation kinetic on filter trapping and regeneration mechanism, KMITL,” 2015.





This material is reserved for educational use only, not allowed for commercial use.

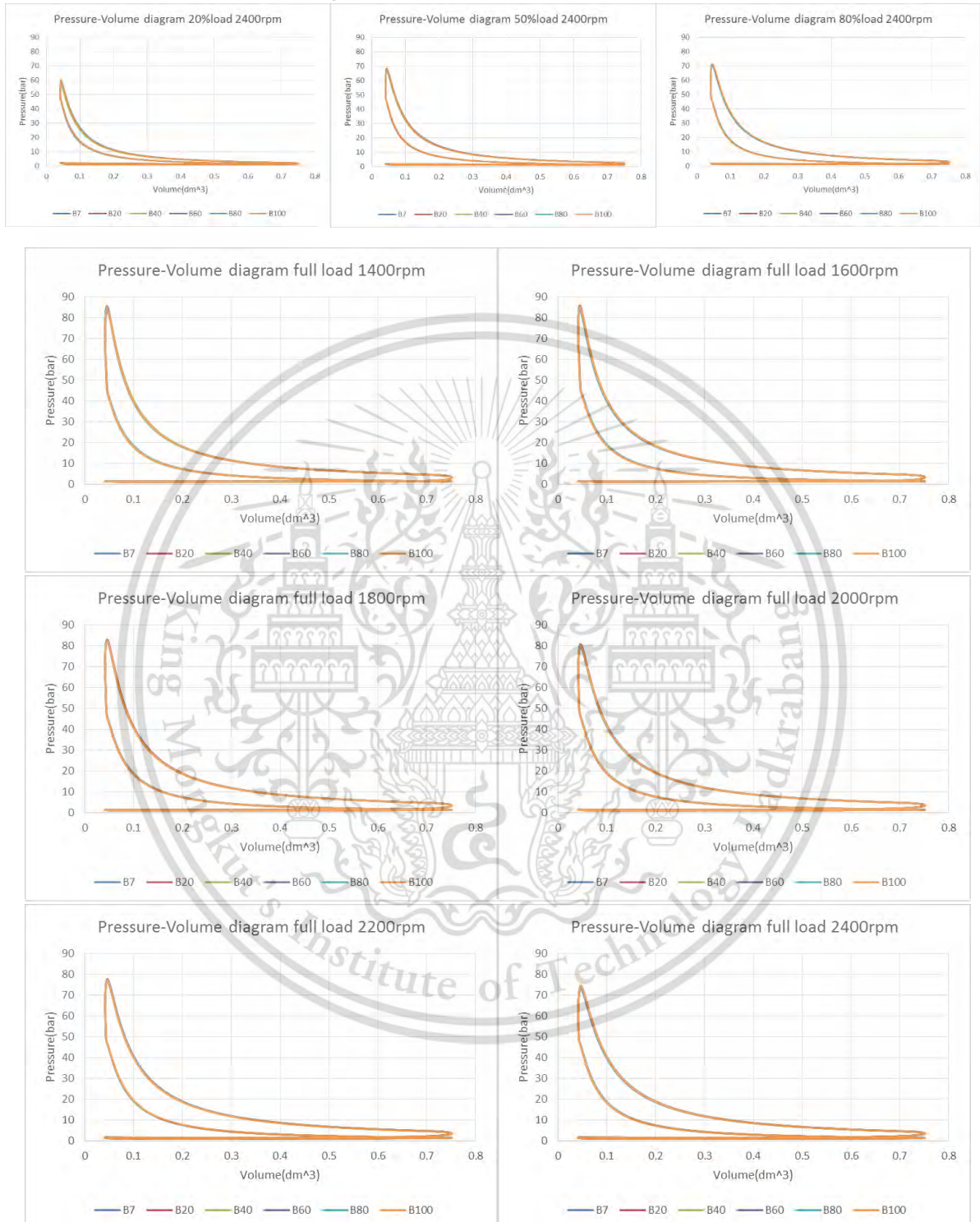
Forbidden to modify the content, and cite the document when use.



This material is reserved for educational use only, not allowed for commercial use.

Forbidden to modify the content, and cite the document when use.

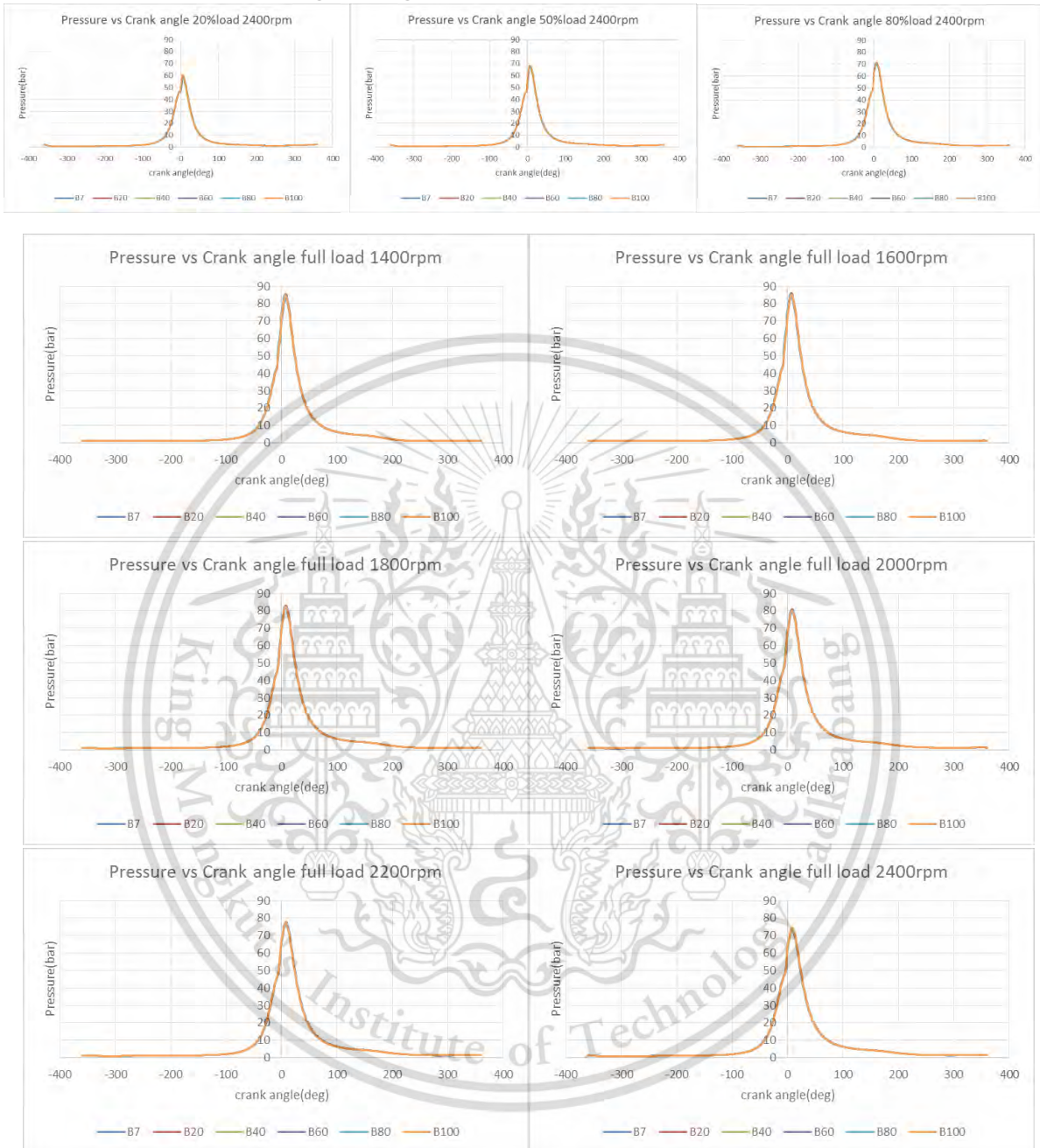
## A-1: Pressure-Volume diagram



This material is reserved for educational use only, not allowed for commercial use.

Forbidden to modify the content, and cite the document when use.

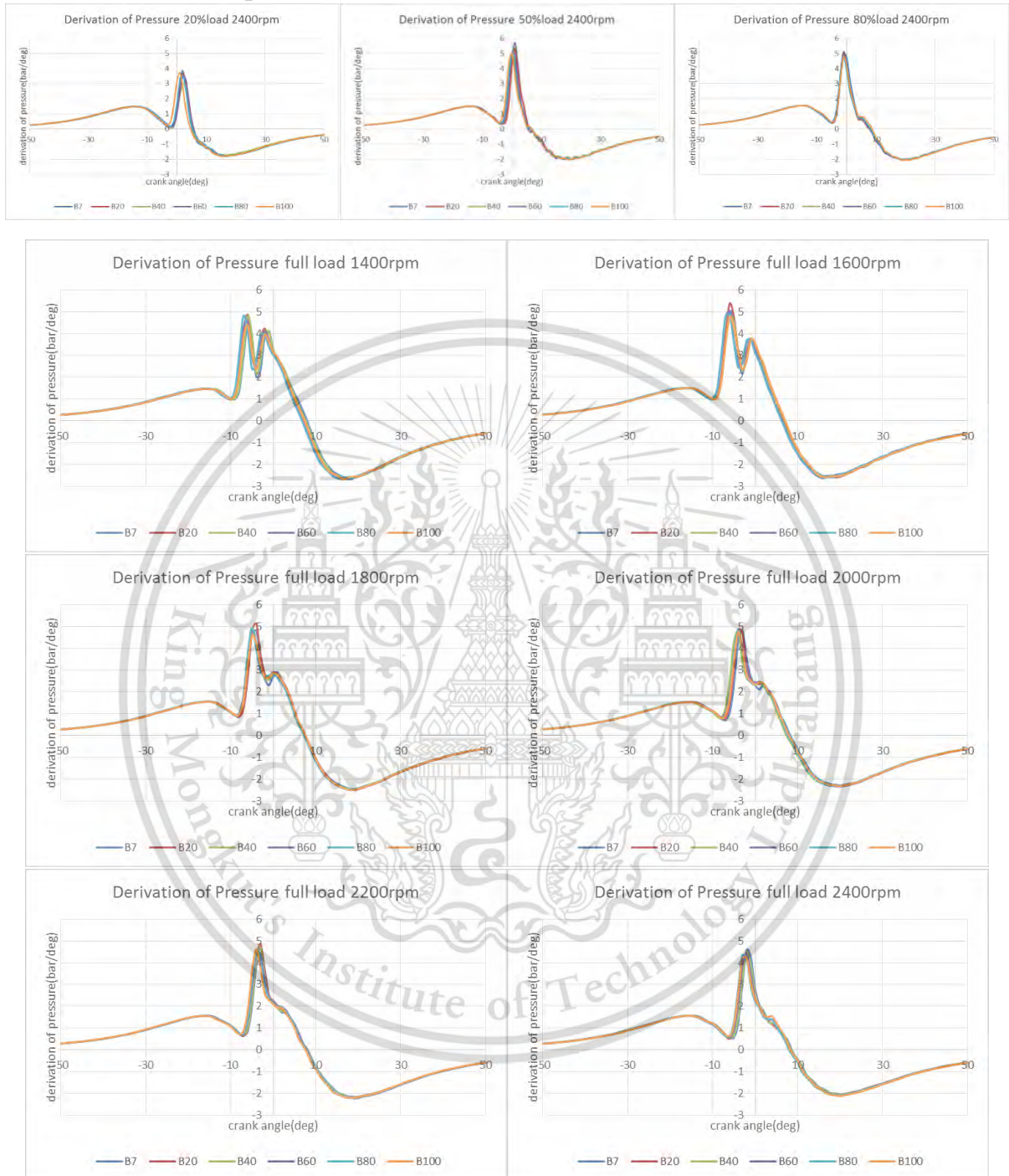
### A-2: Pressure-Crank angle diagram



This material is reserved for educational use only, not allowed for commercial use.

Forbidden to modify the content, and cite the document when use.

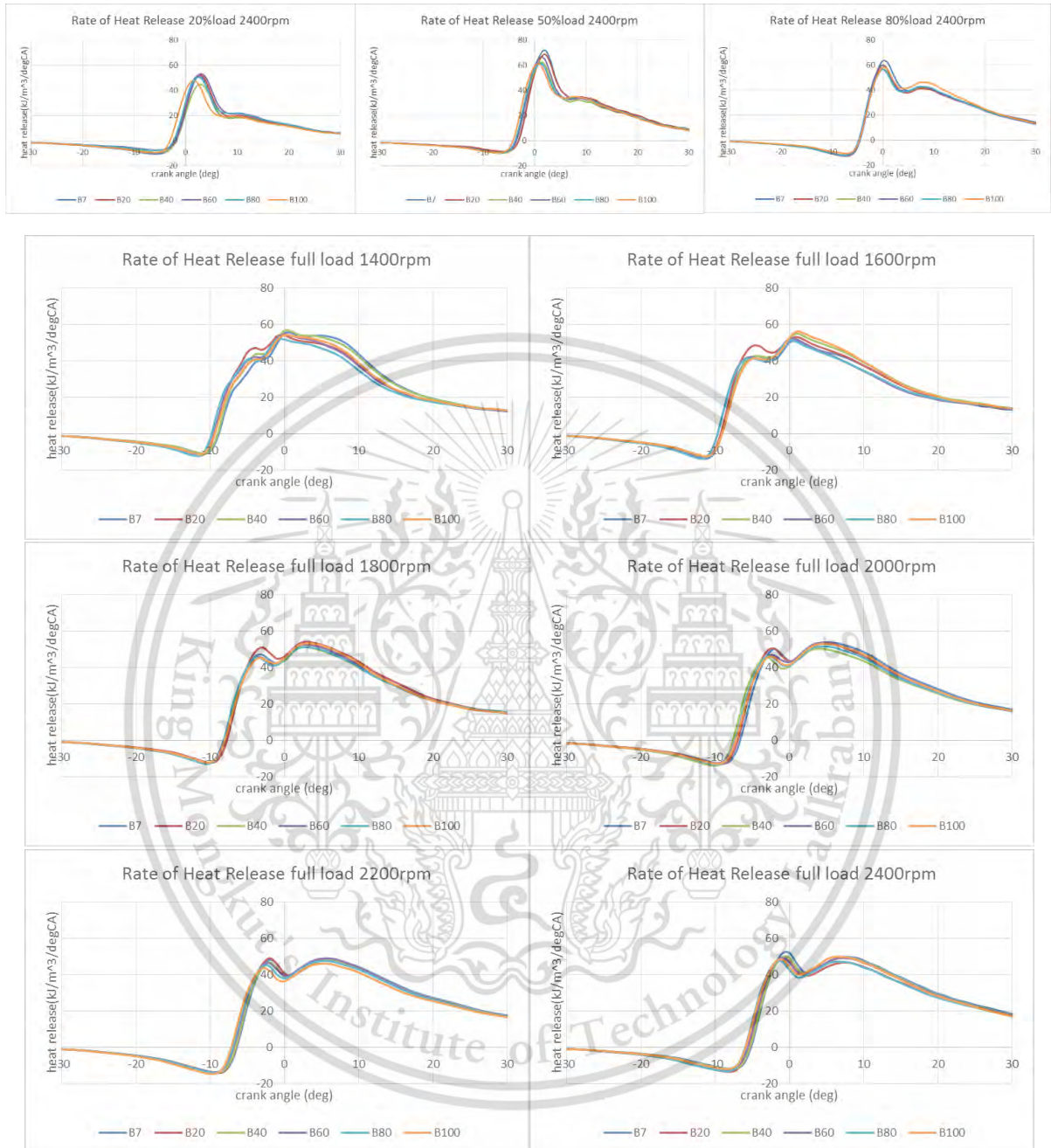
### A-3: Derivation of pressure



This material is reserved for educational use only, not allowed for commercial use.

Forbidden to modify the content, and cite the document when use.

## A-4: Rate of heat release



This material is reserved for educational use only, not allowed for commercial use.

Forbidden to modify the content, and cite the document when use.

## A-5: Cumulative heat release

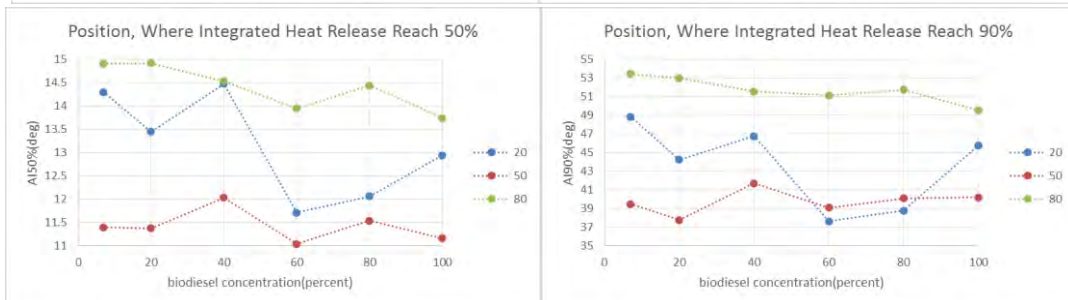
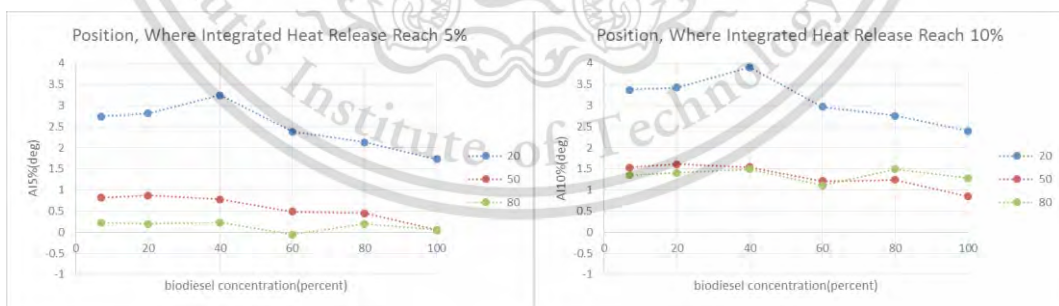
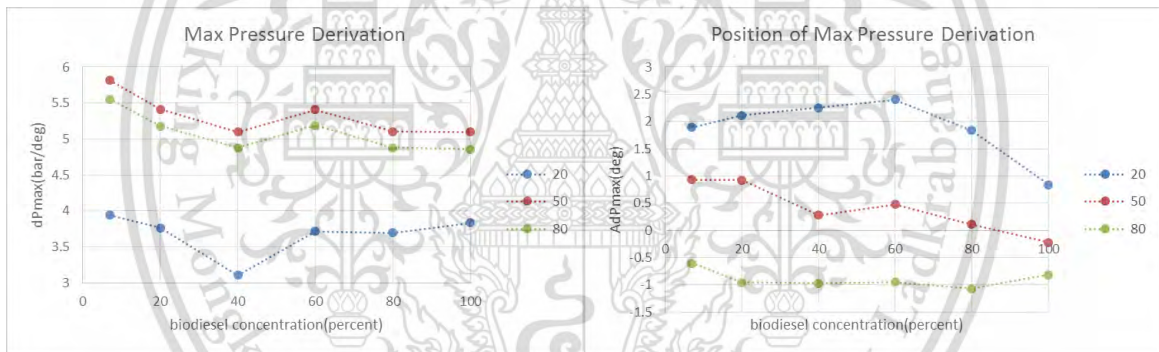
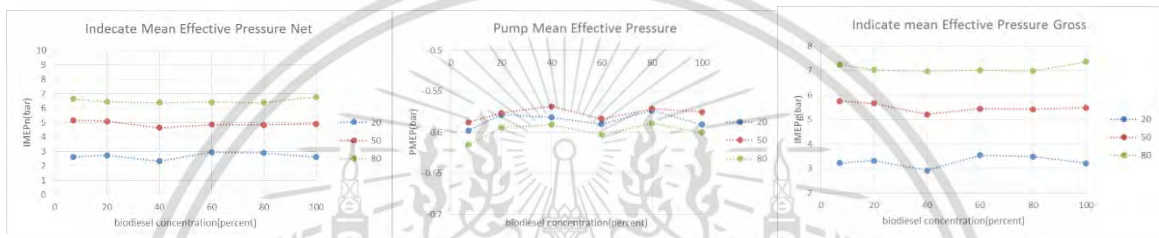
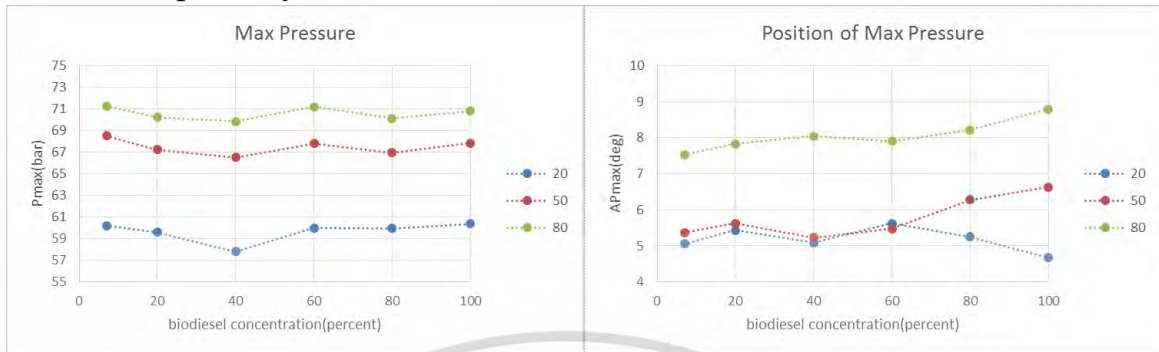


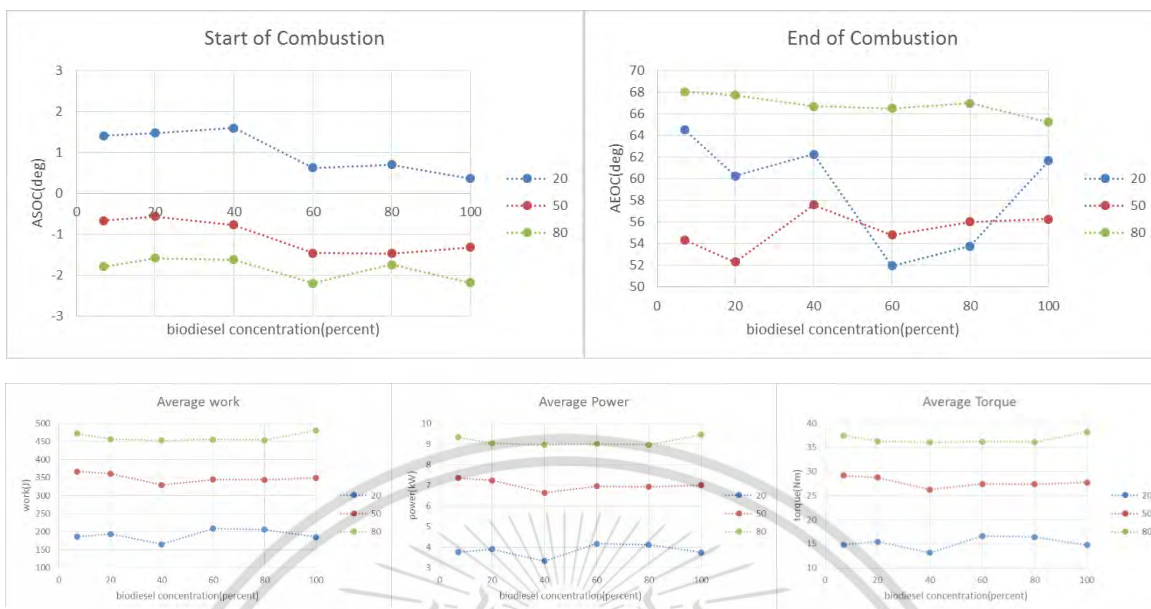
This material is reserved for educational use only, not allowed for commercial use.

Forbidden to modify the content, and cite the document when use.

A-6: Etc

A-6.1: 2400rpm vary load 20%,50%,80%

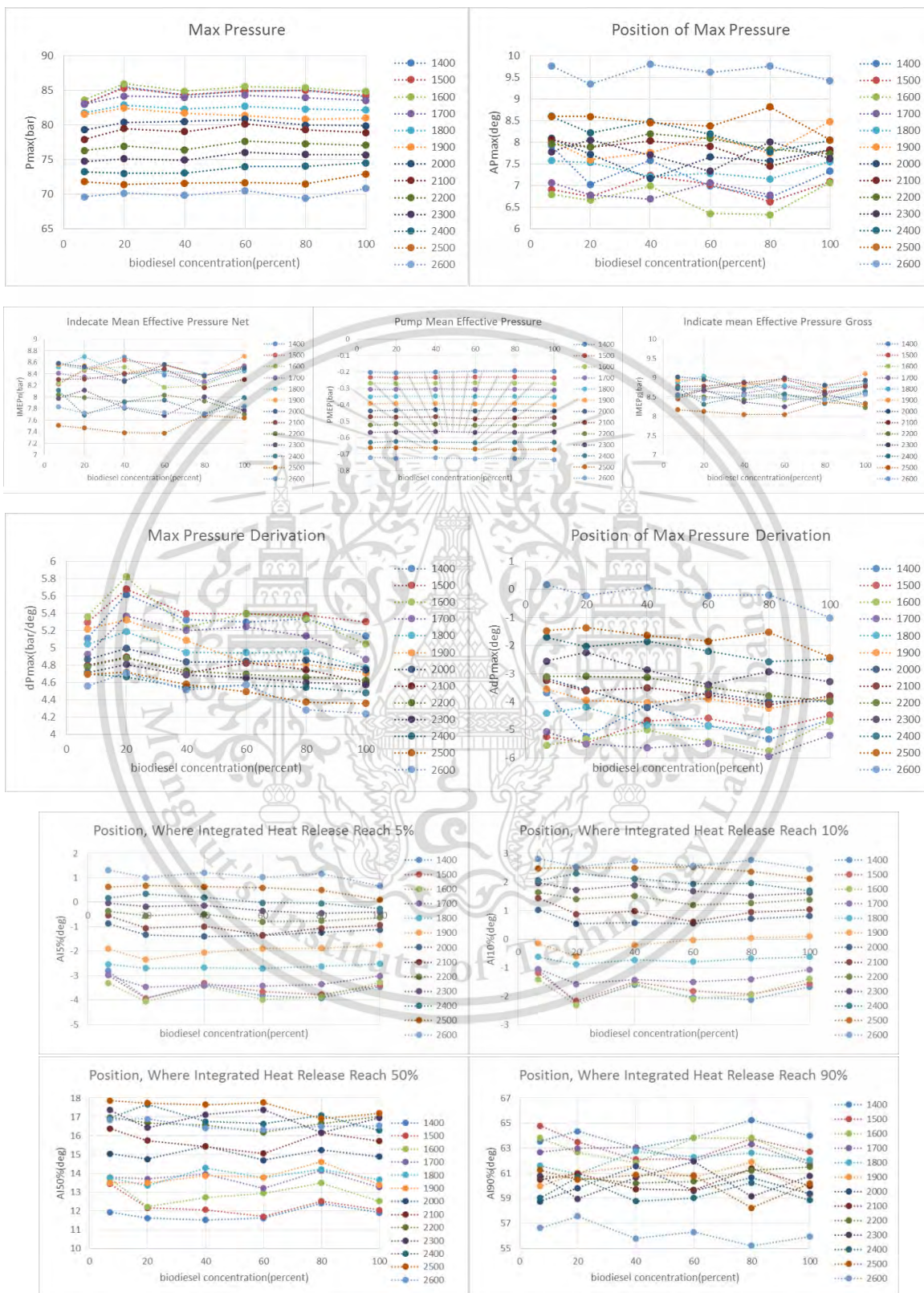




This material is reserved for educational use only, not allowed for commercial use.

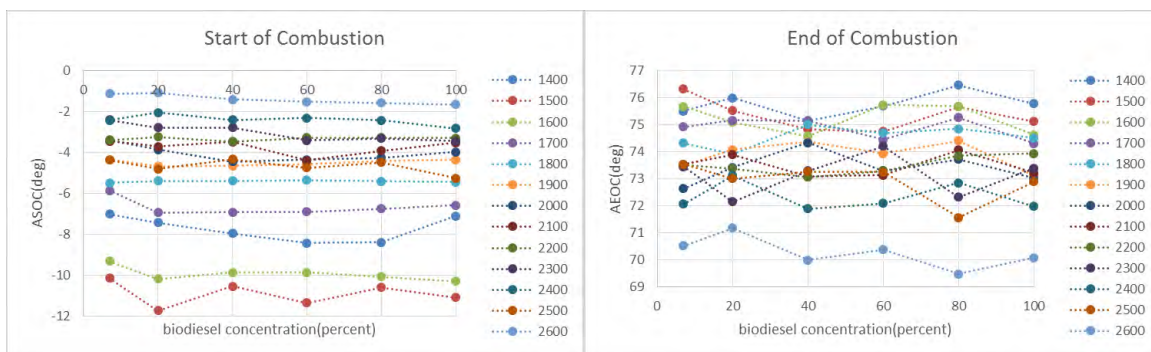
Forbidden to modify the content, and cite the document when use.

A-6.2: Full load

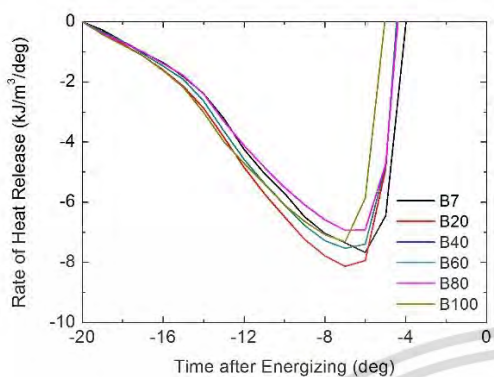


This material is reserved for educational use only, not allowed for commercial use.

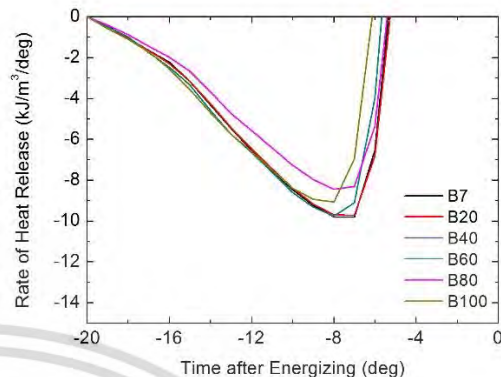
Forbidden to modify the content, and cite the document when use.



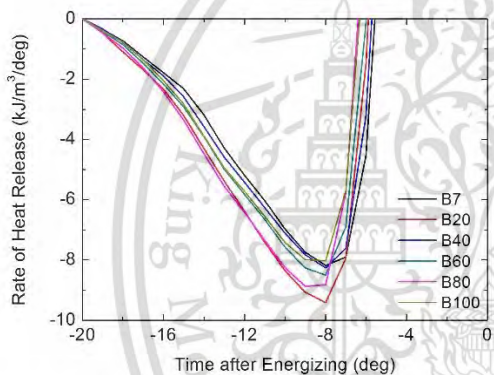
## A6-6.3: Injection timing at full load



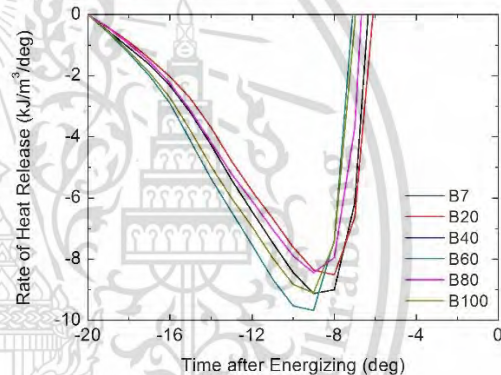
1400RPM



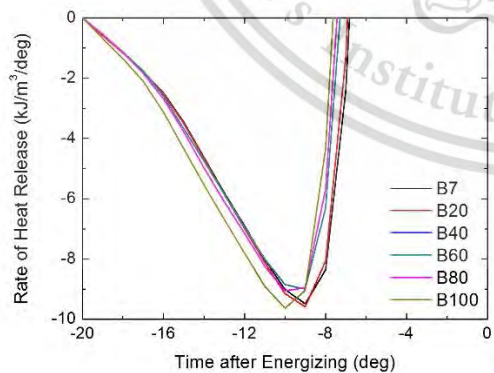
1500RPM



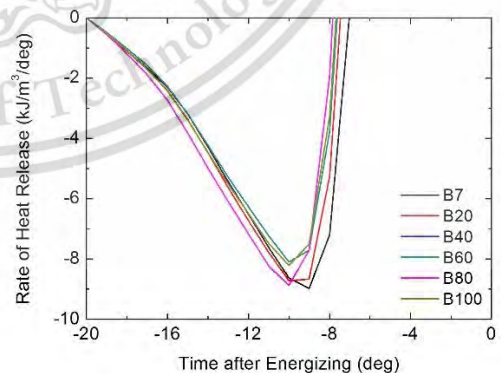
1600RPM



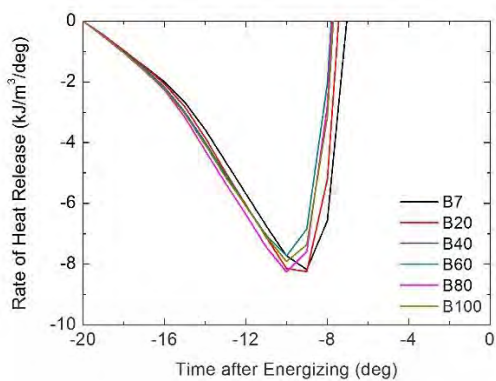
1700RPM



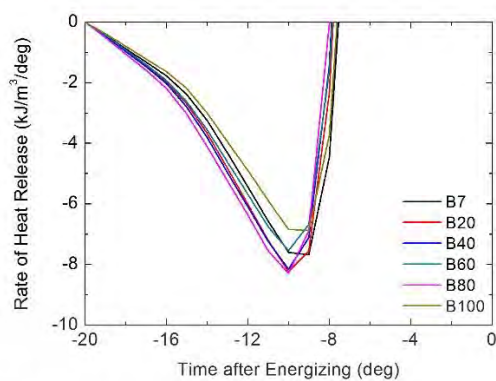
1800RPM



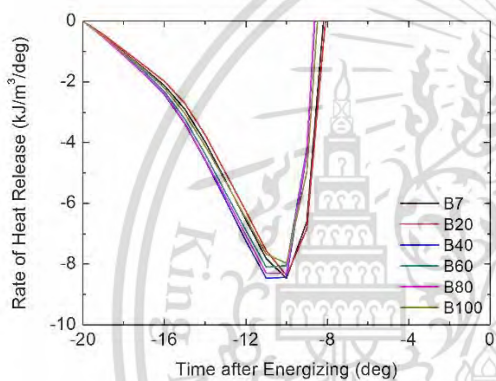
1900RPM



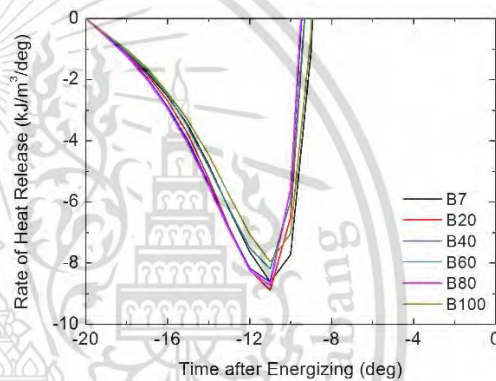
2000RPM



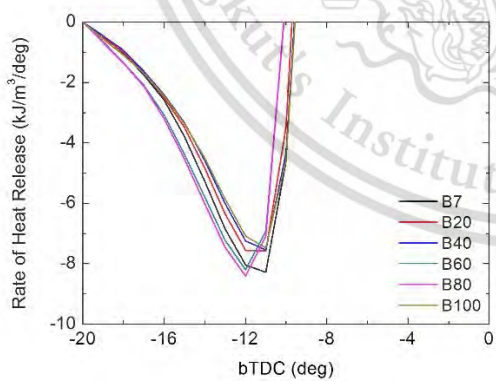
2100RPM



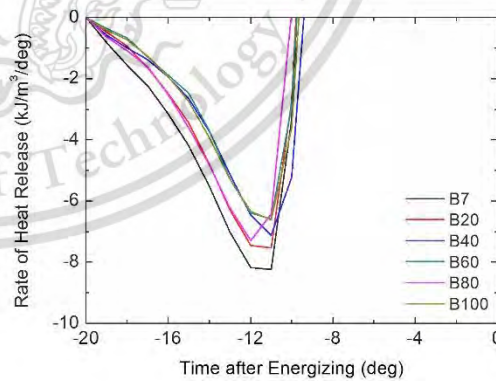
2200RPM



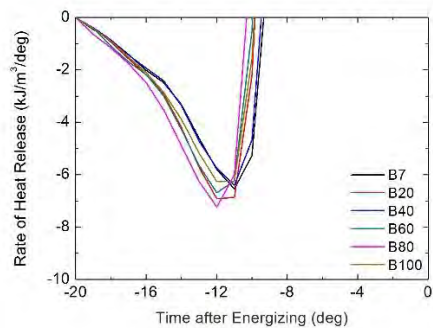
2300RPM



2400RPM



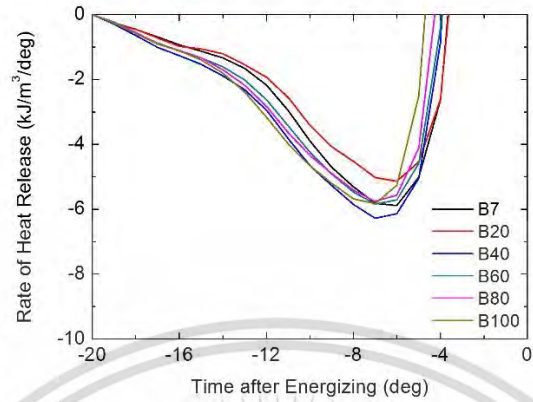
2500RPM



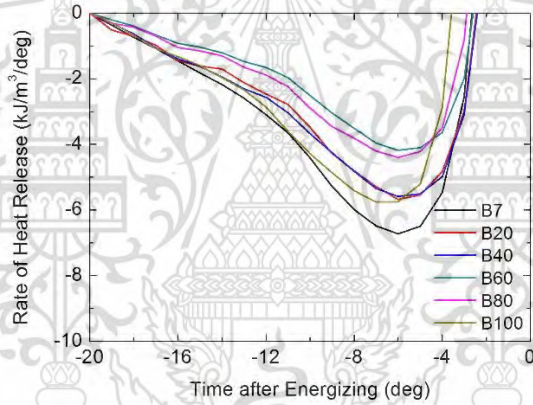
2600RPM



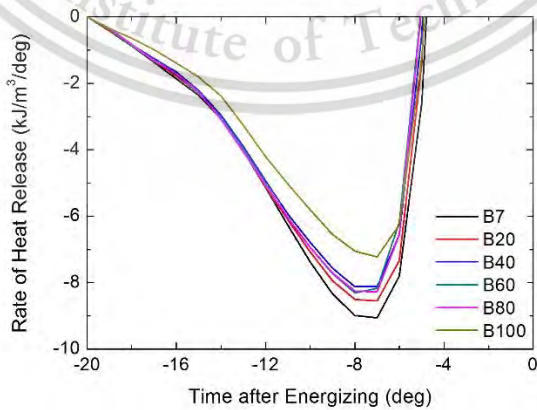
## A6-6.4: Injection timing at partial load at 2400RPM



20% load



50% load



80%load

This material is reserved for educational use only, not allowed for commercial use.

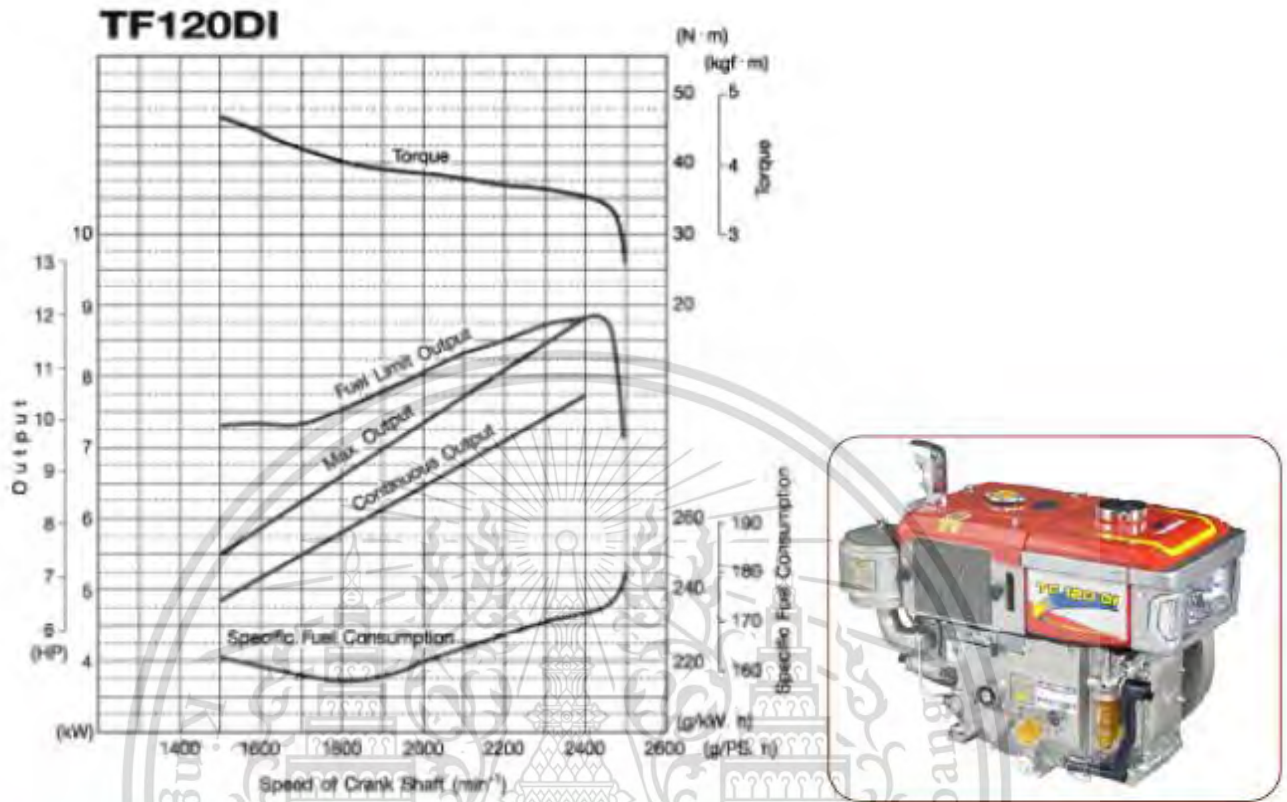
Forbidden to modify the content, and cite the document when use.



This material is reserved for educational use only, not allowed for commercial use.

Forbidden to modify the content, and cite the document when use.

B-1: Diesel engine specification



**SPECIFICATION**

Model	Unit	TF60DI-L	TF90DI-H	TF90DI-L	TF50DI-H	TF110DI-L	TF110DI-Y	TF110DI-H	TF120DI-L	TF120DI-Y	TF120DI-H	
Type		Horizontal water cooled diesel engine										
Combustion system		Direct Injection (DI)										
Number of cylinder		1										
Bore x stroke	mm	80 x 87	80 x 87	85 x 87	85 x 87	88 x 96	88 x 96	88 x 96	92 x 96	92 x 96	92 x 96	
Displacement	lit.	0.437	0.437	0.493	0.493	0.583	0.583	0.583	0.638	0.638	0.638	
Cont. rating output	hp / rpm	7.0 / 2400	7.0 / 2400	8.0 / 2400	8.0 / 2400	9.8 / 2400	9.8 / 2400	9.8 / 2400	10.5 / 2400	10.5 / 2400	10.5 / 2400	
	kW / rpm	5.1 / 2400	5.1 / 2400	5.9 / 2400	5.9 / 2400	7.2 / 2400	7.2 / 2400	7.2 / 2400	7.7 / 2400	7.7 / 2400	7.7 / 2400	
Max. output	hp / rpm	8.0 / 2400	8.0 / 2400	9.0 / 2400	9.0 / 2400	11.0 / 2400	11.0 / 2400	11.0 / 2400	12.0 / 2400	12.0 / 2400	12.0 / 2400	
	kW / rpm	5.9 / 2400	5.9 / 2400	6.6 / 2400	6.6 / 2400	8.1 / 2400	8.1 / 2400	8.1 / 2400	8.8 / 2400	8.8 / 2400	8.8 / 2400	
Specific fuel consumption	g / hp-h	177										
Compression ratio		16.8 : 1	16.8 : 1	16.8 : 1	16.8 : 1	18.3 : 1	18.3 : 1	18.3 : 1	16.1 : 1	16.1 : 1	16.1 : 1	
Applicable fuel oil		Diesel										
Fuel injection pump		Bosch type										
Injection timing	deg	bTDC 20.0					bTDC 19.0					
Injection pressure	kg / cm <sup>2</sup>	200										
F.O. tank capacity	lit.	10.6					11.0					
Lubrication system		Fully sealed forced lubrication with trochoid pump & hydraulic regulator valve										
Lubrication oil		SAE NO. 40 / API GRADE CD / SF										
Lubricating oil capacity (oil pan)	lit.	2.2					2.8					
Cooling system		Radiator	Hopper	Radiator	Hopper	Radiator	Radiator	Hopper	Radiator	Radiator	Hopper	
Cooling water capacity	lit.	1.6	9.4	1.6	9.4	2.1	2.1	11.8	2.1	2.1	11.8	
Starting System		Hand starting										
Dimension	Length	mm					mm					
	Width	mm					mm					
	Height	mm					mm					
Engine Dry Weight	kg	87.5	84.0	88.5	85.0	104.5	104.5	101.5	105.5	105.5	102.5	

This material is reserved for educational use only, not allowed for commercial use.

Forbidden to modify the content, and cite the document when use.

## B-2: Kubota fuel pump specification

## ค่ากำหนดต่างๆ ของเครื่องยนต์ดีเซลคูโบต้า รุ่น RT DI,RT DI PLUS

รายละเอียด		รุ่น	RT DI,RT DI PLUS			
			100	110	125	140
ปั๊ม น้ำมัน เชื้อเพลิง	แรงดันปั๊มน้ำมันเชื้อเพลิง (เพื่อเช็คกระบอกปั๊มกับลูกปั๊ม)	ค่ามาตรฐาน (กก./คร.ชม.)	600 ลดลงเหลือ 500			
		(วินาที)	8			
	ไม่ต่ำกว่า (กก./คร.ชม.)	600 ลดลงเหลือ 500				
		(วินาที)	4			
	แรงดันปั๊มน้ำมันเชื้อเพลิง (เพื่อเช็คลิ้นสว)	ค่ามาตรฐาน (กก./คร.ชม.)	150 ลดลงเหลือ 140			
		(วินาที)	10			
ไม่ต่ำกว่า (กก./คร.ชม.)	150 ลดลงเหลือ 140					
	(วินาที)					
จุดเริ่มต้นน้ำมัน	(องศา)	15-17	17.5-19.5			



This material is reserved for educational use only, not allowed for commercial use.

Forbidden to modify the content, and cite the document when use.

## C-1: Diesel fuel

รายละเอียดแบบท้ายประกาศกรมธุรกิจพลังงาน  
เรื่อง กำหนดลักษณะและคุณภาพของน้ำมันดีเซล (ฉบับที่ ๕)  
พ.ศ. ๒๕๕๕

รายการ	ข้อกำหนด	อัตราสูงต่ำ	น้ำมันดีเซล		วิธีทดสอบ <sup>๔</sup>
			หมุนเร็ว	หมุนช้า	
1	ความถ่วงจำเพาะ ณ อุณหภูมิ 15.6/15.6 องศาเซลเซียส (Specific Gravity at 15.6/15.6 °C)	ไม่ต่ำกว่า และ ไม่สูงกว่า	0.81  0.87	-  0.920	ASTM D 1298
2	จำนวนซีเทน (Cetane Number) หรือ ดัชนีซีเทน (Calculated Cetane Index)				ASTM D 613 ASTM D 976
3	ก่อนวันที่ 1 มกราคม พ.ศ. 2555	ไม่ต่ำกว่า	47	45	ASTM D 445
	ตั้งแต่วันที่ 1 มกราคม พ.ศ. 2555 เป็นต้นไป	ไม่ต่ำกว่า	50	45	
3	ความหนืด (Viscosity, เซนติสโตกส์ cSt)				ASTM D 445
	3.1 ณ อุณหภูมิ 40 องศาเซลเซียส (at 40 °C) หรือ 3.2 ณ อุณหภูมิ 50 องศาเซลเซียส (at 50 °C)	ไม่ต่ำกว่า และ ไม่สูงกว่า	1.8  4.1	-  8.0  6.0	
4	จุดไหลเท (Pour Point, องศาเซลเซียส °C)	ไม่สูงกว่า	10	16	ASTM D 97
5	กำมะถัน (Sulphur, ร้อยละโดยน้ำหนัก %wt.)				
5	ก่อนวันที่ 1 มกราคม พ.ศ. 2555	ไม่สูงกว่า	0.035	1.5	ASTM D 4294
	ตั้งแต่วันที่ 1 มกราคม พ.ศ. 2555 เป็นต้นไป	ไม่สูงกว่า	0.005	1.5	ASTM D 2622
6	การกัดกร่อนแผ่นทองแดง (Copper Strip Corrosion)	ไม่สูงกว่า	หมายเลข 1	-	ASTM D 130
7	เสถียรภาพต่อการเกิดปฏิกิริยา ออกซิเดชัน (Oxidation Stability, กรัม/ลูกบาศก์เมตร g/m <sup>3</sup> )	ไม่สูงกว่า	25	-	ASTM D 2274
8	กากถ่าน (Carbon Residue, ร้อยละโดยน้ำหนัก %wt.)	ไม่สูงกว่า	0.05	-	ASTM D 189
9	น้ำและตะกอน (Water and Sediment, ร้อยละโดยปริมาตร %vol.)	ไม่สูงกว่า	0.05	0.3	ASTM D 2709
10	เถ้า (Ash, ร้อยละโดยน้ำหนัก %wt.)	ไม่สูงกว่า	0.01	0.02	ASTM D 482

( ต่อ -๒- )

รายการ	ข้อกำหนด	อัตราสูงต่ำ	น้ำมันดีเซล		วิธีทดสอบ <sup>17</sup>	
			หมุนเร็ว	หมุนช้า		
11	จุดวาบไฟ (Flash Point,	องศาเซลเซียส °C)	ไม่ต่ำกว่า	52	52	ASTM D 93
12	การกลั่น (Distillation, อุณหภูมิของส่วนที่กลั่นได้โดยปริมาตรในอัตราร้อยละเก้าสิบ (90% recovered)	องศาเซลเซียส °C)	ไม่สูงกว่า	357	-	ASTM D 86
13	โพลีไซคลิก อะโรมาติก ไฮโดรคาร์บอน (Polycyclic Aromatic Hydrocarbon, ก่อนวันที่ 1 มกราคม พ.ศ. 2555 ตั้งแต่วันที่ 1 มกราคม พ.ศ. 2555 เป็นต้นไป	ร้อยละโดยน้ำหนัก % wt.)	ไม่สูงกว่า	11	-	ASTM D 2425
14	สี (Colour)	-	-	-	-	-
14.1	ชนิดของสี (Hue)	-	-	เหลือง	น้ำตาล	-
14.2	ความเข้มของสี (Intensity)	-	ไม่ต่ำกว่า และ ไม่สูงกว่า	4.0	4.5 7.5	ASTM D 1500
15	ไบโอดีเซลประเภทเมทิลเอสเตอร์ ของกรดไขมัน (Methyl Ester of Fatty Acid, ของกรดไขมัน	ร้อยละโดยปริมาตร %vol.)	ไม่ต่ำกว่า และ ไม่สูงกว่า	3	5	EN 14078
16	คุณสมบัติการหล่อลื่น รอยขีดข่วน (Lubridity , Wear Scar	ไมโครเมตร (µm)	ไม่สูงกว่า	460	-	CEC F-06-96
17	สารเติมแต่ง (ถ้ามี) (Additive)	-	-	ให้เป็นไปตามที่ได้รับความเห็นชอบจากอธิบดี กรมธุรกิจพลังงาน		-

หมายเหตุ 17 วิธีทดสอบอาจใช้วิธีอื่นที่เทียบเท่าก็ได้ แต่ในกรณีที่มีข้อโต้แย้งให้ใช้วิธีที่กำหนดในรายละเอียดแนบท้ายนี้

## C-2: Biodiesel fuel

รายละเอียดแบบทำยประกาศกรมธุรกิจพลังงาน  
เรื่อง กำหนดลักษณะและคุณภาพของไบโอดีเซลประเภทเมทิลเอสเตอร์ของกรดไขมัน

พ.ศ. ๒๕๕๒

รายการ	ข้อกำหนด	อัตราสูงค่า	วิธีทดสอบ <sup>๒</sup>
1	เมทิลเอสเตอร์ (Methyl Ester, ร้อยละโดยน้ำหนัก % wt.)	ไม่ต่ำกว่า 96.5	EN 14103
2	ความหนาแน่น ณ อุณหภูมิ 15 °ซ (Density at 15 °C, กิโลกรัม/ลูกบาศก์เมตร kg/m <sup>3</sup> )	ไม่ต่ำกว่า และ ไม่สูงกว่า 860 900	ASTM D 1298
3	ความหนืด ณ อุณหภูมิ 40 °ซ (Viscosity at 40 °C, เซนติสโตกส์ cSt)	ไม่ต่ำกว่า และ ไม่สูงกว่า 3.5 5.0	ASTM D 445
4	จุดวาบไฟ (Flash Point, องศาเซลเซียส °C)	ไม่ต่ำกว่า 120	ASTM D 93
5	กำมะถัน (Sulphur, ร้อยละโดยน้ำหนัก %wt.)	ไม่สูงกว่า 0.0010	ASTM D 2622
6	กากถ่าน (ร้อยละ 10 ของกากที่เหลือจากการกลั่น) (Carbon Residue, on 10 % distillation residue, ร้อยละโดยน้ำหนัก %wt)	ไม่สูงกว่า 0.30	ASTM D 4530
7	จำนวนซีเทน (Cetane Number)	ไม่ต่ำกว่า 51	ASTM D 613
8	เถ้าซัลเฟต (Sulphated Ash, ร้อยละโดยน้ำหนัก %wt.)	ไม่สูงกว่า 0.02	ASTM D 874
9	น้ำ (Water, ร้อยละโดยน้ำหนัก wt.)	ไม่สูงกว่า 0.050	EN ISO 12937
10	สิ่งปนเปื้อนทั้งหมด (Total Contaminate, ร้อยละโดยน้ำหนัก %wt.)	ไม่สูงกว่า 0.0024	EN 12662
11	การกัดกร่อนแผ่นทองแดง (Copper Strip Corrosion)	ไม่สูงกว่า หมายเลข 1	ASTM D 130
12	เสถียรภาพต่อการเกิดปฏิกิริยา ออกซิเดชัน ณ อุณหภูมิ 110 องศาเซลเซียส (Oxidation Stability at 110 °C, ชั่วโมง hours)	ไม่ต่ำกว่า 10	EN 14112

(ต่อ-2)

รายการ	ข้อกำหนด	อัตราสูงสุด	วิธีทดสอบ <sup>๑</sup>
13	ค่าความเป็นกรด (Acid Value . มิลลิกรัมโพตัสเซียมไฮดรอกไซด์/กรัม mg KOH/g)	ไม่สูงกว่า	0.50 ASTM D 664
14	ค่าไอโอดีน (Iodine Value . กรัมไอโอดีน/ 100 กรัม g Iodine / 100 g)	ไม่สูงกว่า	120 EN 14111
15	กรดลิโนเลนิกเมทิลเอสเทอร์ (Linolenic Acid Methyl Ester . ร้อยละโดยน้ำหนัก %wt.)	ไม่สูงกว่า	12.0 EN 14103
16	เมทานอล (Methanol, ร้อยละโดยน้ำหนัก %wt.)	ไม่สูงกว่า	0.20 EN 14110
17	โมโนกลีเซอไรด์ (Monoglyceride ร้อยละโดยน้ำหนัก %wt.)	ไม่สูงกว่า	0.80 EN 14105
18	ไดกลีเซอไรด์ (Diglyceride . ร้อยละโดยน้ำหนัก %wt.)	ไม่สูงกว่า	0.20 EN 14105
19	ไตรกลีเซอไรด์ (Triglyceride . ร้อยละโดยน้ำหนัก %wt.)	ไม่สูงกว่า	0.20 EN 14105
20	กลีเซอรินอิสระ (Free glycerin, ร้อยละโดยน้ำหนัก %wt.)	ไม่สูงกว่า	0.02 EN 14105
21	กลีเซอรินทั้งหมด (Total glycerin, ร้อยละโดยน้ำหนัก %wt.)	ไม่สูงกว่า	0.25 EN 14105
22	โลหะกลุ่ม 1 (โซเดียมและโพแทสเซียม) (Group I metals (Na+K). มิลลิกรัม/กิโลกรัม mg/kg)	ไม่สูงกว่า	5.0 EN 14108 และ EN 14109
	โลหะกลุ่ม 2 (แคลเซียมและแมกนีเซียม) (Group II metals (Ca+Mg). มิลลิกรัม/กิโลกรัม mg/kg)	ไม่สูงกว่า	5.0 pr EN 14538
23	ฟอสฟอรัส (Phosphorus. ร้อยละโดยน้ำหนัก %wt.)	ไม่สูงกว่า	0.0010 ASTM D 4951
24	สารเติมแต่ง (ถ้ามี) (Additive)	ให้เป็นไปตามที่ได้รับความเห็นชอบจากอธิบดี กรมธุรกิจพลังงาน	

หมายเหตุ 1/ วิธีทดสอบอาจใช้วิธีอื่นที่เทียบเท่าก็ได้ แต่ในกรณีที่มีข้อโต้แย้งให้ใช้วิธีที่กำหนดในรายละเอียดแนบท้ายนี้

This material is reserved for educational use only, not allowed for commercial use.

Forbidden to modify the content, and cite the document when use.



This material is reserved for educational use only, not allowed for commercial use.

Forbidden to modify the content, and cite the document when use.

## D-1: Thailand emission standards for small diesel engine vehicle

## ประกาศกระทรวงอุตสาหกรรม

ฉบับที่ ๔๓๕๔ (พ.ศ. ๒๕๕๔)

ออกตามความในพระราชบัญญัติมาตรฐานผลิตภัณฑ์อุตสาหกรรม

พ.ศ. ๒๕๑๑

เรื่อง กำหนดมาตรฐานผลิตภัณฑ์อุตสาหกรรม

รถยนต์ขนาดเล็กที่ใช้เครื่องยนต์แบบจุดระเบิดด้วยการอัด เฉพาะด้านความปลอดภัย :  
สารมลพิษจากเครื่องยนต์ ระดับที่ 7

ประเภทรถยนต์	มวลอ้างอิง (kg)	คาร์บอน มอนอกไซด์	ออกไซด์ ของ ไนโตรเจน	หน่วยเป็น g/km	
				ไฮโดรคาร์บอนรวม กับออกไซด์ ของ ไนโตรเจน	สารมลพิษ อนุภาค
รถยนต์นั่ง มวลเต็มอัตราบรรทุกไม่เกิน 2 500 kg		0.50	0.25	0.30	0.025
รถยนต์นั่งมวลเต็มอัตราบรรทุกเกิน 2 500 kg หรือรถยนต์บรรทุกและรถยนต์นั่งที่ดัดแปลงมา จากรถยนต์บรรทุกที่มีมวลเต็มอัตราบรรทุกไม่ เกิน 3 500 kg	ไม่เกิน 1 305	0.50	0.25	0.30	0.025
	เกิน 1 305 แต่ไม่เกิน 1 760	0.63	0.33	0.39	0.04
	เกิน 1 760	0.74	0.39	0.46	0.06



This material is reserved for educational use only, not allowed for commercial use.

Forbidden to modify the content, and cite the document when use.

CONFERENCE PROCEEDING

# TSME-ICoME 2016



Mechanical Engineering  
Innovation for Green Society



Institution of  
MECHANICAL  
ENGINEERS

The 7<sup>th</sup> TSME-International Conference on Mechanical Engineering  
13-16 December 2016  
Duangtawan Hotel, Chiang Mai, Thailand

Hosted by **CHULA ENGINEERING**

This material is reserved for educational use only, not allowed for commercial use.

Forbidden to modify the content, and cite the document when use.



The 7<sup>th</sup> TSME International Conference on Mechanical Engineering  
13-16 December 2016

**AECXXX** (this number will be assigned after full manuscript is accepted)

## Effect of Palm Methyl Ester Blends Diesel on Small CI Engine Particulate Matter Quantity and Nanostructure

Jiramed Boonsakda<sup>1\*</sup>, Preechar Karin<sup>1</sup>, Chinda Charoenphonphanich<sup>2</sup>, Komkla Siricholathum<sup>1</sup>,  
Katsunori Hanamura<sup>3</sup> and Nuwong Chollacoop<sup>4</sup>

<sup>1</sup>International College, King Mongkut's Institute of technology Ladkrabang

<sup>2</sup>Mechanical Engineering, King Mongkut's Institute of technology Ladkrabang

<sup>3</sup>Department of Mechanical Science and Engineering, Tokyo Institute of Technology

<sup>4</sup>National Metal and Materials Technology Center, National Science and Technology Development Agency

\* Corresponding Author: jiramed.boonsakda@gmail.com, (+66)83555301

### Abstract

Compression Ignition (CI) Engine is popularly used in vehicles due to high thermal efficiency. However CI engine has a particulate matter (PM) problem which palm methyl ester could be one of possible solution to solve this problem. This research focuses on measuring the quantity, size, size distribution and nanostructure of particulate matter in single cylinder CI engine. Particulate matter quantity was collected by opacity smoke meter then captured the nanostructure image by using scanning electron microscope (SEM). The fuels chosen were commercial diesel (B7), blends of 20%, 40%, 60%, 80% and 100% of biodiesel by volume. For quantity and nanostructure analysis, five engine speed modes which consist of 1600, 1800, 2000, 2200 and 2400 rpm were applied on this research. At each engine speed, engine torque were varied with unload, 20%, 40%, 60% and 80% of maximum torque. For particulate matter size and size distribution measured by using laser diffraction technique with same fuel types at 80% load and 2400 rpm. The experimental results indicated that particulate matter quantity decreased when the concentration of biodiesel was increased in blend due to the impact of effective oxygen to more completely combustion. The lowest amount of particulate matter was recognized at 1800-2000 rpm caused by the best engine specific fuel consumption. In addition, when operating at high engine speed, particulate matter was increase because of shorter oxidation time in combustion period. The results of this research might be used as basic information for design and development of Diesel Particulate Filter (DPF) configuration for biodiesel blends diesel CI engines.

**Keywords:** Biodiesel, Biofuel, Particulate matter, Soot, Emission

### 1. Introduction

CI engine is widely used in many application such as agriculture and transportation. Nowadays the energy demand is raising each year but petroleum has limited amount. It makes the price of fuel rapidly increase. Engineers and scientists have to find the alternative fuel which can be used in the standard engine with lower emissions.

In CI engine, the serious issues is the particulate matter (PM) and nitrogen oxide (NO<sub>x</sub>). The pollutants should be removed from exhaust gas because they affected environment and human health such as lung cancer.

The nanostructures of soot primary particles have been characterized using scanning electron microscope (SEM) and transmission electron microscopy (TEM) to understand them in detail. The mean diameter of the single primary and agglomerated particles is usually in the range of ultrafine particle (<100nm) and fine particle (<2.5μm), respectively [1-19]. The composition of PM from a diesel engine may vary widely depending on the operating conditions and fuel composition. PM is traditionally divided into three main fractions: solid fraction (SOL), soluble organic fraction (SOF), and sulfate particulates (SO<sub>4</sub>) that consist of sulfuric acid and water. The SOL of diesel PM is composed primarily of elemental carbon, sometimes referred to as inorganic carbon. This carbon, not chemically bound with other elements, is the finely

dispersed carbon black or soot substance responsible for black smoke emission. Hydrocarbons (HCs) adsorbed on the surface of the carbon particles are presented in the form of fine droplets from the SOF of diesel particulates. At times, this fraction is also referred to as the volatile organic fraction (VOF). The SOF fraction contains most of the polycyclic aromatic HCs (PAHs) and nitro-PAHs emitted with diesel exhaust gases. PAHs are aromatic HCs with two or more benzene rings joined in various forms that are more or less clustered. These require special attention because of their mutagenic and, in some cases, carcinogenic character [9-14].

Nowadays applications of biofuels is a widespread means to reduce amount and particle size of regulated pollutant emissions produced by internal combustion engines because oxygen atoms inside fuel molecules promote more completed combustion, as well as to reduce the greenhouse gas resulting from carbon neutral. The combustion of bio-oxygenated fuel emits carbon dioxide (CO<sub>2</sub>) to the atmosphere for the growth of plants, which are produced by biodiesel fuel and released out of the atmosphere as carbon by photosynthesis. More advantages of biodiesel over other fuels are that it contains much lower sulfur and aromatic HC content [15, 16].

The objective of the present research is to investigate the impact of biodiesel fuel on morphology and quantity of biodiesel particulate matter by using

**AECXXX** (this number will be assigned after full manuscript is accepted)

opacity smoke meter and electron microscopy for better understanding and future design of diesel particulate matter configuration for biodiesel blends diesel engine application [17].

## 2. Experimental Setup and Method

### 2.1 Fuel properties

The fuels chosen in this experiment has six fraction of biodiesel. Commercial grade diesel (B7) and Biodiesel (biodiesel: B100-TIS2313-2549) was used as substrate for another fuel which has 20%, 40%, 60%, and 80% of biodiesel by volume called B20, B40, B60, and B80 respectively. The properties of substrate fuel has shown in "Table. 1". For fuel property of B20 to B80, heating value and density were estimate by interpolation between diesel and biodiesel.

Distillation curve "Fig. 1" below shows the relationship between temperature and percentage of fuel volume which change from liquid to gas phase. Biodiesel is more homogeneous fuel which shown by vaporize temperature. It is very narrow around 340 to 350 degree Celsius. When compare with conventional fuel, biodiesel has higher vaporization temperature due to heavier atomic weight and higher density [Table.1] so the heat of vaporization of biodiesel should be higher than conventional diesel.

Table. 1 Properties of commercial biodiesel fuel derived from palm-olein (biodiesel: B100)

	Diesel	Biodiesel
Density (kg/m <sup>3</sup> )	844.78	864.4
Cetane Number	55	70
Viscosity (centistokes)	3.0	4.5
Chemical Formula	C <sub>16.17</sub> H <sub>32.00</sub>	C <sub>15.26</sub> H <sub>29.48</sub> O <sub>1.70</sub>
Carbon Fraction	82	78
Heating Values (kJ/kg)	46,800	39,550

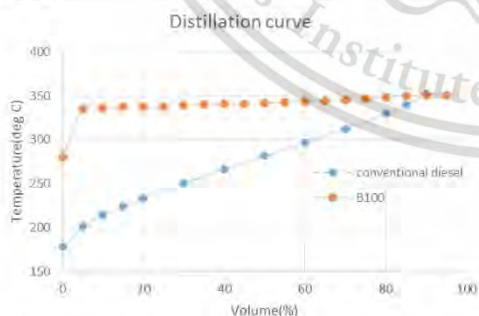


Fig. 1 Distillation curve of conventional diesel and biodiesel.

### 2.2 PM generator

PM was emitted from small CI engine. The engine has displacement of 638cm<sup>3</sup>, compression ratio of 16.1:1 and power output of 8.8 kW. It is a naturally aspirated, single cylinder, four strokes, direct injection, and compression ignition engine. The fuel injection

pressure was approximately 19.6 MPa. Fuel injection timing was constant timing at 19 degree BTDC.

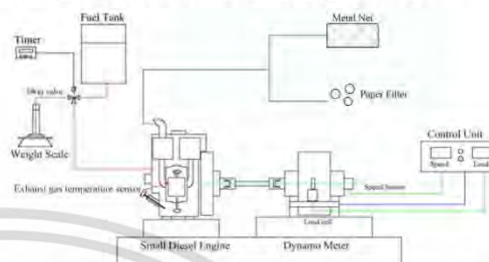


Fig. 2 Schematic diagram of tested small CI engine operation on dynamometer for particulate matter quantity measurement.

### 2.3 Method

The engine was connected to engine dynamometer to control engine load and engine speed. Fuel was supplied from fuel tank to weight scale using timer to control amount of fuel then weight scale measure fuel consumption which supplied to the engine in each condition. Exhaust gas temperature was measured 5cm after exhaust port. PM was trapped by metal net or paper filter depend on experiment as shown in "Fig. 2".

#### 2.3.1 Particle quantity

For PM quantity, The PM emitted from the engine was collected by opacity smoke meter (OKUDA DSM-240) filter paper. PM was collected approximately 20cm after exhaust valve in the same amount of suction period. Then PM quantity was measured by opacity smoke meter in five engine speed modes which consist of 1600, 1800, 2000, 2200 and 2400 rpm. At each engine speed, engine torque were varied with unload, 20%, 40%, 60% and 80% of maximum torque.

#### 2.3.2 Efficiency and particle size distribution

For particle size distribution analysis use laser diffraction technique using "MASTERSIZER 2000" machine. The particle was trapped by metal net after exhaust port around 50cm at 80% load and 2400rpm for every fuel.

#### 2.3.3 Morphology and nanostructures

Morphology and nanostructures of PM was investigated by using a scanning electron microscopy (SEM: EVO@MA10) and a transmission electron microscopy (TEM: JEOL JEM-2010).

## 3. Results and Discussions

### 3.1 PM quantity

"Fig. 3-Fig. 8" show smoke intensities of each fuel, engine load, and engine speed. Conventional diesel emitted the highest amount of smoke. The PM reduced by concentration of biodiesel due to oxygenate fuel. It was clearly observed that biodiesel engine's particulate matter was approximately a half of conventional diesel engine's particulate matter. When increase engine load, smoke intensity increased because more fuel was supplied to the engine. For



**AECXXX** (this number will be assigned after full manuscript is accepted)

engine speed it has a little different amount of smoke due to the engine efficiency of each engine speed. The lowest amount of smoke in each engine load usually occurs around 1800-2000rpm. When increase concentration of biodiesel, trend of engine speed which emitted lowest particulate matter(in the same load) shift to faster engine speed because bio diesel has a faster chemical reaction rate due to Biodiesel is oxygenate fuel which has oxygen in their molecule.

In addition, when operating at high engine speed, particulate matter was increase because of shorter oxidation time in combustion period.

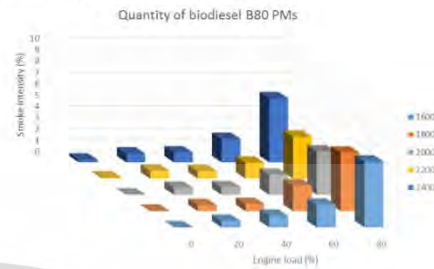


Fig. 7 Smoke intensity of B80

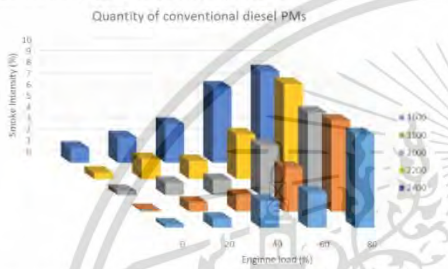


Fig. 3 Smoke intensity of conventional diesel

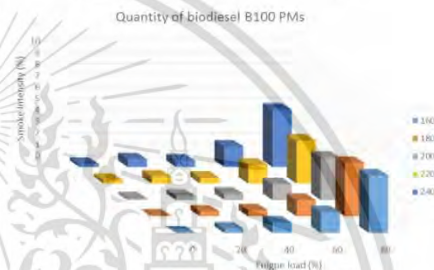


Fig. 8 Smoke intensity of B100

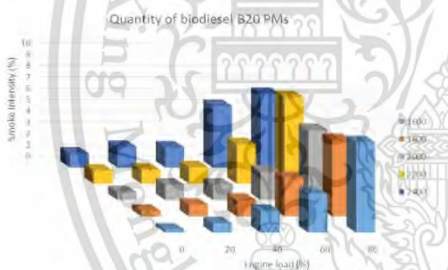


Fig. 4 Smoke intensity of B20

**3.2 Efficiency and exhaust temperature**

From the experiment result “Fig. 9” has shown when increase content of biodiesel, brake specific fuel consumption (BSFC) significantly increase around six percent. When engine dynamometer try to control the same power output of each fuel, biodiesel which has lower heating value have to inject more amount of fuel to compensate the lower energy output.

Although biodiesel has a worse brake specific consumption but when consider on brake specific energy consumption (BSEC), trend is decrease inversely proportional with content of biodiesel. According to biodiesel is an oxygenate fuel which can combust more completely. So the thermal efficiency is increase and energy demand to create the power output is decrease.

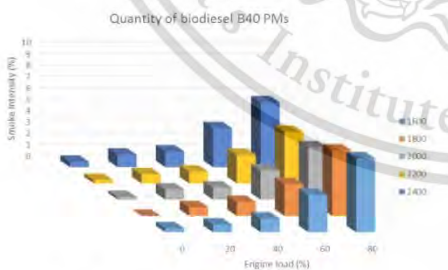


Fig. 5 Smoke intensity of B40

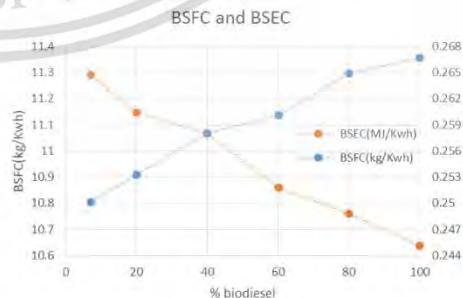


Fig. 9 Brake specific fuel consumption and brake specific energy consumption at 80% load and 2400rpm on each fuel

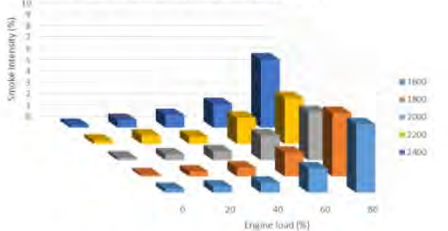


Fig. 6 Smoke intensity of B60

**AECXXX** (this number will be assigned after full manuscript is accepted)

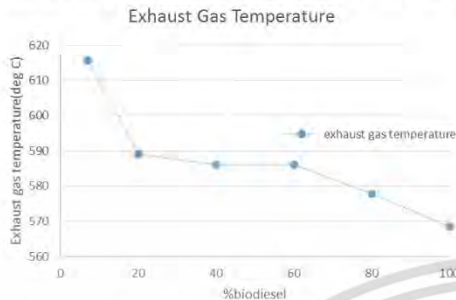


Fig. 10 Exhaust gas temperature at 80% load and 2400rpm on each fuel

Trend of exhaust gas temperature “Fig. 10” is inversely proportional with biodiesel fraction. Due to two reason, first is distillation curve in “ ” which biodiesel start to change their phase from liquid to gas phase at higher temperature than conventional diesel. And mass of biodiesel which use for combustion per cycle is more than conventional diesel from BSFC in “Fig. 9”. It mean in the combustion reaction biodiesel have to absorb much more energy than conventional diesel to change their phase before combustion process. And the second reason is Biodiesel has higher cetane number thus the advance combustion (premixed combustion phase) should be found lead to the shorter combustion duration lead to the lower temperature with biodiesel fuel blends. From those reason, the higher content of biodiesel, the lower exhaust gas temperature.

### 3.3 Particle size distribution

Particle which emitted from internal combustion engine clearly separate into 3 modes [18].

First is nucleation mode, but the nuclei particles are too small for the particle size distribution measure instrument.

Second is accumulation mode which shown in first peak of “Fig. 11”. The size range of agglomerate is ~40-400nm, average size is ~130-142nm, and mode size is ~100-120nm. When compare the average size of particles form laser diffraction technique with image processing technique [19] which the average size of diesel particulate matter is 131nm and biodiesel is 134nm. That result can be confirm that these two methods of measuring get the similar result which have different <10%. The higher content of oxygen in fuel, the higher amount and smaller size of agglomerate because of more complete combustion. Which can see in better BSEC.

Third is coarse mode such as PM<sub>2.5</sub> and PM<sub>10</sub> which shown in second peak of the “Fig. 11”. The higher content of conventional diesel, the higher amount of particle in coarse mode.

The result of particle size distribution in every fuel show the similar trend of particle mode separation. The size of each modes are similar but the amount is different by the fraction of biodiesel.

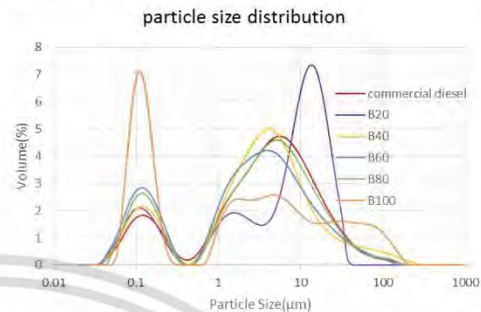


Fig. 11 particle size distribution at 80% load 2400 rpm of each fuel

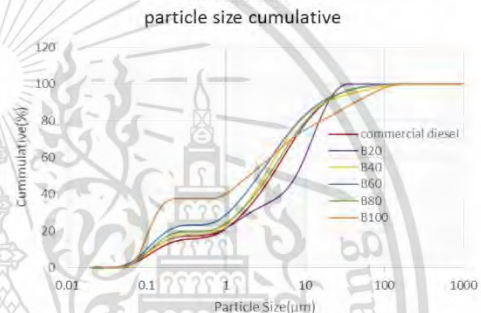


Fig. 12 particle size cumulative at 80% load 2400 rpm of each fuel

### 3.4 Morphology and nanostructures

The morphology of engine’s particulate matter was successfully investigated using electron microscopy. Several type of PM spread all of the filters for example PM<sub>10</sub> which have size around 10 micron, PM<sub>2.5</sub> or fine particle, ultrafine particle and nanoparticle were clearly seen using SEM and TEM. “Fig. 13” shows SEM image of PM<sub>10</sub> from biodiesel engine in the condition of 80% load engine operation. In “Fig. 14 and Fig. 15” shows PM<sub>2.5</sub> from the same condition with “Fig. 13”.

Both of PM<sub>10</sub> and PM<sub>2.5</sub> of diesel and biodiesel engine’s particulate matter consist of many single nanoparticles.



Fig. 13 SEM image of biodiesel blends diesel engine’s PM<sub>10</sub> in the condition of 80% load engine operation.

**AECXXX** (this number will be assigned after full manuscript is accepted)



Fig. 14 SEM image of conventional diesel particulate matter in condition of 80% load operation



Fig. 15 SEM image of biodiesel particulate matter in condition of 80% load operation

In addition, ultrafine particles and nanostructure of PM single particle were investigated using TEM for better understanding. “Fig. 16 and Fig. 17” shows TEM images of diesel and biodiesel engine’s particulate matter ultrafine particles, respectively, in the condition of 80% load engine operation. The average agglomerated particle diameter size are in the range of 40-400nm.

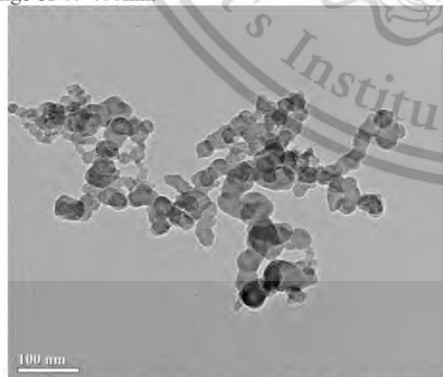


Fig. 16 TEM image of conventional diesel particulate matter ultrafine particles in the condition of 80% load operation

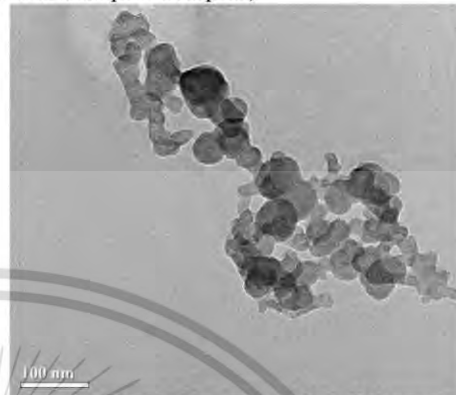


Fig. 17 TEM image of biodiesel particulate matter ultrafine particles in the condition of 80% load operation

Moreover, single nanoparticles of diesel and biodiesel engines was also clearly observed using TEM as shown in “Fig. 18 and Fig. 19”, respectively. The average agglomerated particle diameter size are in the range of 20-50nm. Each carbon platelet, inner core and outer shell of single nanoparticle was also clearly observed by TEM.

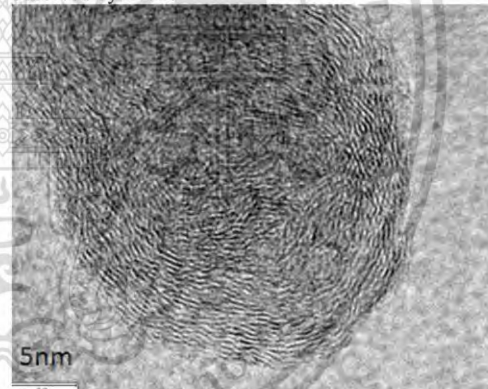


Fig. 18 TEM image of conventional diesel nanoparticle in condition 80% load operation

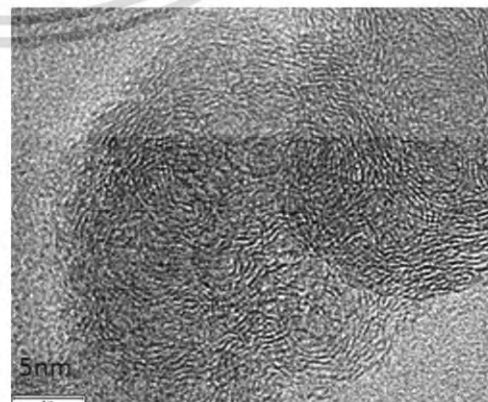


Fig. 19 TEM image of biodiesel nanoparticle in condition 80% load operation



**AECXXX** (this number will be assigned after full manuscript is accepted)

#### 4. Conclusion

The amount of particulate matter (PM) emitted from CI engine depend on several variables. The result shows the parameter which has the highest effect on smoke intensity or PM quantity is engine load, concentration of biodiesel and engine speed respectively. When increase concentration of biodiesel in fuel, PM reduce because oxygen concentration in fuel increase. Higher concentration of oxygen makes more complete combustion, better BSEC, smaller particle, and lower exhaust temperature. The quantities of particulate matter emitted from biodiesel engine are approximately a half of diesel engine's particulate matter. Morphology of CI engine's PM<sub>10</sub>, PM<sub>2.5</sub>, ultrafine particle and nanoparticle was characterized using SEM and TEM successfully. The morphology of biodiesel and conventional diesel doesn't have significant different on every type of particle. Average single nanoparticle sizes of diesel and biodiesel engine's particulate matter is approximately 20-50 nm. Average agglomerate size of diesel and biodiesel engine's particulate matter is ~130-142nm similar to the image processing result from TEM image in the previous research [19].

Smaller particulate matter from biodiesel fuel should be consider to design and development of Diesel Particulate Filter (DPF) configuration for biodiesel blends diesel CI engines in the future.

#### 5. Acknowledgement

The authors gratefully acknowledge the financial support from Thailand Research Fund (TRF).

#### 6. References

- [1]. Heywood BJ. Internal Combustion Engine Fundamental. McGraw-Hill series in mechanical engineering; Singapore, 1998.
- [2]. Smith IO. Fundamentals of soot formation in flames with application to diesel engine particulate emissions. Progress in Energy and Combustion Science; 7:275-291.
- [3]. Maricq MM. Review chemical characterization of particulate emissions from diesel engine: A review. Journal of Aerosol Science; 38:1079-1118.
- [4]. Kittelson BD. Engines and nanoparticles: A review. Journal of Aerosol Science; 29:575-588.
- [5]. Majewski AW, Khair KM. Diesel emissions and their control. SAE Order No.R-303 SAE International; Warrendale USA.
- [6]. Vander Wal AR, Yezerets A, Currier WN, Kim HD, Wang HC. HRTEM Study of diesel soot collected from diesel particulate filters. Carbon; 45:70-77.
- [7]. Fernandez-Alos V, Watson KJ, Vander Wal AR, Mathew PJ. Soot and char molecular representations generated directly from HRTEM lattice fringe images using fringe3D. Combustion and Flame; 158:1807-1813.
- [8]. Neeft PAJ, Nijhuis XT, Smakman E, Makkee M, Moulijn AJ. Kinetics of the oxidation of diesel soot. Fuel; 76-12:1129-1136.
- [9]. Darcy P, Costa DP, Mellottee H, Trichard MJ, Mariadassou DG. Kinetics of catalyzed and non-catalyzed oxidation of soot from a diesel engine. Catalysis Today; 119:252-256.
- [10]. Yezerets A, Currier WN, Eadler AH. Experimental determination of the kinetics of diesel soot oxidation by O<sub>2</sub> - Modeling consequences. SAE Technical paper; 2003-01 0833.
- [11]. Lorentzou S, Pagkoura C, Zygogianni A, Kastrinaki G, Konstandopoulos GA. Catalytic nano-structured materials for next generation diesel particulate filters. SAE Technical paper; 2008-01-0417.
- [12]. Karin P, Hanamura K. Particulate matter trapping and oxidation on catalyst-membrane. SAE International Journal of Fuels and Lubricants; 3-1:368-379.
- [13]. Oki H, Karin P, Hanamura K. Visualization of oxidation of soot nanoparticles trapped on a diesel particulate membrane filter. SAE International Journal of Engine; 2011-01-0602.
- [14]. Karin P, Songsaengchan Y, Laosuwan S, Charoenphonphanich C, Chollacoop N, Hanamura K. Nanostructure of Renewable Oxygenated Fuels Particulate Matter. ASEAN Engineering Journal; 3-1:72-83.
- [15]. Karin P, Songsaengchan Y, Laosuwan S, Charoenphonphanich C, Chollacoop N, Hanamura K. Nanostructure Investigation of Particle Emission by Using TEM Image Processing Method. Energy Procedia, Elsevier; 34, 757-766.
- [16]. Karin, P., Songsaengchan, Y., Laosuwan, S., Charoenphonphanich, C., Chollacoop, N., Hanamura, K. (2013). Physical Characterization of Biodiesel Particle Emission by Electron Microscopy. SAE Technical Paper, 2013-32-9150.
- [17]. Karin, P., Borhanipour, M., Songsaengchan, Y., Laosuwan, S., Charoenphonphanich, C., Chollacoop, N., Hanamura, K. (2015). Oxidation Kinetics of Small CI Engine's Biodiesel Particulate Matter. International Journal of Automotive Technology, Vol. 16, No. 2, pp. 211-219 (2015)
- [18]. Peter E. Particulate Emissions from Vehicles, ISBN 978-0-470-72455-2, John Wiley & Sons Inc.
- [19]. Siricholathum, K. The Impact of biodiesel particulate matter morphology and oxidation kinetic on filter trapping and regeneration mechanism, KMITL

## AUTHOR BIOGRAPHY

**Author:** Mr. Jiramed Boonsakda

**Date of Birth:** 6<sup>th</sup> July 1991

**Address:** 79/129 Mooban Sammakorn minburi Bangchan  
Klongsamwa Bangkok 10510

### Education:

2010 – 2013: Bachelor Degree in Mechanical Engineering, King Mongkut's Institute of Technology Ladkrabang.

2014 – 2016: Master Degree, Automotive Engineering (International Program), International College, King Mongkut's Institute of Technology Ladkrabang.

### Publications:

- 1.) Jiramed Boonsakda, Preechar Karin, Chinda Charoenphonphanich, Komkla Siricholathum, Katsunori Hanamura, and Nuwong Chollacoop, "Effect of Palm Methyl Ester Blends Diesel on Small CI Engine Particulate Matter Quantity and Nanostructure," *7th TSME Int. Conf. Mech. Eng.*, Dec. 2016.
- 2.) P. Karin, J. Boonsakda, K. Siricholathum, E.Saenkhumvong, C. Chareonphonphanich, and K. Hanamura, "Morphology and Oxidation Kinetic of CI Engine's Biodiesel," *International Journal of Automotive Technology.*, 2017, 18, pp. 31–40.